INHIBITION OF METALLO-BETA-LACTAMASE BY RATIONAL AND COMBINATORIAL APPROACHES

by

SUNG-KUN KIM, B.S., M.S.

A DISSERTATION

IN

CHEMISTRY

Submitted to the Graduate Faculty
of Texas Tech University in
Partial Fulfillment of
the Requirements for
the Degree of

DOCTOR OF PHILOSOPHY

Approved

_____
Chairperson of the Committee

_____

_____

Accepted

_____
Dean of the Graduate School

August, 2002

ACKNOWLEDGEMENTS

This research was supported by a grant from the Robert A. Welch Foundation (D-1306) awarded to Professor Robert W. Shaw. I would like to thank Professor Shaw for many years of direction and support. I would like to thank Professor James G. Harman, Professor David B. Knaff, and Professor W. David Nes for suggestions as members of committee. I would like to thank Professor John D. Buynak for providing us with inhibitors. I would like to thank Professor D. Max Roundhill and Dr. Fred Koch for the use of ICP-AES. I would like to thank Professor Moon-Young Yoon at Hanyang University for introducing me to the world of biochemistry.

I would like to thank Michelle Wells, Jennifer Lacina, and Bradley Brown for technical support during the SELEX process, and thank Mitchel Cottenoir and Kyu Mee Kim for intellectual discussions of experiments.

I should thank my parents for support and I am especially indebted to my wife, Sang-Nam Yi, for her many years of sacrifice and patience while I pursued my goal.

TABLE OF CONTENTS

ABSTRACT

The inhibition of the *Bacillus cereus* 5/B/6 metallo-β-lactamase, an enzyme that catalyzes the hydrolysis of nearly all β-lactam antibiotics, has been explored by rational and combinatorial approaches.

Inactivation of the metallo-β-lactamase activity by sodium 7-(dibromomethylene)-cephalosporanate and sodium 3-acetoxymethyl-7-(E-bromomethylidene)-3-cephen-4-carboxylate was time-dependent. The rate constants of inactivation (k_{inact}) were 0.20 and 0.25 min^{-1}, respectively. The values of K_{inact} were found to be 4.7 and 9.0 mM, respectively.

The penicillin derivatives sodium 6-(R-thiolmethyl) penicillate and sodium 6-(S-thiolmethyl) penicillate were reversible, noncompetitive inhibitors of the metallo-β-lactamase. The IC_{50} (inhibitor concentration for 50 % inhibition), K_i (dissociation constant for the enzyme-inhibitor complex), and K_i' (dissociation constant for inhibitor from enzyme-substrate-inhibitor complex) values were 8.3, 4.2 and 11 μM, respectively for sodium 6-(R-thiolmethyl) penicillate and 18, 8.6 and 23 μM, respectively for the S-isomer.

Single-stranded DNA aptamers were developed using the SELEX (systematic evolution of ligands by exponential enrichment), combinatorial chemistry technology. A 61-mer containing a random 30-mer (comprising over 10^{18} sequences) was synthesized. After twenty-one SELEX rounds, one sequence was found. This oligonucleotide synthesized. This 30-mer was a noncompetitive inhibitor of the metallo-β-lactamase with an IC_{50} of 1.2 nM, a K_i of 0.92 nM and a K_i' of 11 nM. Using the MFold program, a

unique stem-loop secondary structure was predicted for a 10-nucleotide portion of the 30-mer. When this 10-mer was synthesized, it also was also found to be a noncompetitive inhibitor of the metallo-β-lactamase. The IC_{50} was the same as that of the 30-mer; however, the K_i (0.31 nM) and K_i' (1.5 nM) were lower than the 30-mer. An 18-mer corresponding to the remainder of the 30-mer sequence did not show detectable inhibition. Both the 30-mer and 10-mer had no effect on the activity of the *B. cereus* 569/H/9 β-lactamase I or bovine carboxypeptidase A, indicating that the inhibition was specific for the metallo-β-lactamase.

The rational drug design approach using chemical synthesis to produce new metallo-β-lactamase inhibitors was successful. The combinatorial chemistry approach (SELEX) was also successful and led to an entirely new class of highly efficient and specific metallo-β-lactamase inhibitors.

LIST OF TABLES

LIST OF FIGURES

LIST OF ABBREVIATIONS AND SIMBOLS

Ala	alanine
Arg	arginine
B. cereus	*Bacillus cereus*
B. fragilis	*Bacteroides fragilis*
bps	base pairs
BSA	bovine serum albumin
CD	circular dichroism
CM	carboxymethyl
cI repressor	bacteriophage λ P_L promoter binding protein
Da	dalton
DD-peptidase	D-alanyl-D-alanine carboxypeptidases/transpeptidases
ddH_2O	distilled deionized H_2O
DEAE	diethylaminoethyl
DE-MALDI-TOF MS	Delayed Extraction Matrix Assisted Laser Desorption/Ionization Time Of Flight Mass Spectrometry
dsDNA	double-stranded DNA
EDTA	ethylenediamine tetraacetic acid
E. coli	*Escherichia coli*
EPR	electron paramagnetic resonance
IC_{50}	inhibitor concentration for 50 % inhibition
ICP-AES	Inductively Coupled Plasma - Atomic Emission Spectroscopy
k_i	biomolecular rate constant with units ($M^{-1}min^{-1}$)

k_{-1}	unimolecular rate constant with units (min^{-1})
k_2	unimolecular rate constant with units (min^{-1})
K_i	dissociation constant for inhibitor from enzyme-inhibitor complex
K_i'	dissociation constant for inhibitor from enzyme-substrate-inhibitor complex
k_{inact}	rate constant for the conversion of the initial reversible enzyme inhibitor complex to the irreversibly inhibited enzyme
K_{inact}	$(k_{-1} + k_2)/k_1$
LB Medium	Luria-Bertani Medium
Lys	lysine
MOPS	3-(N-morpholino) propanesulfonic acid
NMR	nuclear magnetic resonance
PAGE	polyacrylamide gel electrophoresis
pRE2	plasmid DNA expression vector
pRE2/bla	plasmid DNA expression vector containing the *B. cereus* 5/B/6 metallo-β-lactamase structural gene
SDS	sodium dodecyl sulfate
SELEX	Systematic Evolution of Ligands by EXponential enrichment
SEM	standard error of the mean
ssDNA	single-stranded DNA
TA	20 mM Tris (pH = 7.0) and 20 mM acetate
TFA	trifluoroacetic acid
T_m	temperature at which 50 % of a given oligonucleotide is hydridized

	to its complementary strand
Tris	2-amino-2-(hydroxy-methyl)-1,3-propanediol
UV	ultraviolet
V	volt(s)

CHAPTER I

INTRODUCTION

β-lactam antibiotics

β–lactamases (β–lactamhydrolyases, EC 3.5.2.6) are highly efficient enzymes that catalyze the hydrolysis of the β–lactam rings of antibiotics such as penicillins, cephalosporins, monobactams and carbapenems, causing these compounds to lose their bactericidal activity (Fisher et al., 1981; Maugh, 1981) (Figure 1). The β–lactam antibiotics are analogs of a peptidoglycan that is involved in bacterial cell wall synthesis. The targets of the β–lactam antibiotics are DD-peptidases (D-alanyl-D-alanine carboxypepidases/transpeptidases) that catalyze the formation of the peptide cross-links of the peptidoglycan in the final stages of the bacterial cell wall synthesis. Bacterial cell wall synthesis takes place on the external surface of the cytoplasmic membrane and is easily accessible for the antibacterial agents. The β–lactam antibiotics inhibit DD-peptidases by forming a rather stable covalent acyl-enzyme complex with the enzyme that has a longer half-life than that formed with the peptidoglycan, thus disrupting the construction of the bacterial cell wall, thereby causing the death of bacteria (Kelly et al., 1988; Ghuysen, 1988). Since the mammalian cells have a different membrane with no cell wall structures, the β–lactams are highly specific for bacteria and have few side effects even at high concentrations of β–lactam antibiotics (Maugh, 1981).

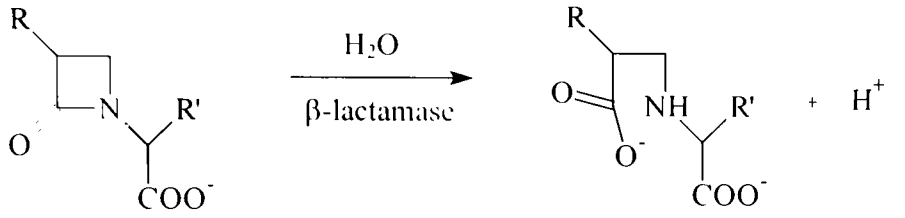

Figure 1. Catalysis of hydrolysis of a generic β–lactam by a β–lactamases (Livermore, 1991).

Figure 2 shows the general structures of penicillins and cephalosporins. Figure 3 shows the comparison of the structure of penicillins with the structure of D-alanyl-D-alanine-peptidoglycan. Held in a strained configuration by the ring system, the β–lactam and the adjacent atoms have a spatial configuration similar to that of peptidoglycan.

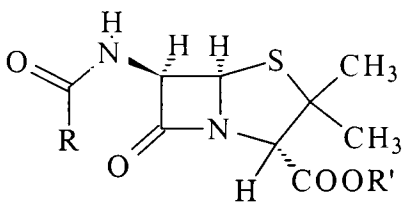

Penicillins

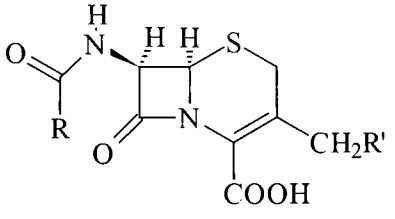

Cephalosporins

Figure 2. Structures of two classes of β–lactam antibiotics: Penicillins and Cephalosporins.

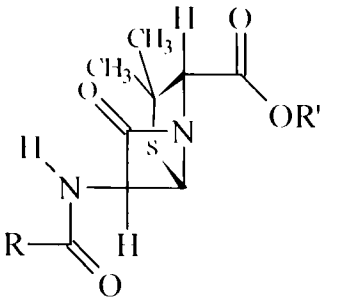

Penicillins

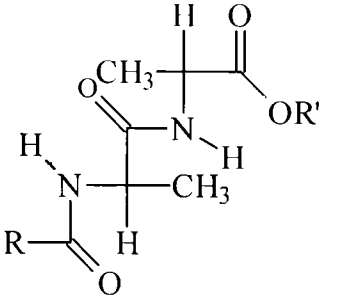

D-alanyl-D-alanine-peptidoglycan

Figure 3. The comparison of the structure of penicillins with the structure of D-alanyl-D-alanine-peptidoglycan (Suskoviae et al., 1991).

Bacteria that acquire the genes for the production of β-lactamases become resistant to β–lactam antibiotics (Neu, 1992). Studies of the chemical reaction mechanisms of β–lactamases are of vital importance in designing new antibiotic compounds and new β–lactamase inhibitors (Abraham and Waley, 1979; Brenner and Knowles, 1984). Research to develop new β–lactam antibiotics has been attempting to keep ahead of the spread of the bacterial drug-resistance by making slight alterations in the structures of the existing β–lactam antibiotics. Cephalosporins, for example, have

passed through four generations (Maugh, 1981; Pitout et al., 1997). The use of β–lactam/β–lactamase inhibitor combinations has also increased. There are limits on chemical manipulation of the existing groups of antibiotics. Therefore, it is increasingly important to design new types of antibiotics and mechanism-based β–lactamase inhibitors and to understand the mechanisms by which β–lactamases function. The design of a therapeutically useful β–lactam antibiotics or inhibitors requires a detailed understanding of the function of β–lactamases.

Classification of β–lactamases

β–lactamases are produced by a wide range of bacteria. An incomplete list of bacteria that produce β–lactamases include *Bacillus anthracis*, *Bacillus cereus, Bacillus fragilis, Escherichia coli, Aeromonous hydrophilia, Bacteroides, Staphylococcus epidermidis, Streptococcus, Pseudomonas aeruginosa, Providencia, Haemophilus, Xanthomonas maltophilia, Acinetobacter, Citrobacter, Enterobacter* and *Branhamella* (Danziger and Pendland, 1995). β–lactamases are classified on the basis of their primary structures and catalytic properties. There are currently four classes of β–lactamases: class A, B, C and D (Ambler, 1980; Ambler et al., 1991; Joris et al., 1991; Frere, 1995). Class A, C and D β–lactamases are serine-active-site enzymes that resemble serine proteases and form an acyl-enzyme intermediate with an active-site serine during the catalysis of β–lactam antibiotics (Rahil and Pratt, 1991). Class A β–lactamases are soluble enzymes, and the class C β–lactamases are very similar to class A β–lactamases except they are membrane bound (Hussain et al., 1987). Class D β–lactamases do not exhibit primary

sequence similarities to class A and C β–lactamases (Joris et al., 1991; Ledent et al., 1993). The class B β–lactamases, on the other hand, are quite different from the other classes of β–lactamases. They are metallo-β–lactamases, which require divalent metal ions for enzymatic activity (Ambler, 1980; Abraham and Waley, 1979). Native class B β–lactamases are isolated with one or two zinc ions bound to their active sites (Carfi et al., 1995; Concha et al., 1996).

The β–lactam antibiotics that are substrates of class B β–lactamases include penicillin derivatives and cephalosporin derivatives. (Felici et al., 1993, 1997; Felici and Amicosante, 1995). *B. cereus* 569/H/9 β-lactamase I is 8,800 times less active with cephalosporin C than the metallo-β-lactamase (Abraham and Waley, 1979). Hydrolysis of β–lactam antibiotics such as carbapenems, cephamycins and imipenem, which are normally resistant to the serine β-lactamase, is also catalyzed by the class B β–lactamases (Felici et al., 1993; Felici and Amicosante, 1995; Rasmussen et al., 1994). The inhibitors for other classes of β–lactamases such as penem, 6-β–iodopenicillanic acid, penicillanic acid sulfone and clavulanic acid do not inhibit class B β–lactamases (Felici and Amicosante, 1995; Matagne et al., 1995). Recently a series of mercaptoacetic acid thiol esters (Payne et al., 1997; Yang and Crowder, 1999) and thiomandelic acid (Mollard et al., 2001) have been identified as metallo-β-lactamase inhibitors. Also, understanding the structure and dynamics of metallo-β-lactamases has been studied (Carfi et al., 1995; Concha et al., 1996; Scrofani et al., 1999; Concha et al., 2000). However, there is still a need to develop more effective inhibitors for metallo-β-lactamases.

Metallo-β–lactamases have been detected in an increasing number of pathogenic

bacteria including *Bacillus*, *Bacteroides*, *Xanthomonas*, *Aeromonas*, *Pseudomonas*, *Stenotrophomonas*, *Klebsiella*, *Flavobacterium*, *Legionella*, *Enterobacter* and *Serratia* (Fecili and Amicosante, 1995; Payne, 1993; Payne et al., 1997). These findings underline the spreading of metallo-β–lactamases genes among pathogenic bacteria.

Metallo-β–lactamase from *Bacillus cereus* 5/B/6

The first metallo-β–lactamase was identified in *B. cereus* 569 (Sabath and Abraham, 1966). It was shown that a part of the cephalosporinase activity in the crude penicillinase preparation from *B. cereus* strain 569 required Zn^{2+} for maximum activity. This enzyme was reported to have unique thermal stability. Heating at 60 °C for 30 min. does not abolish the catalytic activity of this enzyme (Crompton et al., 1962; Davies et al., 1974). The first purified metallo-β–lactamases were reported to have been obtained by Kuwabara et al. (1970). From *B. cereus* 569/H, a spontaneous mutant of strain 569 produces class B β–lactamases constitutively (Kogut et al., 1956). The purification procedure was Kuwabara and Lloyd (1971).

Another *B. cereus* strain (5/B) was found to produce one class A β–lactamase and one metallo-β–lactamase. This metallo-β–lactamase is very similar to the metallo-β–lactamases produced by *B. cereus* 569 and 569/H except with slightly different substrate specificity (Crompton et al., 1962). *B. cereus* 5/B/6, a mutant form of *B. cereus* 5/B, produces only the metallo-β–lactamase due to a mutation in the structural gene required for the synthesis of the class A β–lactamases (Davies et al., 1975; Abraham and Waley, 1979). The metallo-β-lactamases from *B. cereus* strain 5/B/6 was later purified in

a similar manner as *B. cereus* 569/H/9 (Thatcher, 1975). The metallo-β–lactamases from these strains of *B. cereus*, which are isolated with one or two Zn^{2+} ions at the active site, were among the first to be studied of the class B enzymes (Ambler, 1985; Bicknell et al., 1986; Sutton et al., 1987; Meyers and Shaw, 1989). The metallo-β-lactamases from these strains of *B. cereus* are very similar. They both consist of 227 amino acid residues among which 209 residues are identical (Lim et al., 1988). Although these β-lactamases are isolated with a Zn^{2+} bound at the active site, other metal ions including Co^{2+}, Cd^{2+}, Mn^{2+}, Hg^{2+} and Cu^{2+} support some catalytic activity of the enzymes (Davies and Abraham, 1974; Hilliard and Shaw, 1992; Hilliard, 1995).

The metallo-β-lactamases from *B. cereus* 569/H/9 and 5/B/6 are secreted extracellularly. The latter enzyme has a 29 amino acid leader sequence before it is secreted from the cell. The gene for this enzyme has been cloned, sequenced and characterized in great detail in *E. coli*. It has also been expressed as an intracellular enzyme with the signal sequence at relatively low levels in *E. coli* (Lim et al., 1988). It was also revealed that the metallo-β-lactamases from *B. cereus* strains 5/B/6 and 569/H/9 differ by only 18 amino acid residues (Lim et al., 1988). Even though the procedure for production and purification of this enzyme from *B. cereus* 5/B/6 cultures was greatly improved (Meyers and Shaw, 1989), hyperexpression in *E. coli* was still desirable. The construct used at that time did not achieve this goal (Lim et al., 1988). The main cause of the low levels of expression was postulated to be the presence of the 29 amino acid leader peptide at the 5' end of this β-lactamase which signals the secretion of the enzyme from the *B. cereus* cell (Shaw et al., 1991).

Site-directed mutagenesis was performed to remove the leader sequence and

introduce a NdeI restriction endonuclease site (Shaw et al., 1991) at the initiator codon of the *B. cereus* 5/B/6 β-lactamase structural gene as a fragment between a NdeI and a SacI site. This construct allowed the cloning of just the *B. cereus* 5/B/6 β-lactamase structural gene sequence into the *E. coli* expression vector pRE2 (Reddy et al., 1989). This recombinant plasmid pRE2 was chosen because a gene cloned into the unique NdeI and SacI restriction endonuclease sites within its polylinker region is correctly oriented and under the control of its strong P_L promoter. The resulting plasmid is denoted as pRE2/*bla*. In the *E.coli* MZ-1, the temperature sensitive cI repressor binds to the P_L promoter and prevents the expression of the *B. cereus* 5/B/6 β-lactamase gene on plasmid pRE2/*bla* at low temperatures. The cI protein is denatured at higher temperatures allowing the expression of *B. cereus* 5/B/6 β-lactamases at high levels (Nagai and Thogersen, 1984; Zuber et al., 1987). Subsequent purification of wild type and mutant *B. cereus* 5/B/6 β-lactamases resulted in a high yield of the metallo-β-lactamase that is identical to that purified from *B. cereus* 5/B/6 (Myers and Shaw, 1989; Shaw et al., 1991). There are the crystal structures available for metallo-β–lactamases (Carfi et al., 1995; Concha et al., 1996). We have used a variety of other techniques to investigate the catalytic specificity and active sites of this enzyme. These include site-directed mutagenesis and mechanism-based inactivators.

Rational drug design and enzyme inhibition

Mechanism-based inhibition

Mechanism-based inhibitors have been utilized extensively to probe the reaction mechanisms of the serine-active-site β-lactamase (Buynak et al., 1994, 1995). Besides

their value for basic research, inhibitors utilized in clinics also offer great benefits. We have studied the mechanism-based inhibition of the 5/B/6 enzyme by compounds synthesized by Prof. John Buynak at Southern Methodist University (Figure 4). Similar compounds have previously been reported to be inhibitors of the serine hydroxyl (class A) enzyme but have not previously been found to be effective inhibitors of metallo-β-lactamases. We have utilized Delayed Extraction Matrix Associated Laser Desorption Ionization Time of Fight (DE-MALDI-TOF) mass spectrometry techniques to determine the molar masses of the inhibited protein species produced as a result of reactions with the compounds of Figure 4.

Reversible inhibition

We have also studied the reversible inhibition of *B. cereus* 5/B/6 metallo-β-lactamase by penicillin derivatives synthesized by Prof. John Buynak at Southern Methodist University (Figure 5). Penicillin derivative inhibitors for other classes of β–lactamases such as 6-β–iodopenicillanic acid and penicillanic acid sulfone do not inhibit class B β–lactamases (Felici and Amicosante, 1995; Matagne et al., 1995). Most of metal ion chelating agents such as EDTA that are known as metallo-β-lactamase inhibitors have no pharmaceutical relevance (Payne, 1993). Finding the inhibitors for metallo-β-lactamsase will benefit metallo-β-lactamase research, both in terms of mechanistic studies of the enzyme and in terms of developing new drug preparations.

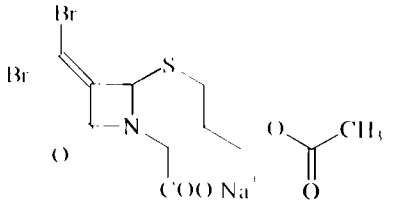

Sodium 7-(dibromomethylene)-cephalosporanate (**1**)*

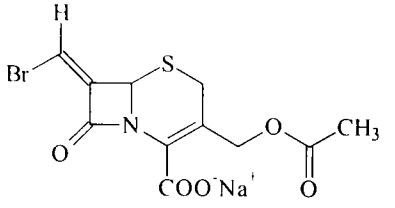

Sodium 3-acetoxymethyl-7-(E-bromomethylidene)-3-cephem-4-carboxylate (**2**)*

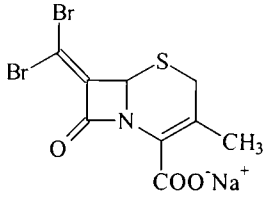

Sodium 7-(dibromomethylidene)-3-methyl-3-cephem-4-carboxylate (**3**)#

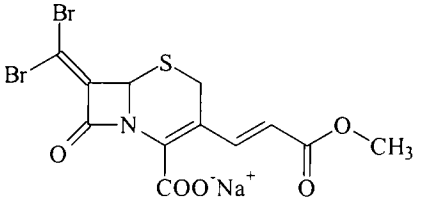

Sodium 3-(2'E-carbomethoxyethylene)-7-(dibromomethylidene)-3-cephem-4-carboxylate (**4**)#

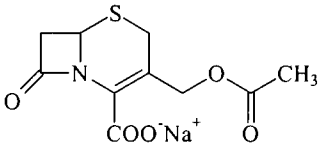

Sodium 3-acetoxymethyl-3-cephem-4-carboxylate (**5**)#

Figure 4. The structures of compounds tested as mechanism-based inhibitors of β-lactamases in this study (* Buynak et al., 1995; # Buynak, not published).

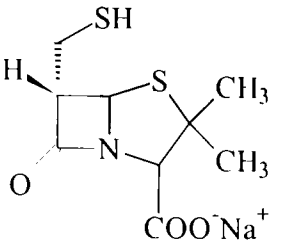

Sodium 6-(R-thiolmethyl) penicillate (**6**)

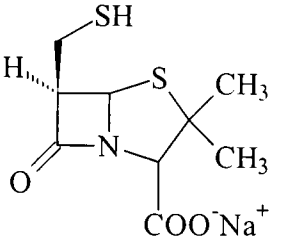

Sodium 6-(S-thiolmethyl) penicillate (**7**)

Figure 5. The structures of penicillin derivatives tested as reversible inhibitors of β-lactamases in this study (Buynak, not published).

Inductively Coupled Plasma-Atomic Emission Spectroscopy (ICP-AES)

Inductively Coupled Plasma-Atomic Emission Spectroscopy (ICP-AES) has utilized to study the metal ion stoichiometry in the metallo-β-lactamase. ICP-AES is a multi-element analysis technique that will dissociate a sample into its constituent atoms and ions and cause them to emit light at a characteristic wavelength by exciting them to a higher energy level. This is accomplished by the use of an inductively coupled plasma source, usually argon. A monochromator can separate specific wavelengths of interest,

and a detector is used to measures the intensity of the emitted light. This information can be used to calculate the concentration of that particular element in the sample.

Site-directed mutagenesis

A site-directed mutagenesis study has been undertaken in order to obtain clues about residues that may be potentially important in substrate binding and catalysis.

The QuikChange (Stratagene) site-directed mutagenesis kit can be used to make point mutations. This method is one of the PCR-based methods. This method is very simple and efficient. The QuikChange site-directed mutagenesis method is performed using *Pfu* DNA polymerase, which has a 6-fold higher fidelity in DNA synthesis than *Taq* DNA polymerase. The procedure utilized a supercoiled, double-stranded DNA vector with DNA extension during temperature cycling by means of *Pfu* DNA polymerase. On incorporation of the oligonucleotide primers, a mutated plasmid containing staggered nicks is generated. Following temperature cycling, the product is treated with *Dpn* I. The *Dpn* I endonuclease (target sequence: 5'-G^{m6}ATC-3') is specific for methylated and hemimethylated DNA and is used to digest the parental DNA template and to select for mutation-containing synthesized DNA. DNA isolated from almost all *E. coli* strains is *dam* methylated and therefore susceptible to *Dpn* I digestion. The nicked vector DNA incorporating the desired mutations is then transformed into *E. coli* TAP 56.

In 1990, the laboratories of G.F. Joyce (La Jolla), J.W. Szostak (Boston), and L. Gold (Boulder) independently developed a technique, which allows the simultaneous screening of a large number of nucleic acid molecules for different functionalities. This method is commonly known as '*in vitro* selection' (Ellington and Szostak, 1990), '*in vitro* evolution' (Joyce, 1989), or 'SELEX' (Systematic Evolution of Ligands by Exponential enrichment) (Tuerk and Gold, 1990). With the *in vitro* selection technique large random pools of nucleic acids can be screened for a particular functionality, such as the binding to small organic molecules (Famulk, 1994), large proteins (Tuerk and Gold, 1990; Chen and Gold, 1994) or the alteration or *de novo* generation of ribozyme catalysis (Robertson and Joyce, 1990; Bartel and Szonstale, 1993). Functional molecules ('aptamera' from 'aptus'; lat. = to fit) are selected from the mainly non-functional pool of RNA or DNA by column chromatography or other selection techniques that are suitable for the enrichment of any desired property.

The method is conceptually straightforward: a starting, degenerate oligonucleotide pool is generated using a standard DNA-oligonucleotide synthesizer. The instrument synthesizes an oligonucleotide with a completely random base-sequence, which is flanked by defined primer binding sites. The immense complexity of the generated pool justifies the assumption that it may contain a few molecules with the correct secondary and/or tertiary structures that bind tightly and specifically to a target enzyme and inhibit the enzymatic activity. These are selected, for example, by affinity chromatography or filter binding. Because a pool of such high complexity can be expected to contain only a very small fraction of functional molecules, several

purification steps are usually required. Therefore, the very rare "active" molecules are amplified by the polymerase chain reaction (PCR). In this way, iterative cycles of selection can be carried out. Successive selection and amplification cycles result in an exponential increase in the abundance of functional sequences, until they dominate the population. A generalized diagram of the SELEX protocol is shown in Figure 6.

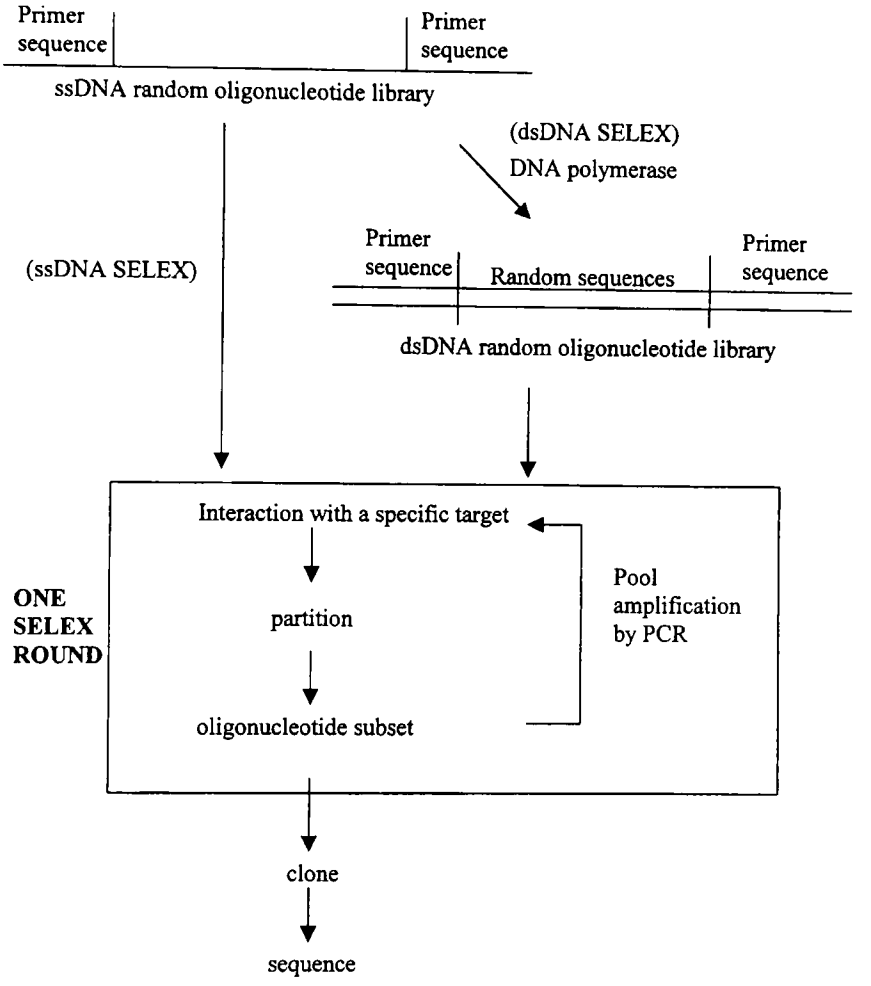

Figure 6. Diagrammatic representation of the SELEX procedure (modified from Gold et al., 1995). Primer sequences permit amplification. The steps in the SELEX process are further described in the Methods.

We synthesized a pool of $4^{30} = 1.2 \times 10^{18}$ 61-mer oligonucleotides that have 15 and 16 nucleotides to serve as polymerase chain reaction (PCR) primers at their 5' and 3' termini respectively, and also contain an internal 30-nucleotide completely random sequences. Single-stranded DNA has been selected that not only binds tightly and specifically to the *B. cereus* 5 B 6 metallo-β-lactamase, but also is able to inhibit this enzyme.

Prediction of secondary structure of aptamers

MFold program is an adaptation of the *mfold* package (version 2.3) by Zuker (1989) and Jaeger et al. (1989, 1990) that has been modified to work with the Wisconsin Package™ Their method uses the energy rules developed by Turner et al. (1988) to predict optimal secondary structures for a RNA molecule and the energy rules compiled and developed by SantaLucia et al. (1977) to predict optimal and suboptimal secondary structures for a single-stranded DNA molecule. This approach will provide a first-approximation prediction of secondary structure from sequence.

CHAPTER II

MATERIALS AND METHODS

Materials

The metallo-β-lactamase from *B. cereus* 5/B/6 was produced from *E. coli* MZ1 carrying the pRE2/*bla* plasmid and purified according to the procedures described previously (Shaw et al., 1991). The purity was ascertained by specific activity, native and SDS PAGE, and DE-MALDI-TOF. T4 DNA ligase was purchased from Promega. Restriction endonucleases NdeI and SacI were purchased from New England Biolabs, Inc. and were used according to the manufacturer's recommendations. DNA molecular weight markers (BstNI digested pBR322 and BstEII digested λ DNA) were purchased from New England Biolabs, Inc. The QuikChange Site-directed mutagenesis kit was purchased from Stratagene. DEAE-Sephacel, Sephadex G-25 (superfine), CM-Sepharose CL 6B and various columns were purchased from Pharmacia or Bio-Rad Laboratories. The Gene Clean II Kit was purchased from BIO101. Automated DNA sequencing was done on ABI PRISMTM 310 Genetic Analyzer from Applied Biosystems Inc. Synthetic oligonucleotides for SELEX were synthesized using Beckman Oligo 1000M oligonucleotide synthesizers. PCR reactions were carried out using a Perkin Elmer Certus Thermal Cycler. *Pfu* polymerase was purchased from Stratagene. The cell suspensions were sonicated using a Heat System Ultrasonics, Inc. model W-375 sonicator. PCI (Phenol: Chloroform: Isoamyl alcohol (25:24:1) and electrophoresis grade agarose were obtained from Amresco. Bovine carboxypeptidase A and hippuryl-L-phenylalanine were purchased from Sigma. PCR 20 bp low ladder, ethidium bromide, dimethysulfoxide

(DMSO), acrylamide, bisacrylamide, benzylpenicillin, cephalosporin C (potassium salt), ampicillin, cesium chloride, EDTA, ethanol, glucose, sodium hydroxide, potassium hydroxide, rubidium chloride, urea, MOPS, Tris, $ZnSO_4$ and various other inorganic salts and organic solvents of reagent grade or better were obtained from Sigma Chemical Co. Difco brand bacto-agar, casamino acids and yeast extract used to make all media and plates were obtained through Fisher Scientific.

Method for assay of the purified *B. cereus* 5/B/6 metallo-β-lactamase and *B. cereus* 568/H/9 β-lactamase I

For metallo-β-lactamase activity assays, the activities using cephalosporin C as substrate were determined as previously reported (Myers and Shaw, 1989). The activity assay procedure was essentially the same as the spectrophotometric method of Davies et al. (1974) in which the substrate absorbance at 260 nm is continuously monitored during hydrolysis. One unit of activity was defined as the amount of enzyme required to catalyze the hydrolysis of 1 μmol of substrate in one minute at 30 °C. All assays were carried out near V_{max} using 4.3 mM cephalosporin C (approximately 10 K_m) dissolved in 50 mM MOPS/1 mM $ZnSO_4$, pH = 7.0. The assays were performed in a 0.1 cm pathlength quartz cuvette and the total reaction volume was maintained at 250 μL.

For β-lactamase I activity assays, Davies et al. (1974) described the method of β-lactamase I activity assays. The method was modified. The enzyme sample was incubated with 20 mM EDTA (pH = 7.0) for 15 min. at room temperature prior to the assay. The enzymatic hydrolysis of 1.1 mM benzylpenicillin in 10 mM sodium citrate (pH = 7.0) and 1 mM EDTA was continuously monitored at 231 nm at 30 °C. One unit of β-

lactamase activity was defined as the amount of enzyme required to hydrolyze one μmole of substrate min. at 30 °C at pH = 7.0.

The protein concentrations were determined by the method of Lowry (Lowry et al., 1951) using bovine serum albumin as a standard. This method was used throughout for all protein determinations.

Method for preparing the sample for ICP-AES

The purified metallo-β-lactamase (0.5 mM) was adjusted to 25 mM in EDTA from a 250 mM EDTA (pH = 7.0) stock solution and incubated on ice until less than 0.1 % of the original metallo-β-lactamase activity remained. The metallo-β-lactamase required 7 hours incubation. The sample was loaded onto a 1.5 x 50 cm G-25 Sephadex superfine gel filtration column equilibrated with 25 mM MOPS (pH = 7.0). The buffer had previously been passed over a small Chelex 100 column to remove trace metal ions. The column was eluted at 15 mL/hour. 3 mL fractions were collected in acid/EDTA rinsed tubes and the absorbance of each fraction was determined at 280 nm and 220 nm (the absorbance maximum for the EDTA-Zn (II) complex). Those fractions displaying an absorbance at 280 nm were pooled and concentrated by ultrafiltration using a 23 mm Amicon Ym-10 membrane.

For the holoenzyme, the enzyme went through the same gel filtration column equilibrated with 25 mM MOPS (pH = 7.0) and 1 mM $ZnSO_4$.

Method for site-directed mutagenesis

β-lactamase was produced in the expression vector plasmid construct pRE2/*bla* and mutagenesis was carried out in this plasmid by a modification of the QuikChange method (Papworth et al., 1996).

Two complementary oligonucleotides containing the desired mutation were synthesized (Table 1). 5 μL of 10 x reaction buffer from QuikChange kit, 50 ng of pRE2/bla as a template, 125 ng of each designed oligonucleotide primers, 1 μL of dNTP mix and ddH_2O were added to a final volume of 50 μL. One μL of *pfu* turbo DNA polymerase (2.5 U/μL) from QuikChange kit was added. Each reaction was overlaid with 30 μL of mineral oil. In PCR reactions, each reaction was cycled using the cycling parameters outlined in Table 2. Following temperature cycling, PCR tubes were placed on ice for 2 minutes to cool the reaction to less than 37 °C. One μL of the *Dpn* I restriction enzyme (10 U/μl) was added directly to each amplification reaction below the mineral oil overlay and incubated at 37 °C for 1 hour to digest the parental supercoiled dsDNA. The PCR products were transformed (Hanahan, 1983) into *E. coli* strain MZ-1 to recover nicked mutant DNAs.

Table 1. Sequences of mutagenic oligonucleotide primers used to introduce amino acid changes within the structural gene of the *B. cereus* 5/B/6 β–lactamases gene. The changed codon that introduced the amino acid substitution is underlined in each primer.

Mutation	Mutagenic Primers
Lys171Ala	5'GCTGGAGGCTGTTTAGTTGCATCTGCGTCCTCCG3'
Lys171Ala RC*	5'CGAGGACGCAGATGCAACTAAACAGCCTCCAGC3'
Lys171Arg	5'GCTGGAGGCTGTTTAGTTAGATCTGCGTCCTCG3'
Lys171Arg RC*	5'CGAGGACGCAGATCTAACTAAACAGCCTCCAGC3'

*RC : Reverse complementary oligonucleotide

Table 2. Cycling parameters for the QuikChange site-directed mutagenesis method

Cycles	Temperature	Time
1	95 °C	30 seconds
16	95 °C	30 seconds
	55 °C	1 minute
	68 °C	9 minutes

Method for mechanism-based inactivation studies for metallo-β-lactamase

In studies involving the time-dependent inactivation of metallo-β-lactamases, preincubation mixtures contained possible inhibitors in 100 mM succinate and 1 mM $ZnSO_4$ buffer, pH = 6.0 at 30 °C. The metallo-β-lactamases were added to the preincubation mixtures. The final concentration of the enzyme was 60 μM. At the point indicated, 4.3 mM cephalosporin C was used as a substrate, and 50 mM succinate and 1 mM $ZnSO_4$ buffer (pH = 6.0) was used as an essay buffer. The enzyme activity remaining was determined (Myers and Shaw, 1989).

Method for data analysis of time-dependent inhibition

To analyze the time-dependent inhibition data, the following kinetic scheme for the formation of covalent bonding between inhibitor and enzyme was anticipated (Kitz and Wilson, 1962).

$$E + I \underset{k_{-1}}{\overset{k_1}{\rightleftharpoons}} E{:}I \xrightarrow{k_2} E' \qquad (1)$$

In which E = free enzyme, E:I = noncovalent enzyme-inhibitor complex, E' = covalently inhibited enzyme.

k_1 is bimolecular rate constant with units ($M^{-1}min^{-1}$); k_{-1} and k_2 have units (min^{-1}).

$$[E]_T = [E] + [E{:}I] + [E'] \qquad (2)$$

$$\text{Inhibition rate} = \frac{d[E']}{dt} = \frac{-d([E] + [E{:}I])}{dt} = k_2[E{:}I] \qquad (3)$$

$$\text{Rate E:I formation} = \frac{d[E:I]}{dt} = k_2[E][I] \cong k_1([E]_T - [E:I])[I] \quad (4)$$

$$\text{Since } [E] = ([E]_T - [E:I] \quad [E]) \cong ([E]_T - [E:I]) \text{ (at early times)} \quad (5)$$

$$\text{Rate E:I decomposition} = \frac{-d[E:I]}{dt} = k_{-1}[E:I] + k_2[E:I] \quad (6)$$

$$\text{At steady state,} \quad \frac{d[E:I]}{dt} = 0 = \frac{-d[E:I]}{dt} \quad (7)$$

$$k_1([E]_T - [E:I])[I] = k_{-1}[E:I] + k_2[E:I] \quad (8)$$

$$k_1[E]_T[I] - k_1[E:I][I] = (k_{-1} + k_2)[E:I] \quad (9)$$

$$k_1[E]_T[I] = (k_1[I] + k_{-1} + k_2)[E:I] \quad (10)$$

$$[E:I] = \frac{k_1[E]_T[I]}{k_1[I] + k_{-1} + k_2} = \frac{[E]_T[I]}{[I] + (k_{-1} + k_2)/k_1} \quad (11)$$

$$\text{Let } K_{inact} = \frac{k_{-1} + k_2}{k_1}, \quad (12)$$

Note:

When $k_2 << k_{-1}$, $K_{inact} \cong \frac{k_{-1}}{k_1}$

i.e. $K_{inact} \cong \frac{k_{-1}}{k_1} = \frac{[E][I]}{[E:I]} = K_{diss}$ for E:I

$$\text{Therefore, } [E:I] = \frac{[E]_T[I]}{[I] + K_{inact}} \quad (13)$$

From (3),

$$\frac{-d([E] + [E:I])}{dt} = \frac{k_2[E]_T[I]}{[I] + K_{inact}} \quad (14)$$

$$\frac{-d([E] + [E:I])}{[E]_T} = \frac{k_2[I]dt}{[I] + K_{inact}} \cong \frac{-d([E] + [E:I])}{([E] + [E:I])} \quad (15)$$

Integrate both sides of this equation,

$$\left[\ln([E] + [E{:}I])\right]_{\text{at } t = t,\ [E]_I = [E] + [E{:}I]}^{\text{at } t = 0,\ [E]_I = [E] + [E{:}I]} = \ln \frac{([E] + [E{:}I])}{[E]_I} \qquad (16)$$

$$\left[\frac{k_2[I]t}{[I] + K_{inact}}\right]_{t = 0}^{t = t} = \frac{k_2[I]t}{[I] + K_{inact}} - 0, \qquad (17)$$

$$\text{i.e.,} \quad \ln \frac{([E] + [E{:}I])}{[E]_I} = \frac{k_2[I]t}{[I] + K_{inact}} \qquad (18)$$

Therefore, a plot of ln of this function versus t gives a straight line with slope.

$$\text{Slope} = \frac{k_2[I]}{[I] + K_{inact}} \qquad (19)$$

$$\text{Let} \quad \frac{k_2[I]}{[I] + K_{inact}} = k_{obs} \text{ (observed inactivation rate constant)} \qquad (20)$$

k_1 has units: $M^{-1}min^{-1}$.

k_{-1} has units: min^{-1}.

k_2 has units: min^{-1}.

$K_{inact} = \frac{k_{-1} + k_2}{k_1}$ has units: M.

Therefore, k_{obs} has units: $\frac{M\ min^{-1}}{M} = min^{-1}$.

Taking the reciprocal of equation (20),

$$\frac{1}{k_{obs}} = \frac{[I] + K_{inact}}{k_2[I]} = \frac{1}{k_2} + \frac{K_{inact}}{k_2[I]} \qquad (21)$$

Therefore, a plot of $1/k_{obs}$ versus $1/[I]$ gives a straight line with a slope K_{inact}/k_2 and an intercept of $1/k_2$.

Therefore, K_{inact} and k_2 can both be obtained; k_2 is inactivation rate constant (k_{inact}).

Irreversible inhibition, progressive with time in accordance with Equation 18, was obtained with compounds 1 and 2 (Figures 30 and 32). The values of k_{obs} obtained were then plotted according to Equation 21 (Figures 31 and 33). A plot of the reciprocal of the rate ($1/k_{obs}$) as a function of the reciprocal of the inhibitor concentration ($1/[I]$) fits a straight line. Extrapolating the line to its intercept on the ordinate gives $1/k_{inact}$. Extrapolating to the intercept on the abscissa gives $-1/K_{inact}$.

Method for DE-MALDI-TOF MS

The DE-MALDI-TOF MS experiments were performed on samples of the enzyme inhibited by the mechanism-based inactivators in an attempt to determine what fragment of the inhibitors was covalently added to the enzyme. To prepare protein samples for mass spectrometric analysis, reaction of possible inhibitors with 60 μM enzyme in 100 mM succinate and 1 mM $ZnSO_4$ buffer (pH = 6.0) at 30 °C were carried out until the activity decreased to a constant, low value. The reaction mixtures were then passed through Sephadex G-25 superfine (Sigma) columns equilibrated with 50mM MOPS and 1mM $ZnSO_4$ buffer (pH = 7.0) to remove the excess inhibitors. Protein solutions that were free of excess inhibitor were concentrated with ultrafiltration using a 23 mm Amicon Ym-10 membrane. MALDI mass spectra were acquired using a PerSeptive Biosystems, Inc. Voyager DE time-of-flight mass spectrometer operating in the linear mode. The instrument has a 1.2-meter flight tube and an adjustable accelerating voltage up to 25 kV in the delayed extraction mode. Radiation from a nitrogen laser (337

nm, 3-ns pulse width) was used to desorb ions from the target. Each spectrum was produced by accumulating data collected from 128 to 256 laser shots. The matrix solution for MALDI was saturated sinapinic acid in a solvent system of acetonitrile/water. Ordinarily, 0.3 % (v v) Trifluoroacetic acid (TFA) is added in the solvent system (Beavis and Chait, 1989), but TFA was absent in this solvent system because in the presence of 0.3 % (v/v) TFA, the amount of the mass-shifted inhibitor-enzyme adduct was much smaller than in the absence of TFA. Internal calibration was performed with bovine trypsinogen ($[M+H]^+$; 23994.0) and human carbonic anhydrase II ($[M+H]^+$; 29115.8).

Method for reversible inhibition studies for metallo-β-lactamase

To test reversible inhibitors, the preincubation mixtures contained possible inhibitors in 50 mM MOPS buffer, pH = 7.0 at 30 °C for 15 minutes. The metallo-β-lactamases were incubated with the same final concentration of the possible inhibitors as the preincubation mixture in 50 mM MOPS buffer (pH = 7.0) for 15 minutes. The enzyme activity remaining was determined (Myers and Shaw, 1989).

Method for SELEX

Oligonucleotides

Oligonucleotides were produced using a Beckman Instruments, Inc. OLIGO 1000M DNA synthesizer. One 61 base single-stranded DNA was synthesized containing 30 bases of randomized sequence (30N) between two primer regions encompassing SacI and NdeI recognition sites:

61-mer

5'CGCGAGCTCCGCGCG 30N CGCGCGCATATGGCGC3'

SacI NdeI

This template DNA was amplified by PCR with the corresponding primers:

5' Primer (16-mer) possessing NdeI site:

5'GCGCCATATGCGCGCG3'

3' Primer (15-mer) possessing SacI site:

5'CGCGAGCTCCGCGCG3'

Gel shift assay

The electrophoretic mobility shift assay used 6 % (w/v) polyacrylamide gels (29:1 mono:bis) in 20 mM Tris-acetate (TA) buffer (pH = 7.0), polymerized with 0.07 % (w/v) ammonium persulfate and 0.028 % (v/v) TEMED. The stock enzyme in 150 mM ammonium sulfate, 10 mM sodium citrate (pH = 7.0), 1 mM $ZnSO_4$, and 30 % (v/v) glycerol, was heated for 30 min at 60 °C to denature any possible other proteins. This enzyme is stable at 60 °C. The enzyme was centrifuged and the supernatant was collected. The enzyme was diluted with dilution buffer (20 mM TA and 1 mM $ZnSO_4$, pH = 7.0). The synthesized library of 61-mer ssDNA described above was used for SELEX selection. The ssDNA was incubated with the enzyme at 30 °C for 15 min in TA buffer with an appropriate concentration of NaCl. The total reaction volume was 20 μL. The amounts of the ssDNA, enzyme and NaCl in the incubated buffer were adjusted (Table 3). After 15 min, 40 % (v/v) glycerol was added to samples to give 10 % (v/v) glycerol as a final concentration. Samples were run in the 6 % (w/v) polyacrylamide gel at 200 V for 25 to 30 minutes. From the seventeenth round to the twenty-first round, the time period of the incubation of ssDNA and enzyme was 2.5 hours.

Table 3. Salt concentration conditions of SELEX.

Round	ssDNA	Enzyme	NaCl
1	3 μM	20μM	10 mM
2	3 μM	20 μM	10 mM
3	1.5 μM	20 μM	10 mM
4	1.5 μM	10 μM	10 mM
5	1.5 μM	10 μM	10 mM
6	1.5 μM	5 μM	10 mM
7	1.5 μM	5 μM	10 mM
8	1.5 μM	2 μM	10 mM
9	1.5 μM	1.5 μM	10 mM
10	1.5 μM	1.5 μM	10 mM
11	1.5 μM	1.5 μM	10 mM
12	1.5 μM	1.5 μM	10 mM
13	1.5 μM	1.5 μM	15 mM
14	1.5 μM	1.5 μM	15 mM
15	1.5 μM	1.5 μM	15 mM
16	1.5 μM	1.5 μM	20 mM
17	1.5 μM	1.5 μM	50 mM
18	1.5 μM	1.5 μM	50 mM
19	1.5 μM	1.5 μM	50 mM
20	1.5 μM	1.5 μM	50 mM
21	1.5 μM	1.5 μM	50 mM

The enzyme:ssDNA complexes were separated from free DNAs on the 6 % (w/v) polyacrylamide gels described above. The resulting gel was soaked in the incubation buffer with the ethidium bromide for 10 minutes and was destained in ddH_2O. The enzyme:ssDNA complexes were visualized by UV illumination using TM-36 Chromato-UVE transilluminater from UVP Inc. and were excised. The band containing ssDNA was crushed by a disposable pipette tip in the PCR tube and the ssDNA was amplified.

Generation of single-stranded DNA by asymmetric PCR

The ssDNA was subjected to amplification with 2.5 units of the *pfu* polymerase. The reaction mixture, including 200 ng of 5' primer (16mer) and 100 ng of 3'primer (15mer), was subjected to 30 cycles of 45 seconds at 94 °C, 45 seconds at 55 °C, and 6 seconds at 72 °C. This was followed by ten minutes at 72 °C to allow all annealed primers to finish extending. The optimal 10x buffer for PCR was 100 mM Tris-HCl (pH = 8.8), 35 mM $MgCl_2$ and 250 mM KCl. The final concentration of dNTP was 2 mM. The total reaction volume was 100 μL.

The PCR products were purified from 12 % (w/v) polyacrylamide gel (29:1 mono:bis). The ssDNA was extracted by the modified crush and soak method (Maxam and Gilbert, 1977) with the following modifications: After cutting out the segment of the gel using a sharp scalpel or razor blade, the slice was transferred to a microcentrifuge tube. The slice was crushed by a disposable pipette tip. The slice was weighed to determine its volume and 1-2 volumes of elution buffer (0.5 M ammonium acetate, 1 mM EDTA (pH = 8.0), and 0.1 % (w/v) SDS was added. The tube was incubated at 45 °C on a rotary platform for 2.5-3 hours. After centrifuging the tube at 12,000 g for 1 minute, the

supernatant was transferred to a fresh microcentrifuge tube. To avoid any fragments of polyacrylamide, a plastic column containing glass wool was used to centrifuge the supernatant. A one-half volume aliquot of elution buffer was added to the remaining pellet to be vortexed and recentrifuged. The supernatant and gel fragments were poured into the plastic column and spun for 15 seconds. 2-2.5 volumes of 100 % ethanol was added to the sample from this column and placed at - 20 °C for 1 hour and at –80 °C for 10–15 minutes. The tube was spun for 10-15 minutes. This ethanol precipitation step will help the removal of ethidium bromide to provide the right conformation of ssDNA. The supernatant was discarded. The pellet was washed with 70 % ethanol and was dried.

To confirm that the PCR product was ssDNA containing a 30 base insertion, the initial pool of ssDNA containing 30 random bases was compared with the PCR product on 12 % (w/v) polyacrylamide (29:1 mono:bis) and 8 M urea gel in TBE buffer (Sambrook et al., 1989).

Cloning and sequencing

The plasmid pRE2/bla was digested with restriction endonucleases NdeI and SacI (Reddy, Peterkofsky and McKenney, 1989). All these double-digestion mixtures were electrophoretically separated on 1.0 % (w/v) agarose gel in TBE buffer at 60 V in the absence of ethidium bromide for 3 hours. The linearized pRE2 vector and the metallo-β-lactamase gene fragment were then located by staining the gels in 5 μg/mL ethidium bromide solution and visualized under UV. The restricted linear pRE2 and the metallo-β-lactamase gene fragment were then excised from the gels, and the DNAs were extracted by the Gene Clean Kit (purchased from BIO 101).

The ssDNA was amplified by PCR to make dsDNA. After ethanol precipitation, the fixed regions was digested with restriction endonuclease NdeI and SacI. The digested fragment was loaded on 12% (w/v) polyacrylamide gels (29:1 mono:bis) and was then purified by the modified crush and soak method.

Ligation of the fragments with the linear pRE2 vector was accomplished with T4 DNA ligase (purchased from Promega Co.) at 4 °C overnight or at room temperature for 3 hours. For each ligation, 100 ng of linearized pRE vector, 1.11 ng of fragment and 3 units of T4 DNA ligase were mixed together in ligation buffer in a total volume of 10 μL. After incubation, the mixture was used to transform *E. coli* strain TAP 56 competent cell prepared by the Hanahan method (Hanahan, 1983). Transformed cells were incubated at 30 °C for 2 5 hours and were then put into LB medium that contained 1.0 % (w/v) casamino acids, 0.5 % (w/v) yeast extract, 0.5 % (w/v) sodium chloride (adjusted to pH = 7.0 with NaOH) and 50 μg/mL ampicillin. The culture was incubated at 30 °C overnight. The subcloned plasmid DNA was prepared by the boiling miniprep method (Sambrook et al., 1989). The DNA extracted by boiling miniprep was sequenced by an ABI PRISMTM 310 Genetic Analyzer. After finding the sequence, the 30-mer insertion was synthesized by on a Beckman Instruments Inc. OLIGO 1000M DNA synthesizer. The synthesized 30-mer was purified by 12 % (w/v) polyacrylamide gel for all further experiments.

Method for assay of bovine carboxypeptidase A

The assay of bovine carboxypeptidase A is based on the method of Folk and Schirmer (1963). The rate of hydrolysis of hippuryl-L-phenylalanine is determined by monitoring the increase in absorbance at 254 nm (25 °C, pH = 7.5). The enzyme was

dissolved in 10 % lithium chloride to a concentration of 1 – 3 units per mL. Hippuryl-L-phenylalanine (0.001 M) was dissolved in 0.05 M TrisHCl, pH = 7.5 with 0.5 M sodium chloride. In a 1 cm of cuvette, 1.0 mL of substrate was added and incubated in the spectrophotometer at 25 °C for 3 – 4 minutes to reach temperature equilibration and establish blank rate. Fifty µL of diluted enzyme was added to record increase in A_{254}.

The enzyme was preincubated with/without the inhibitor in the buffer for 15 min. at 25 °C.

CHAPTER III

RESULTS

Inductively coupled plasma-atomic emission spectroscopy (ICP-AES)

Metal stoichiometries have been determined for the Zn^{2+}-β–lactamases by the ICP-AES. After the appropriate blanks were subtracted, the stoichiometries were calculated on the basis of the protein concentration of each sample. These results are summarized in Table 4. From the results, it is evident that holoenzyme has at least two Zn^{2+} ions and apoenzyme has no Zn^{2+}ion.

Table 4. ICP-AES determination of metal bound by metallo-β–lactamases

Sample	moles of zinc/ mole of protein
Holoenzyme	3.0 ± 0.5 (± SEM, N =2)
Apoenzyme	0.044

Site-directed mutagenesis

The three-dimensional structure of the enzyme reveals that the residue Lys171 may be involved in stabilization of the Michaelis complex and/or the tetrahedral intermediate of the reaction (Fabiane et al., 1998). We mutagenized this position to Ala and Arg.

Table 5 shows the specific activities of the mutant enzymes made by the QuikChange mutagenesis kit. The activity of Lys171Ala had only 8.0 % and the activity of Lys171Arg was 32.0 % of that of control wild type enzyme.

Table 5 Specific activities of crude sonicates from *E. coli* strain MZ-1 expressing mutant 5 B 6 β-lactamases.

Metallo-β-lactamases	Percent Wild Type Specific Activity*
Wild Type	100 %
Lys171Ala	8.0 % ± 1.0 %
Lys171Arg	32.0 % ± 2.1 %

* The data shown represent the mean ±SEM, N=3. The substrate used in these experiments was cephalosporin C.

Mechanism-based inhibition studies

Compounds **1**, **2**, **3**, **4** and **5** were tested as mechanism-based inhibitor using cephalosporin C as substrate (see Methods).

It was observed that at pH = 7.0 initially the activity of the enzyme incubated with sodium 7-(dibromoethylene) cephalosporanate (**1**) dropped rapidly before the enzyme recovered much of its activity and then started losing activity in a time-dependent manner (Figure 7). On the other hand, at pH = 6.0, (Figure 8), there is a monotonic sharp decrease followed by an approach to equilibrium, resulting in simpler inhibition kinetics. At a concentration of 3 mM with sodium 7-(dibromoethylene) cephalosporanate (**1**), 50 % inactivation was obtained in 12 minutes. Also, at a concentration of 6 mM with the inhibitor, 50 % inactivation was obtained in less than 6 minutes.

Sodium 3-acetoxymethyl-7-(E-bromomethylidene)-3-cephem-4-carboxylate (**2**) (Figure 9) displayed a sharp decrease in activity at pH = 6.0. At the concentration of 3 mM, sodium 3-acetoxymethyl-7-(E-bromomethylidene)-3-cephem-4-carboxylate (**2**), 50 % inactivation was obtained in 10 minutes.

In the case of sodium 7-(dibromomethylidene)-3-methyl-3-cephem-4-carboxyate (**3**) (Figure 10), there was a negligible effect on the activity by 3 mM compound **3** on 60 μM enzyme. Likewise, sodium 3-(2'E-carbomethoxyethylene)-7-(dibromomethylidene)-3-cephem-4-carboxyate (**4**) (Figure 11) displayed the same result at the same ratio of inhibition to enzyme. However, sodium 3-acetoxymethyl-3-cephem-4-carboxylate (**5**) (Figure 12) showed a slight inhibition at a ratio of inhibitor to enzyme of 200:1.

As control experiments, penicillin G and cephalosporin C were tested as a function of time to determine if they were irreversible inhibitors. Penicillin G (Figure 13) did not show a significant inhibitory effect on the wild type β-lactamases at a compound to enzyme molar ratio of 100:1 (6 mM: 60 μM). Cephalosporin C (Figure 14) showed product inhibition. At the concentration of 6 mM cephalosporin C, 50 % inactivation was obtained in 35 minutes. Also, at the concentration of 16.4 mM cephalosporin C, 50 % inactivation was obtained in 25 minutes.

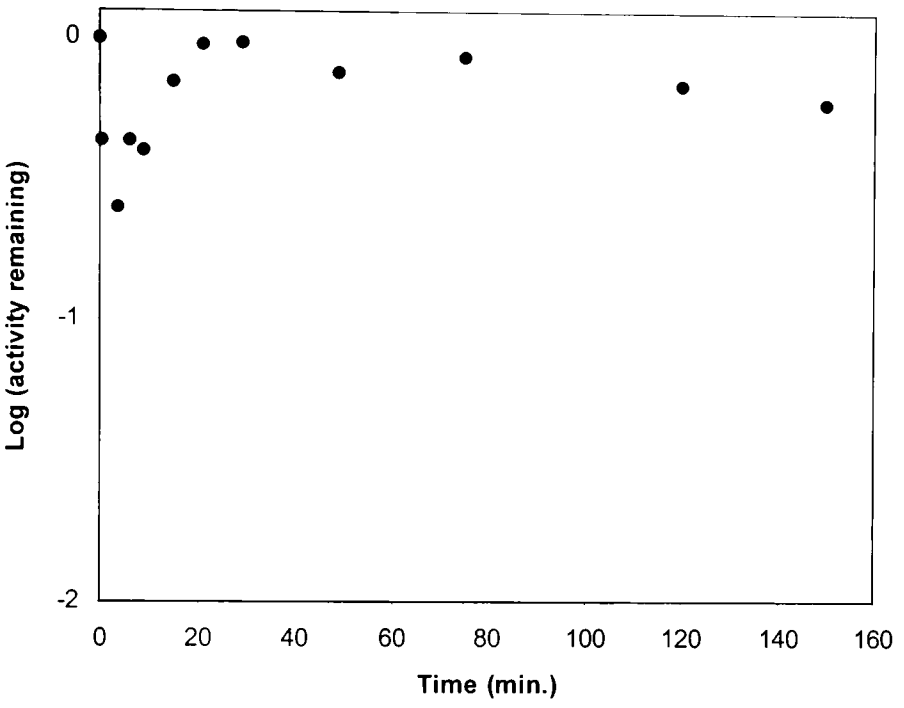

Figure 7. Time-dependent inhibition of *B. cereus* 5/B/6 metallo-β-lactamase by sodium 7-(dibromomethylene)-cephalosporanate (**1**) at pH = 7.0. Inhibitor to enzyme ratio was at 50:1; substrate was cephalosporin C. Preincubation buffer was 100 mM MOPS/ 1 mM $ZnSO_4$, pH = 7.0, and the assay buffer was 50 mM MOPS/ 1 mM $ZnSO_4$, pH = 7.0.

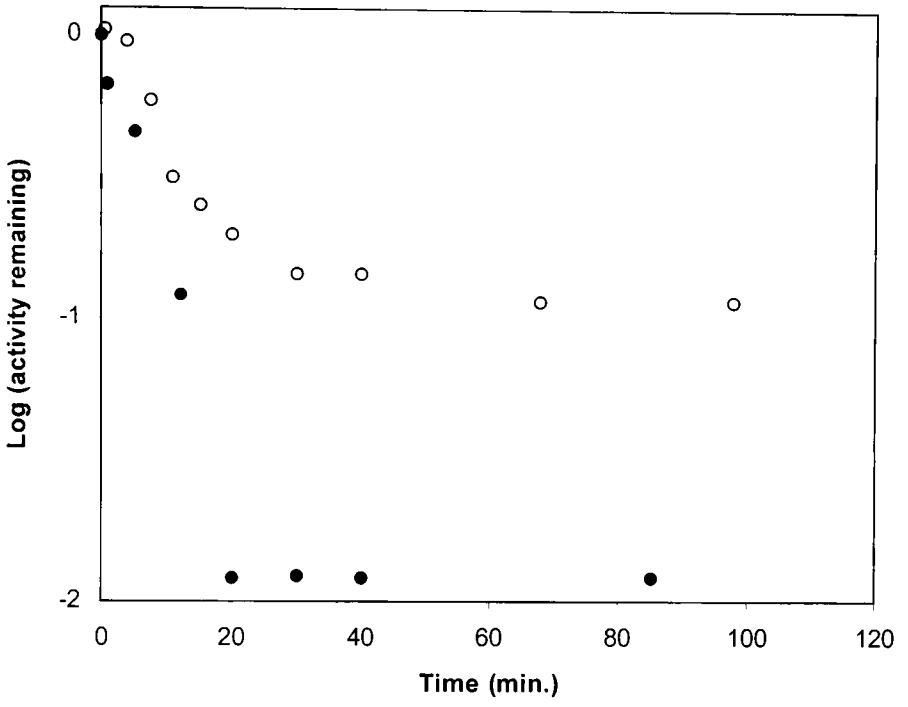

Figure 8. Time- and concentration dependence of inactivation of metallo-β-lactamase activity by 7-(dibromomethylene)-cephalosporanate (1) at pH = 6.0. The concentrations of the inhibitor were (○) 3 mM and (●) 6 mM; the concentration of the enzyme was 60 μM. Preincubation buffer was 100 mM succinate/ 1 mM $ZnSO_4$; the assay buffer was 50 mM succinate/ 1 mM $ZnSO_4$ at pH = 6.0.

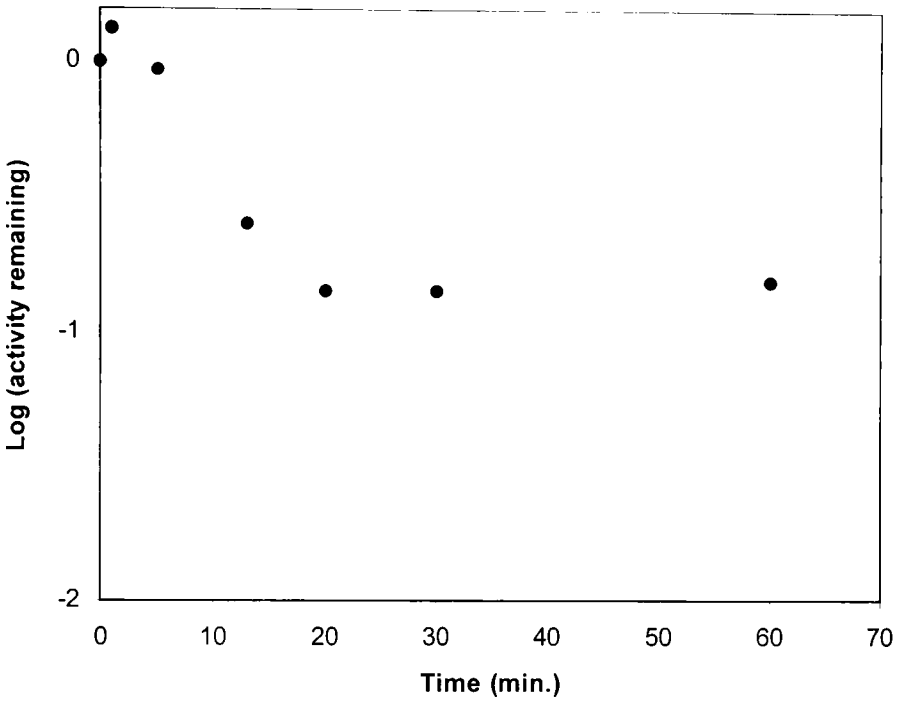

Figure 9. Time-dependent inactivation of metallo-β-lactamase activity by sodium 3-acetoxymethyl-7-(E-bromomethylidene)-3-cephem-4-carboxylate (**2**). The concentration of the inhibitor was (●) 3 mM; the concentration of the enzyme was 60 μM. Preincubation buffer was 100 mM succinate/ 1 mM $ZnSO_4$; the assay buffer was 50 mM succinate/ 1 mM $ZnSO_4$ at pH = 6.0.

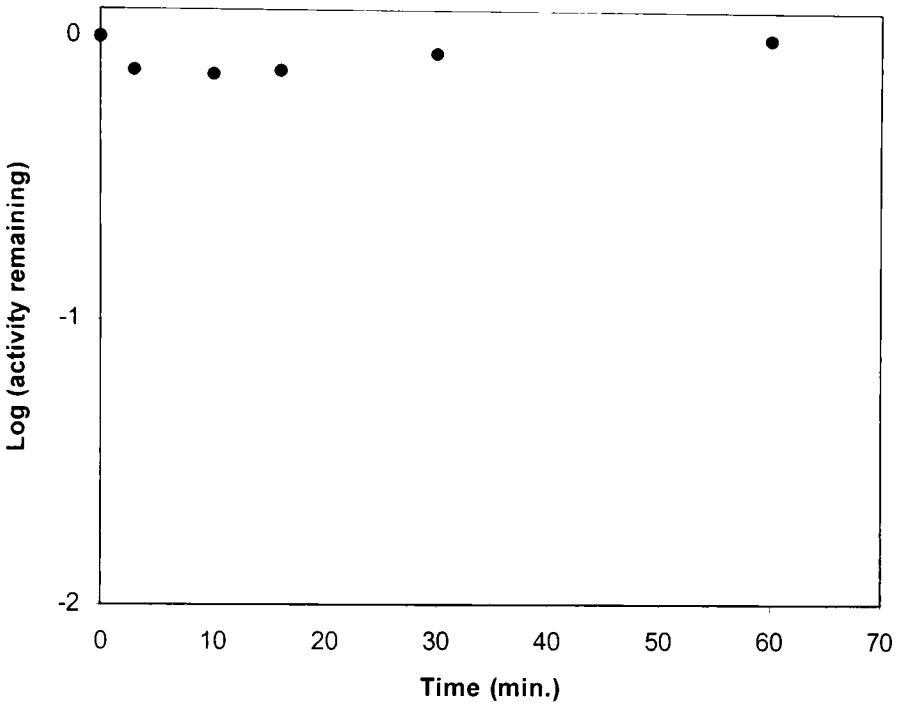

Figure 10. Time-dependent inactivation of metallo-β-lactamase activity by sodium 7-(dibromomethylidene)-3-methyl-3-cephem-4-carboxyate (**3**). The concentration of the inhibitor was (●) 3 mM; the concentration of the enzyme was 60 μM. Preincubation buffer was 100 mM succinate/ 1 mM $ZnSO_4$; the assay buffer was 50 mM succinate/ 1 mM $ZnSO_4$ at pH = 6.0.

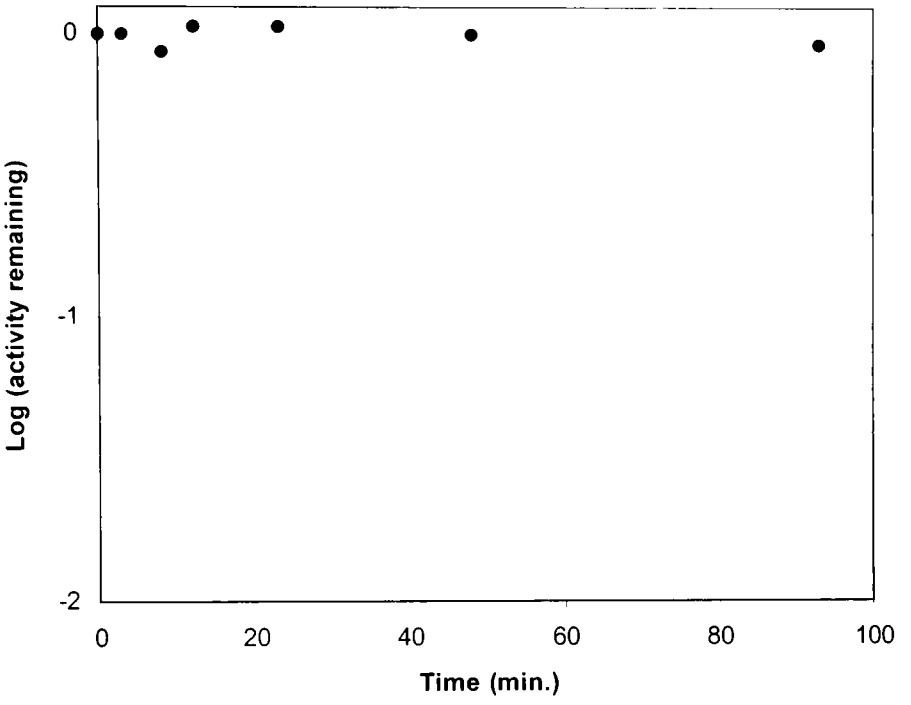

Figure 11. Time-dependent inactivation of metallo-β-lactamase activity by sodium 3-(2'E-carbomethoxyethylene)-7-(dibromomethylidene)-3-cephem-4-carboxyate (**4**). The concentration of the inhibitor was (●) 3 mM; the concentration of the enzyme was 60 μM. Preincubation buffer was 100 mM succinate/ 1 mM $ZnSO_4$; the assay buffer was 50 mM succinate/ 1 mM $ZnSO_4$ at pH = 6.0.

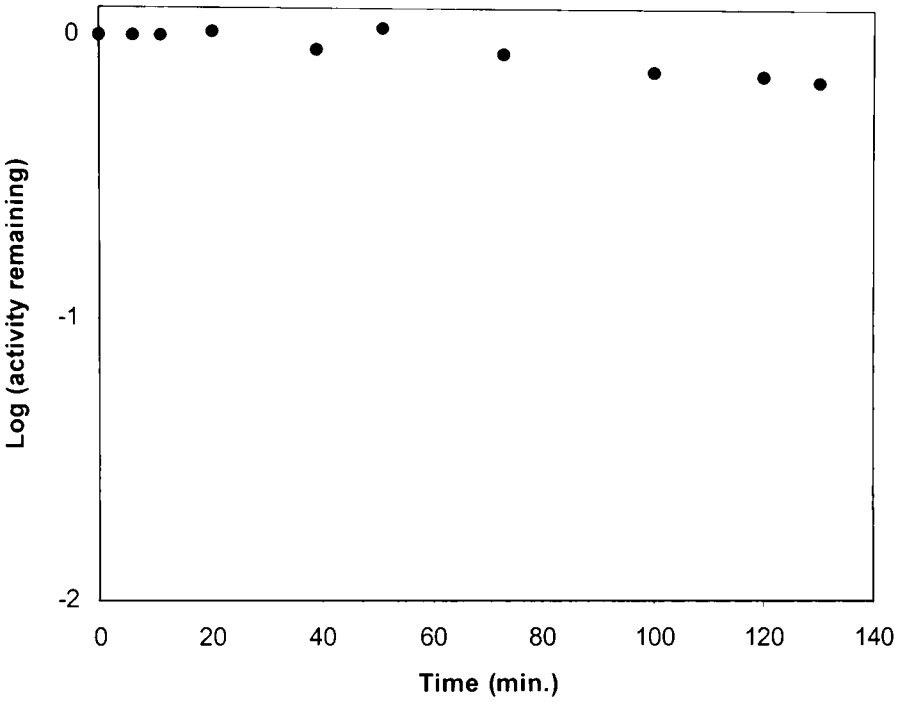

Figure 12. Time-dependent inactivation of metallo-β-lactamase activity by sodium 3-acetoxymethyl-3-cephem-4-carboxylate (**5**). The concentrations of the inhibitor were (●) 12 mM; the concentration of the enzyme was 60 μM. Preincubation buffer was 100 mM succinate/ 1 mM $ZnSO_4$; the assay buffer was 50 mM succinate/ 1 mM $ZnSO_4$ at pH = 6.0.

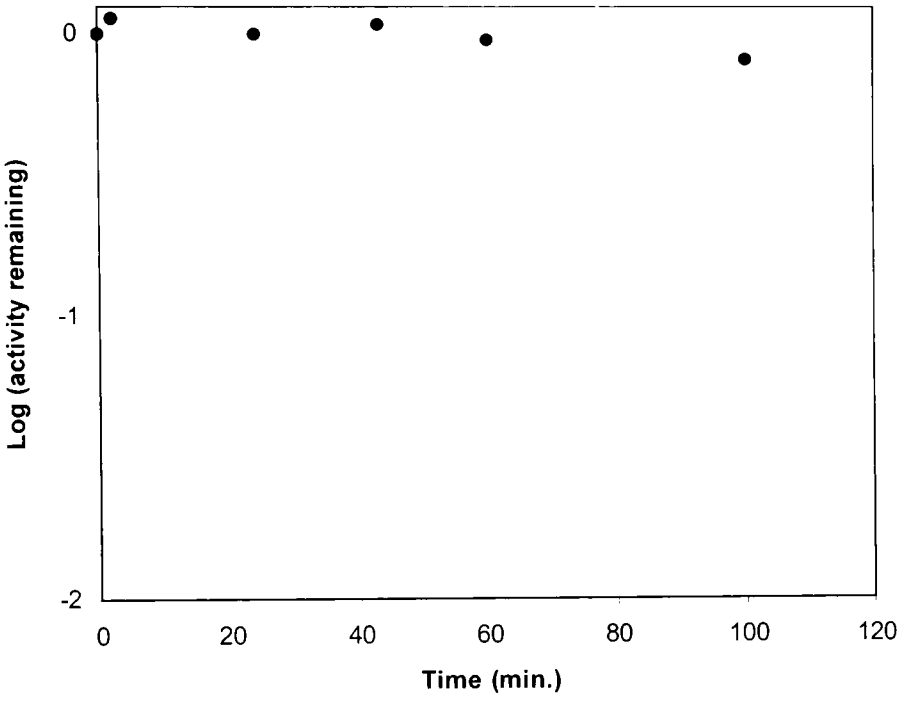

Figure 13. Time-dependent inactivation of metallo-β-lactamase activity by penicillin G. The concentration of the inhibitor was (●) 6 mM; the concentration of the enzyme was 60 μM. Preincubation buffer was 100 mM succinate/ 1 mM $ZnSO_4$; the assay buffer was 50 mM succinate/ 1 mM $ZnSO_4$ at pH = 6.0.

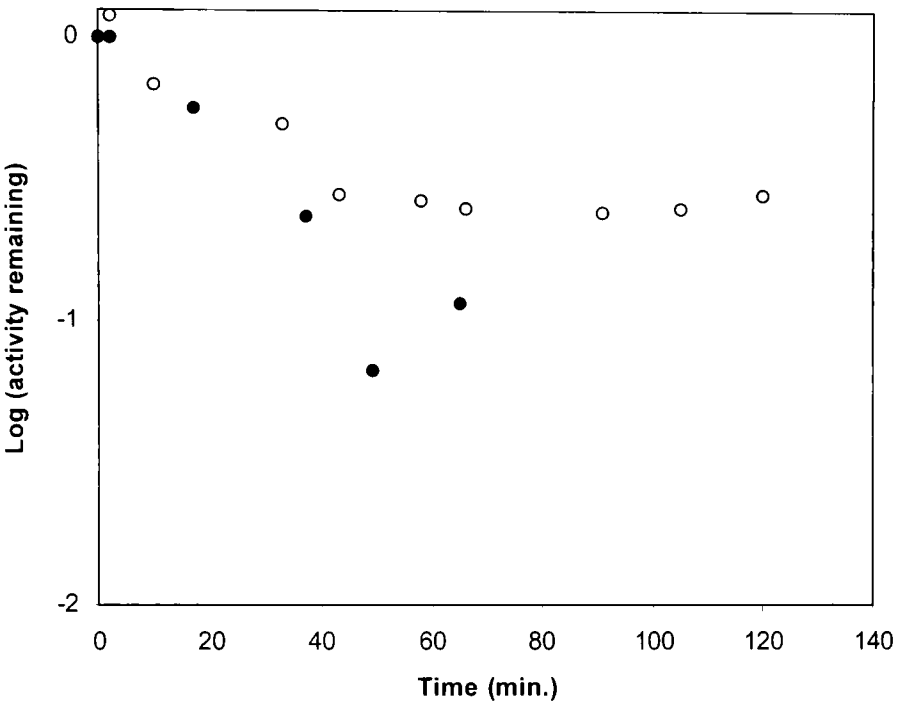

Figure 14. Time- and concentration dependence of inactivation of metallo-β-lactamase activity by cephalosporin C. The concentrations of the inhibitor were (○) 6 mM and (●) 16.4 mM; the concentration of the enzyme was 60 μM. Preincubation buffer was 100 mM succinate/ 1 mM $ZnSO_4$; the assay buffer was 50 mM succinate/ 1 mM $ZnSO_4$ at pH = 6.0.

DE-MALDI-TOF studies

The masses of the uninhibited and inhibited enzymes from reaction with the putative inhibitor compounds 1, 2, 3, 4, and 5, were determined using DE-MALDI TOF mass spectrometry. The molar mass of the uninhibited enzyme (25,168 Da) was identical to that predicted from the protein sequence for the *B. cereus* 5/B/6 enzyme. Figure 15 shows the DE-MALDI TOF mass spectra of the standard proteins and of uninhibited enzyme. The bovine trypsinogen and human carbonic anhydrase II internal standard peaks are shown at 23994.0, 29115.8 Da as $[M + H]^+$. The control enzyme exhibits a peak as $[M + H]^+$ at 25169.0 ± 2.9 Da that is equivalent to the mass for the unprotonated enzyme (25,168 Da). On the shoulder of peaks of the proteins, there were two small peaks present. The peak of $[M - 131]^+$ corresponds to a loss of the N-terminal methionine group (Wolf et al., 1998); the peak of $[M + 206]^+$ corresponds to the addition of sinapinic acid accompanied with dehydration (Beavis and Chait, 1989).

In Figure 16, the enzyme inhibited with soduim 7-(dibromomethylene) cephalosporanate (**1**) in 50 mM succinate buffer (pH = 6.0) and 1 mM $ZnSO_4$ displayed a mass of 25549.4 ± 6.4 Da $[M + H]^+$. The inhibitor has a mass of 427.1 Da. The difference in mass between inhibited enzyme peak and uninhibited enzyme peak gives a value of 380.2 Da. This suggests that a sizeable portion of the inhibitor is bound to the enzyme.

When the enzyme was inhibited with this compound and washed with ddH_2O by ultrafiltration using a 23 mm Amicon Ym-10 membrane, the mass obtained was consistently 25400.9 ± 5.9 Da $[M + H]^+$ (Figure 17). When 0.3 % TFA was added to the matrix, the uninhibited enzyme peak appeared (Figure 18) presumably resulting from the more acidic condition of the sample.

The mass of enzyme inhibited with sodium 3-acetoxymethyl-7-(E-bromomethylidene)-3-cephem-4-carboxylate (**2**) is 25471.8 ± 7.0 $[M + H]^+$ (Figure 19). This inhibition was also acid labile. Although sodium 7-(dibromomethylidene)-3-methyl-3-cephem-4-carboxyate (**3**) and sodium 3-(2'E-carbomethoxyethylene)-7-(dibromomethylidene)-3-cephem-4-carboxyate (**4**) did not indicate time-dependent inhibition, the DE-MALDI-TOF mass spectra display mass shifts. The enzyme preincubated with **3** has a mass $[M + H]^+$ of 25393.3 ± 8.6 (Figure 20). The enzyme preincubated with **4** displayed a mass $[M + H]^+$ of 25452.3 ± 3.7 (Figure 21). The mass $[M + H]^+$ of the enzyme preincubated with sodium 3-acetoxymethyl-3-cephem-4-carboxylate (**5**) was 25902.6 ± 10.0 (Figure 22). Unlike compound **1**, **2**, **3** and **4**, more than one mole of the compound **5** was likely bound per mole of the enzyme.

As control experiments, penicillin G and cephalosporin C were tested. The mass of the enzyme preincubated with penicillin G shows the uninhibited enzyme peak, which is at 25169.8 ± 1.5 Da as $[M + H]^+$ (Figure 23). Cephalosporin C also showed essentially the mass of uninhibited enzyme (25166.4 ± 0.5 Da as $[M + H]^+$) (Figure 24). This infers that there were no covalent bonds between the enzyme and these substrates.

The results of the DE-MALDI-TOF MS are summarized in Table 6.

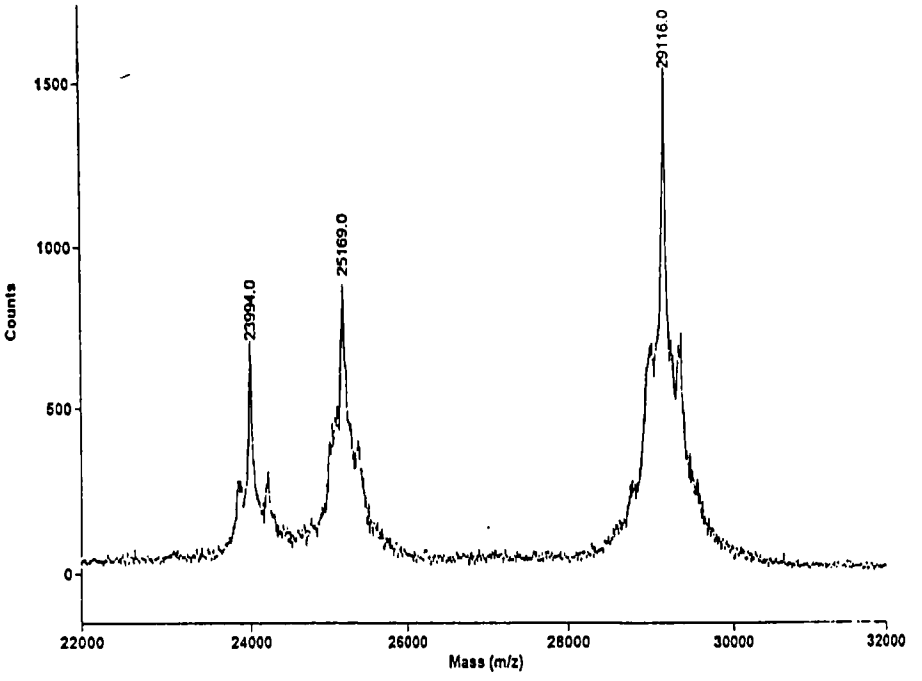

Figure 15. MALDI mass spectrum of uninhibited enzyme and internal standard proteins. The bovine trypsinogen (23994.0 Da as $[M + H]^+$) and human carbonic anhydrase II (29115.8 Da as $[M + H]^+$) were used as internal standard proteins.

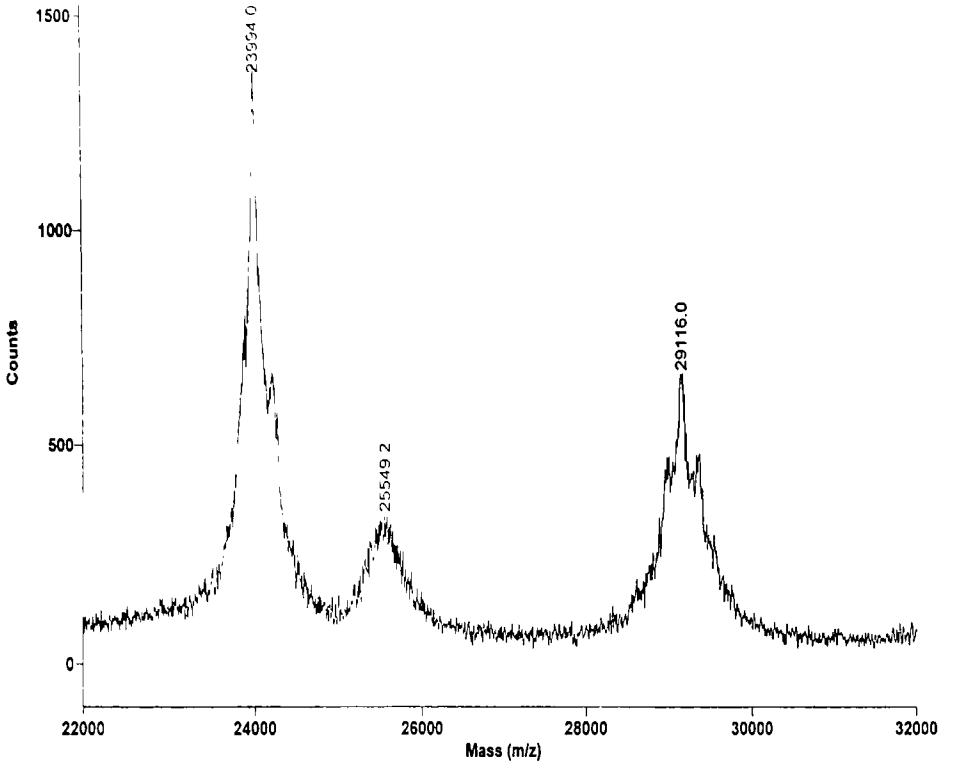

Figure 16. MALDI mass spectrum of *B. cereus* 5/B/6 metallo-β-lactamase inhibited with soduim 7-(dibromomethylene) cephalosporanate (**1**) and standard proteins. The sample was in 50 mM succinate buffer (pH = 6.0) and 1 mM $ZnSO_4$.

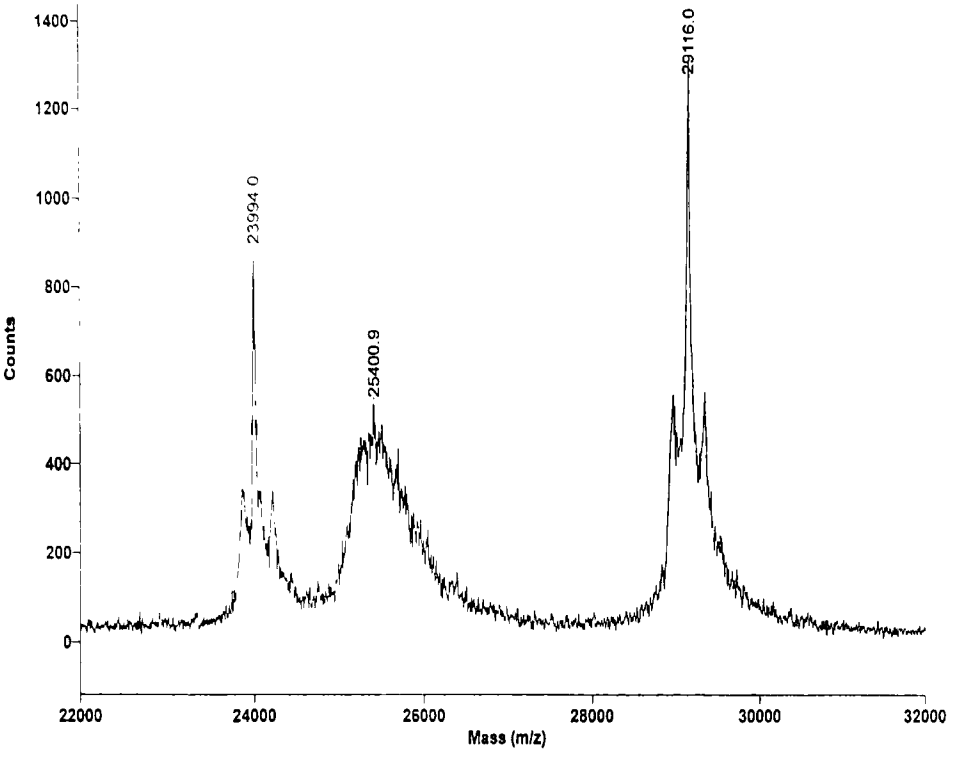

Figure 17. MALDI mass spectrum of *B. cereus* 5/B/6 metallo-β-lactamase inhibited with soduim 7-(dibromomethylene) cephalosporanate (**1**) after washing with ddH_2O.

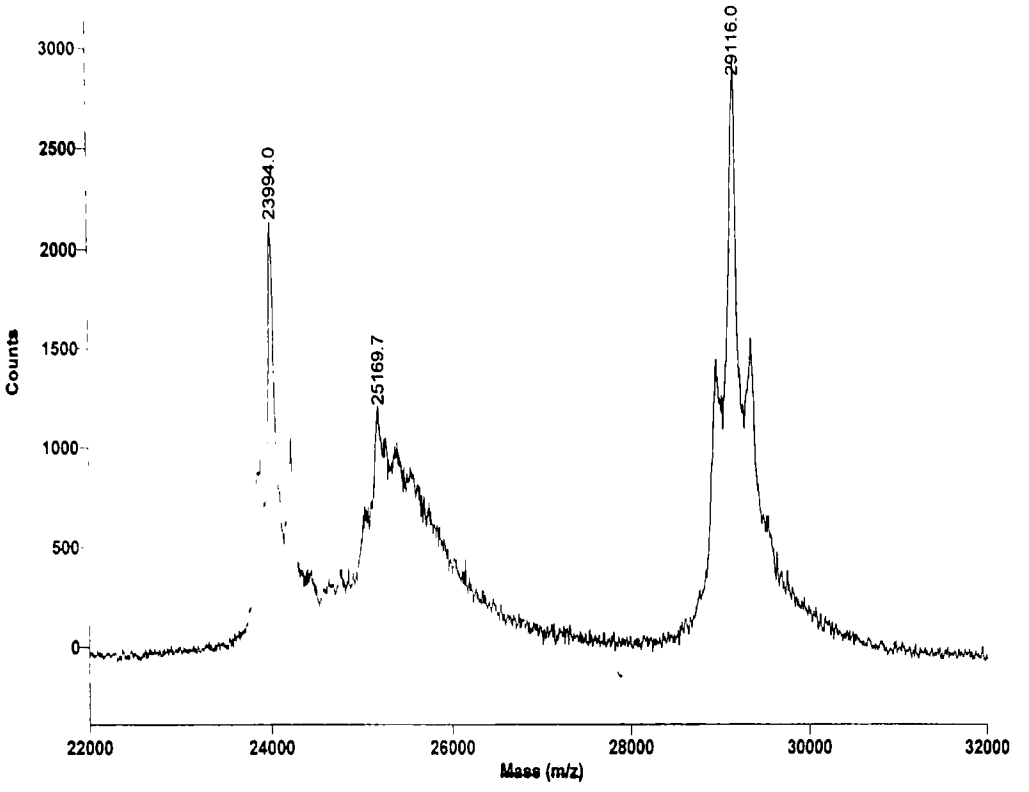

Figure 18. MALDI mass spectrum of *B. cereus* 5/B/6 metallo-β-lactamase inhibited with soduim 7-(dibromomethylene) cephalosporanate (**1**) after washing with ddH_2O and adding 0.3 % TFA to the matrix.

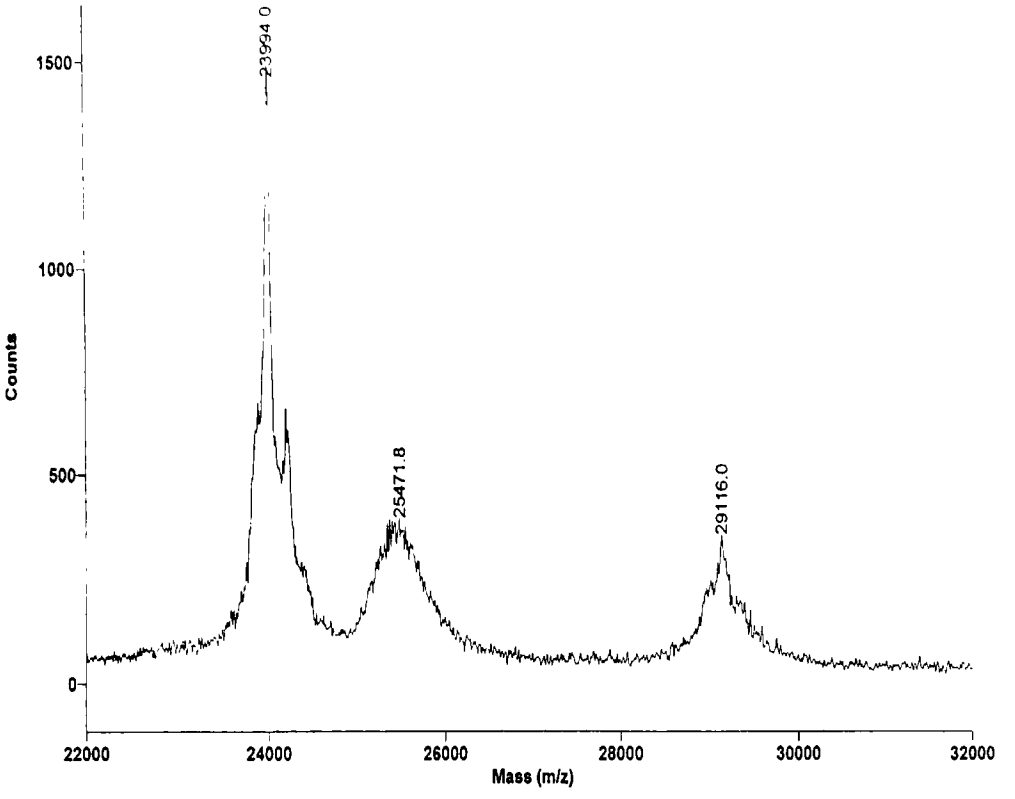

Figure 19. MALDI mass spectrum of 60 μM *B. cereus* 5/B/6 metallo-β-lactamase preincubated with 3 mM sodium 3-acetoxymethyl-7-(E-bromomethylidene)-3-cephem-4-carboxylate (**2**).

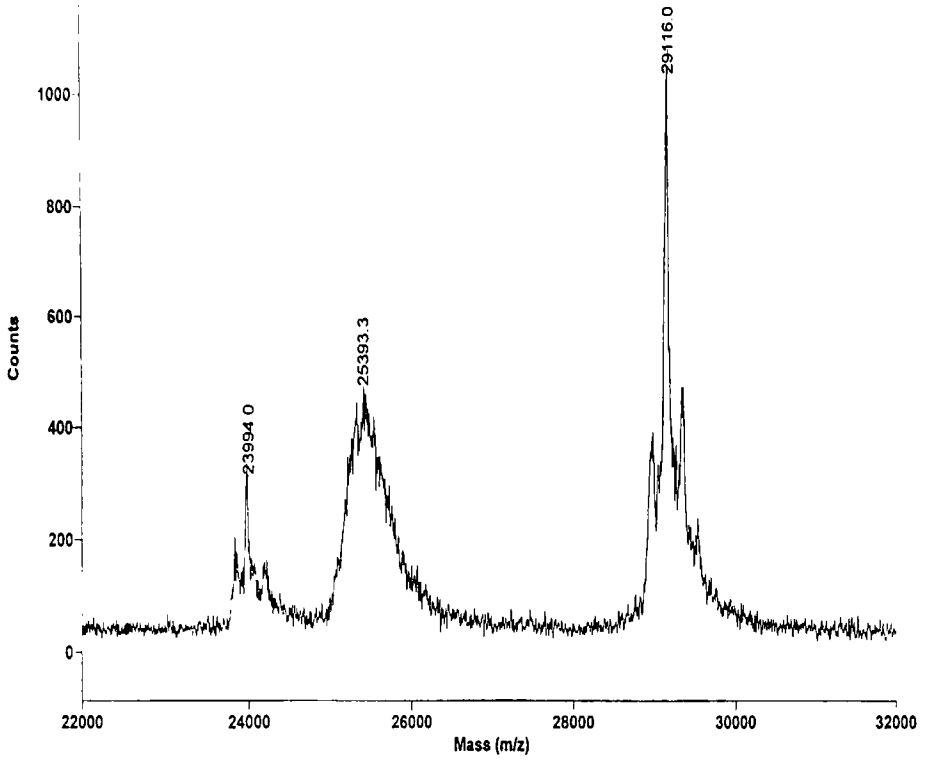

Figure 20. MALDI mass spectrum of 60 μM *B. cereus* 5/B/6 metallo-β-lactamase preincubated with 3 mM sodium 7-(dibromomethylidene)-3-methyl-3-cephem-4-carboxyate (**3**).

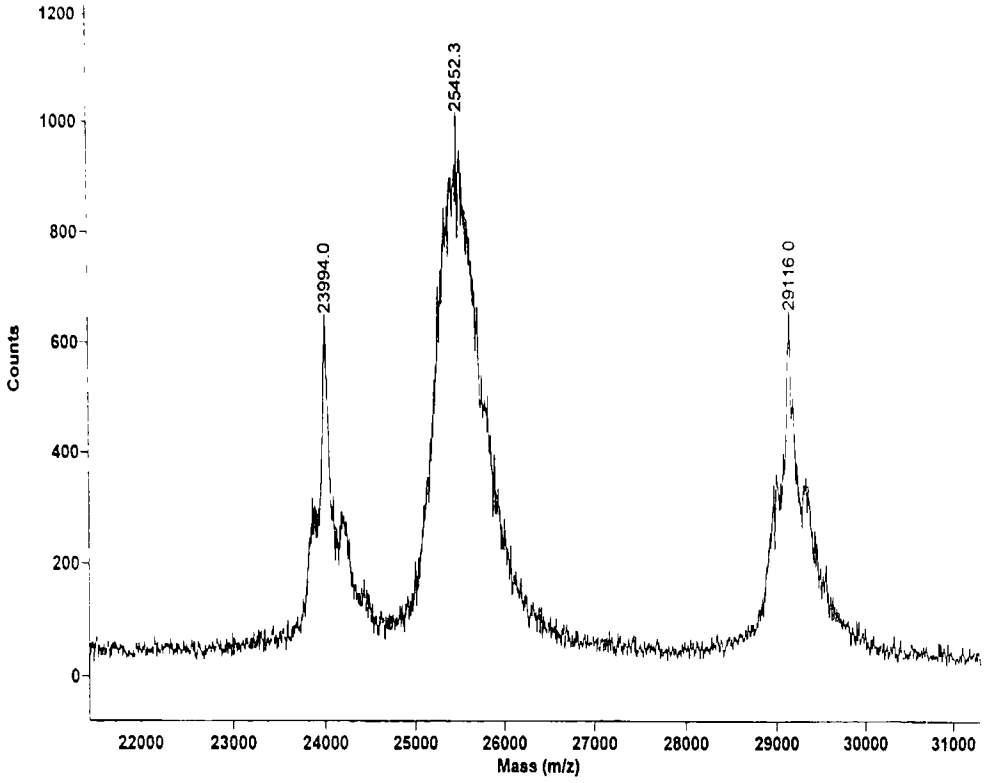

Figure 21. MALDI mass spectrum of 60 μM *B. cereus* 5/B/6 metallo-β-lactamase preincubated with 3 mM sodium 3-(2'E-carbomethoxyethylene)-7-(dibromomethylidene) -3-cephem-4-carboxyate (**4**).

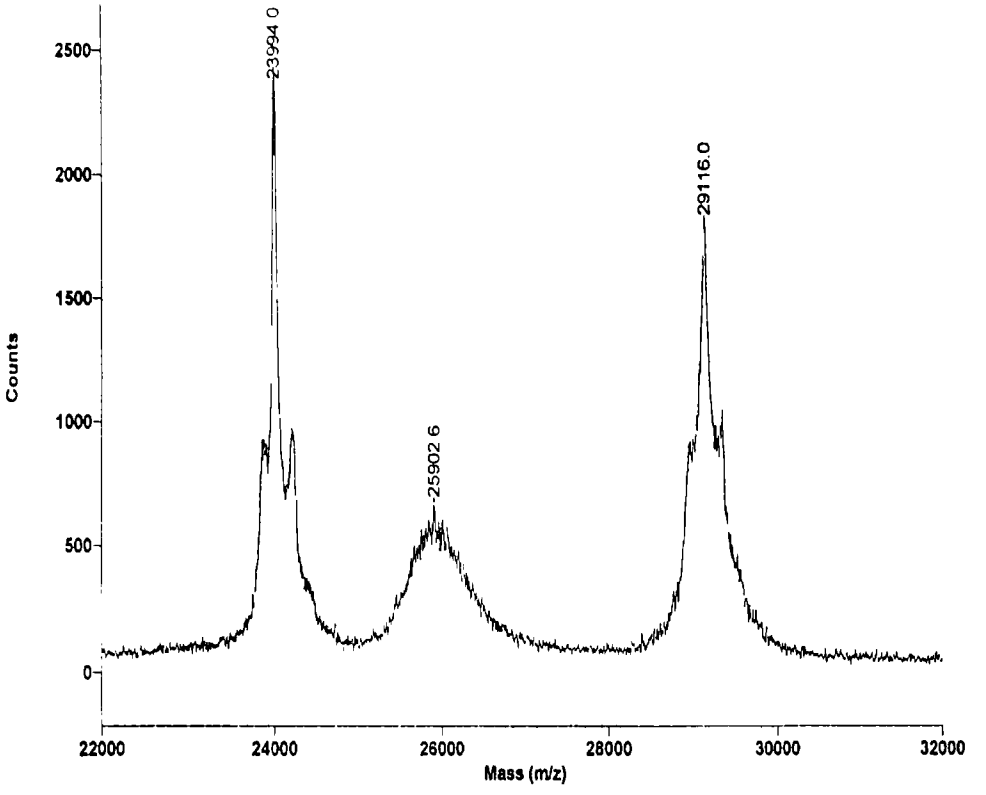

Figure 22. MALDI mass spectrum of 60 μM *B. cereus* 5/B/6 metallo-β-lactamase preincubated with 12 mM sodium 3-acetoxymethyl-3-cephem-4-carboxylate (**5**).

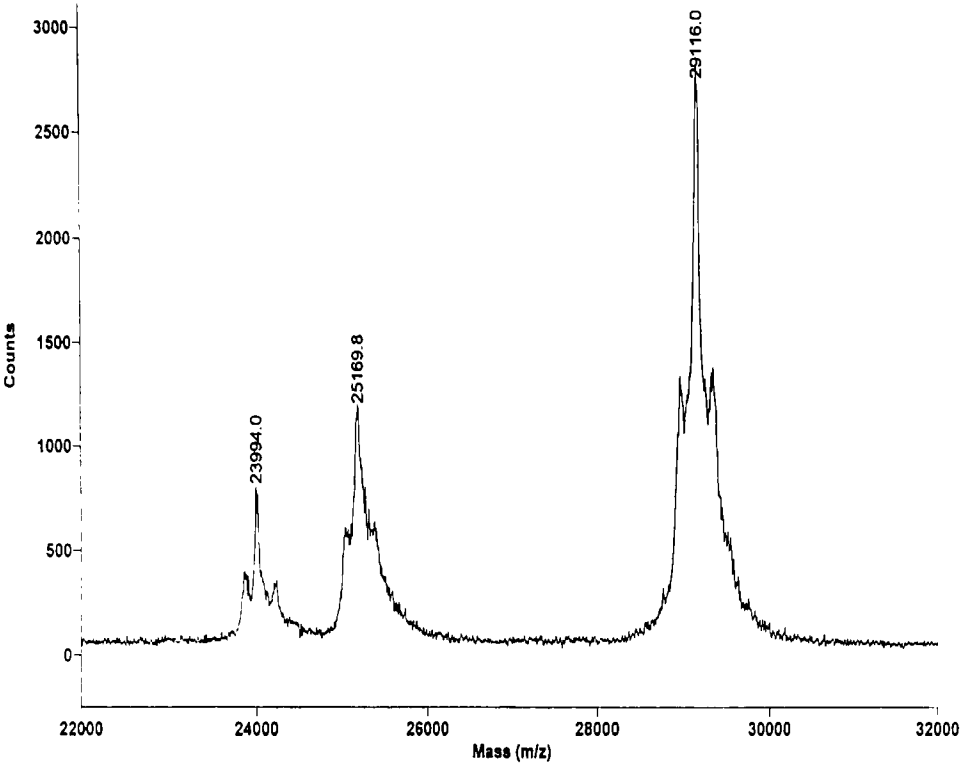

Figure 23. MALDI mass spectrum of 60 μM *B. cereus* 5/B/6 metallo-β-lactamase preincubated with 6 mM penicillin G.

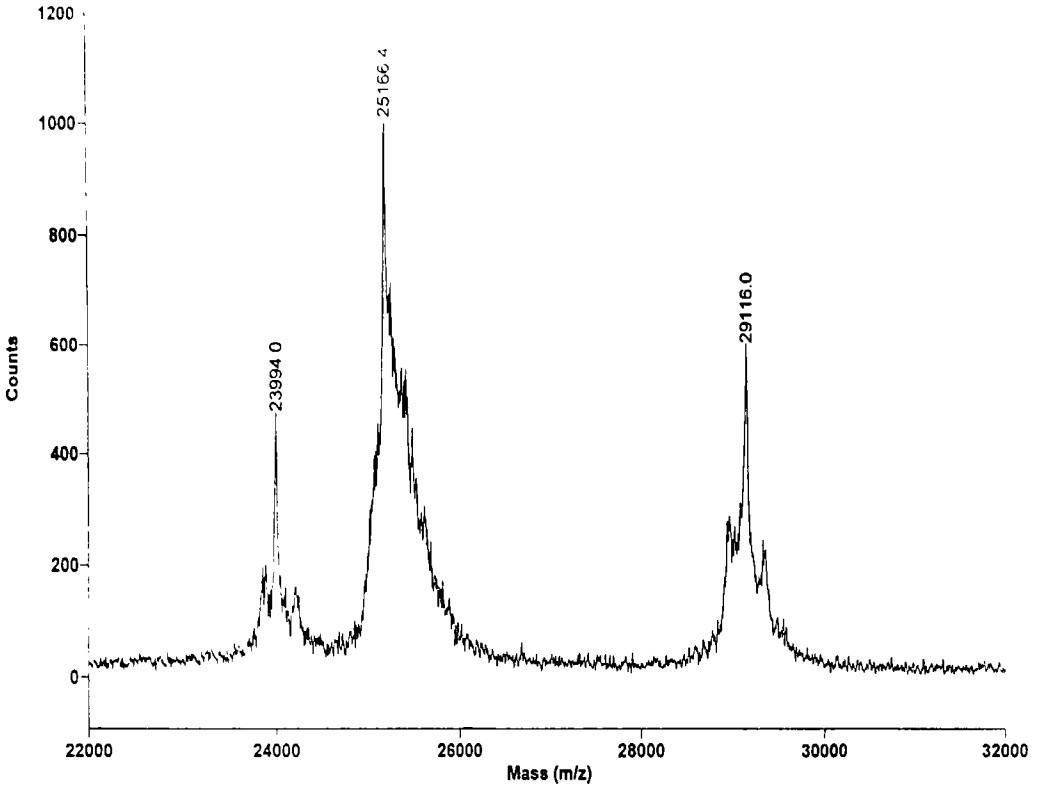

Figure 24. MALDI mass spectrum of 60 μM *B. cereus* 5/B/6 metallo-β-lactamase preincubated with 16.4 mM cephalosporin C.

Table 6. Summary of masses observed after the incubation of the enzyme and substrates or possible inhibitors.

Sample	The average mass of DE-MALDI-TOF	The mass difference of (Inhibited - Uninhibited Enzyme)
Cephalosporin C	25166.4	-2.6
Penicillin G	25169.8	0.8
Sodium 7-(dibromomethylene)-cephalosporanate (**1**)	25549.2	380.2
Sodium 3-acetoxymethyl-7-(E-bromomethylidene)-3-cephem-4-carboxylate (**2**)	25471.8	302.8
Sodium 7-(dibromomethylidene)-3-methyl-3-cephem-4-carboxyate (**3**)	25393.3	224.3
Sodium 3-(2'E-carbomethoxyethylene)-7-(dibromomethylidene)-3-cephem-4-carboxyate (**4**)	25452.3	283.3
Sodium 3-acetoxymethyl-3-cephem-4-carboxylate (**5**)	25902.6	733.6

Separation of inhibited enzymes by CM Sepharose CL-6B

Due to the fact that the peaks of enzyme-inhibitor complexes may result from mixtures of uninhibited enzyme, inhibited enzyme and matrix (sinapinic acid) adduct peaks, the DE-MALDI-TOF MS peaks were broad. In an attempt to separate the inhibited enzyme from uninhibited enzyme, CM Sepharose CL-6B cation exchange column was used.

The elution profiles of the CM Sepharose CL-6B for the enzyme incubated compounds **1**, **2**, **3**, **4** and **5** were shown in Figure 25, 26, 27, 28 and 29, respectively.

An ammonium sulfate step-gradient was carried out on the column. The elution profiles from Figure 25, 26, 29 showed protein peaks in the wash, which contained 0 mM ammonium sulfate. On the other hand, the elution profiles from Figure 27 and 28 did not show noticeable protein peaks in the wash. All elution profiles indicated predominant protein peaks were eluted at the 100 mM ammonium sulfate. The proteins were collected and concentrated for DE-MALDI-TOF MS. The results of DE-MALDI-TOF mass spectra are summarized in Table 7.

From the DE-MALDI-TOF results, compounds 1 and 2 that showed inhibition with the enzyme also showed the mass shift in the first peak and the major peak. The mass shifts were different from those before CM Sepharose CL-6B. The mass shifts indicate that several different sizable portions of the inhibitors may be bound to the enzyme.

Compounds **3** and **4** showed different mass shifts from those before CM Sepharose CL-6B in the major peak. This also suggests that several different fragments of these compounds bind to the enzyme that may be nonspecific because compounds **3** and **4** did not show inhibition.

The mass shift of compound **5** that did not inhibit the enzyme was close to the mass of uninhibited enzyme in the major peak, suggesting that the nonspecific binding compounds were lost from the enzyme.

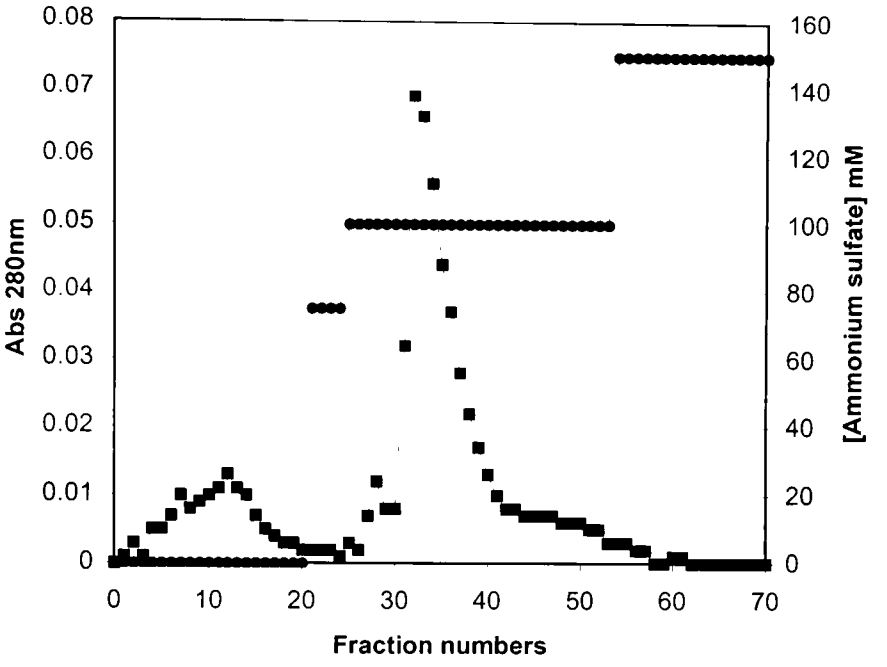

Figure 25. The elution profile of CM Sepharose CL-6B for the enzyme incubated with compound **1**. Filled squares represent protein absorbance at 280 nm; Filled circles represent step gradient with ammonium sulfate.

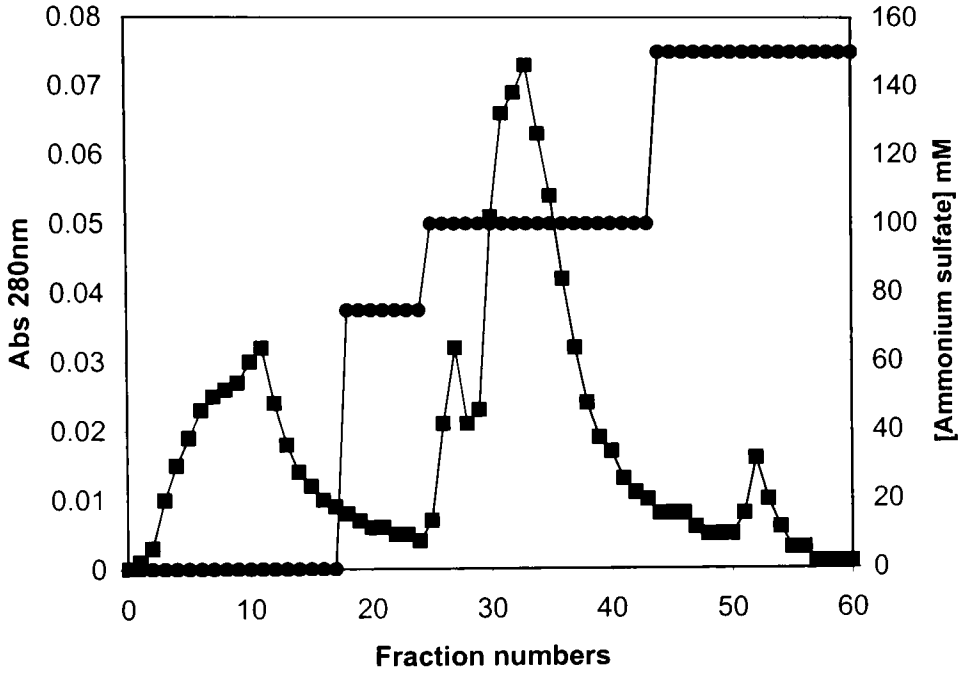

Figure 26. The elution profile of CM Sepharose CL-6B for the enzyme incubated with compound **2**. Filled squares represent protein absorbance at 280 nm; Filled circles represent step gradient with ammonium sulfate.

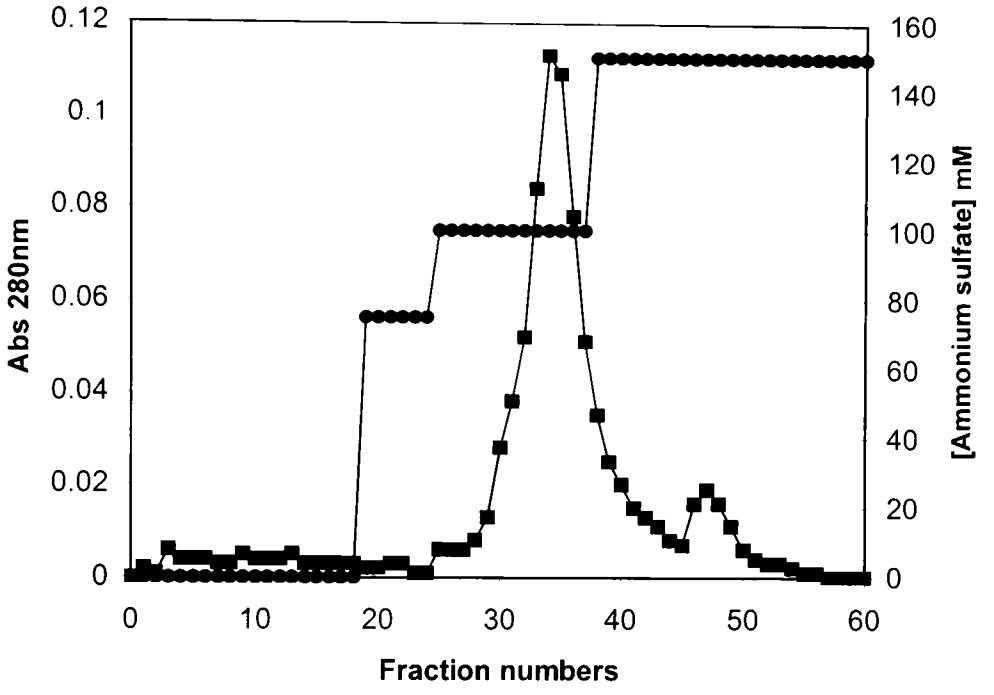

Figure 27. The elution profile of CM Sepharose CL-6B for the enzyme incubated with compound **3**. Filled squares represent protein absorbance at 280 nm; Filled circles represent step gradient with ammonium sulfate.

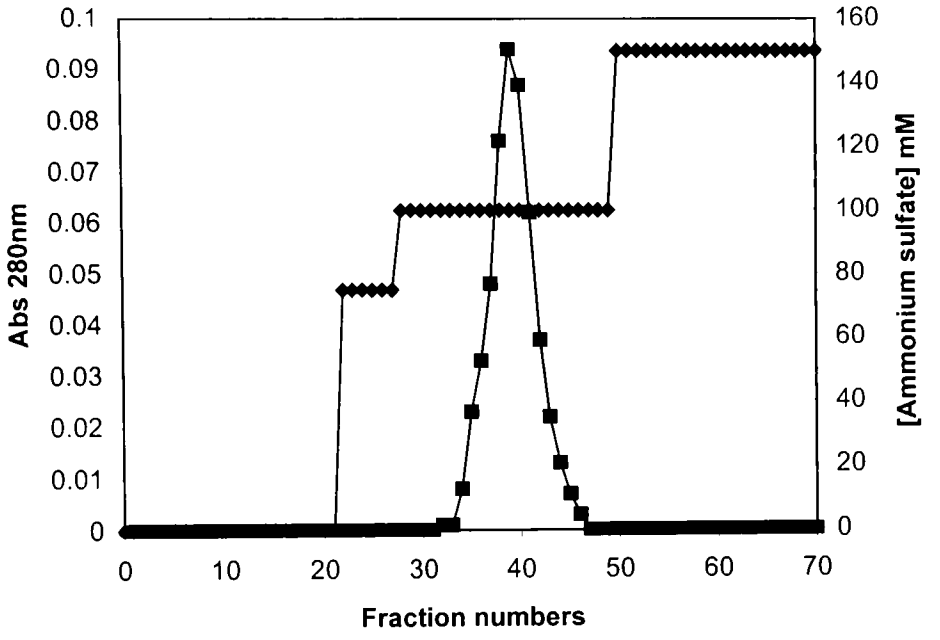

Figure 28. The elution profile of CM Sepharose CL-6B for the enzyme incubated with compound **4**. Filled squares represent protein absorbance at 280 nm; Filled circles represent step gradient with ammonium sulfate.

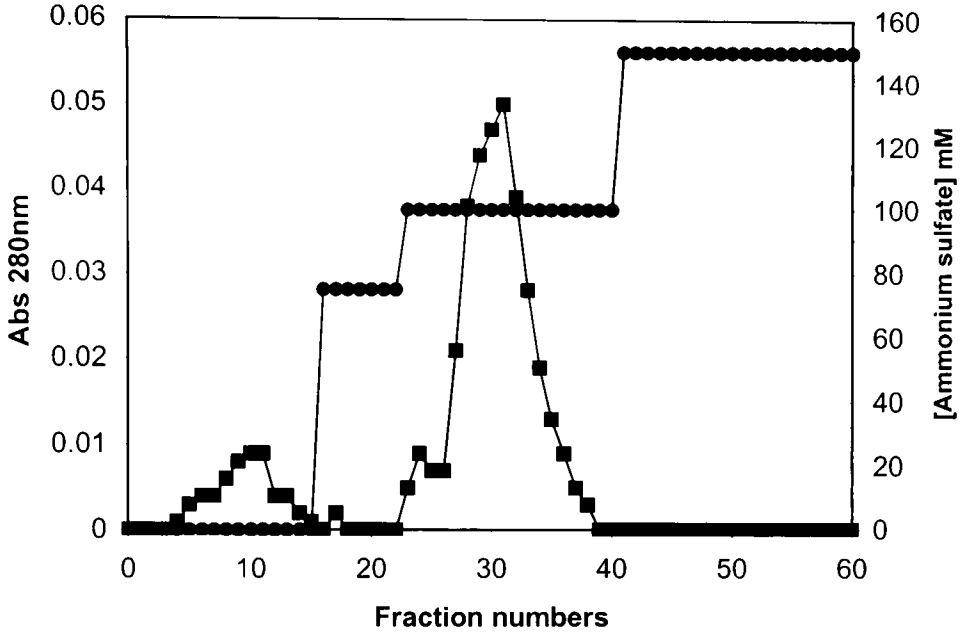

Figure 29. The elution profile of CM Sepharose CL-6B for the enzyme incubated with compound **5**. Filled squares represent protein absorbance at 280 nm; Filled circles represent step gradient with ammonium sulfate.

Table 7. Summary of masses observed after CM Sepharose CL-6B chromatography

Sample	The average mass of protein in the first peak	The mass difference of (Inhibited Uninhibited Enzyme)	The average mass of protein in the major peak	The mass difference of (Inhibited Uninhibited Enzyme)
1	25545.9	376.9	25373.1	204.1
2	25581.8	412.8	25467.4	298.4
3	ND*	NA	25237.4	68.4
4	ND*	NA	25333.1	164.1
5	ND*	NA	25181.1	12.1

ND* = not determined, due to small amounts of these compounds.

Determination of K_{inact} value for the mechanism-based inhibitors

Metallo-β-lactamase was inactivated by compound **1** (Figure 30) and compound **2** (Figure 32) as a function of time. First-order inactivation constants were determined by linear regression analysis of the slopes of the lines. From the plot of the reciprocal of the initial rate constant of inactivation as a function of the reciprocal of the inactivator concentration (compound **1** (Figure 31); compound **2** (Figure 33)), the rate constant of inactivation (k_{inact}) and the K_{inact} values were acquired (see Methods). The kinetic constants obtained for compound **1** and compound **2** are compared in Table 8.

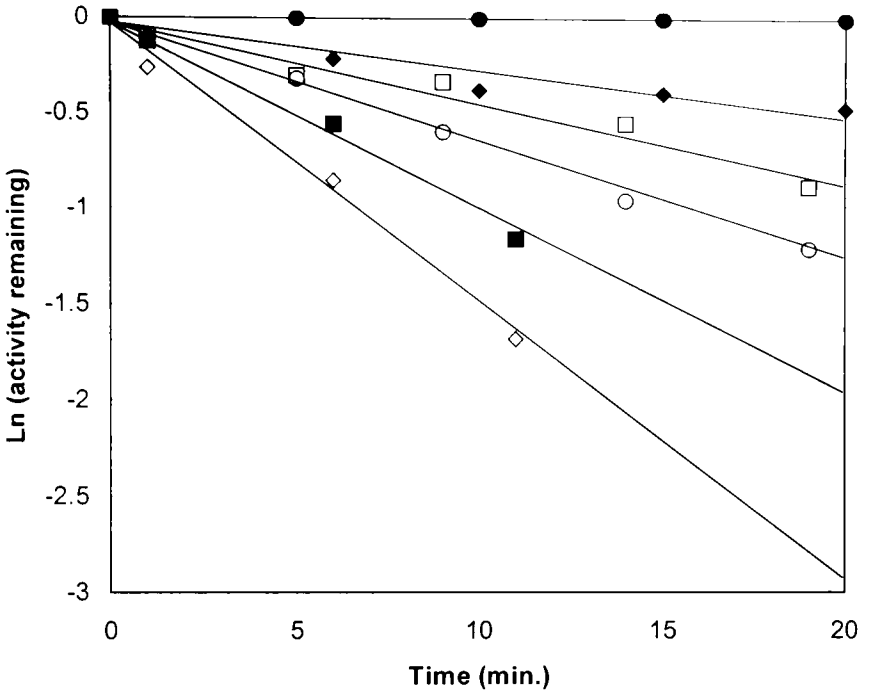

Figure 30. Time- and concentration dependence of inactivation of *B. cereus* 5/B/6 metallo-β-lactamase activity by compound **1**. Filled circle: [I] = 0 mM; filled diamond: [I] = 0.6 mM; open square: [I] = 1.2 mM; open circle; [I] = 2.5 mM; filled square: [I] = 5.0 mM; filled circle; [I] = 10.0 mM. I = compound **1**.

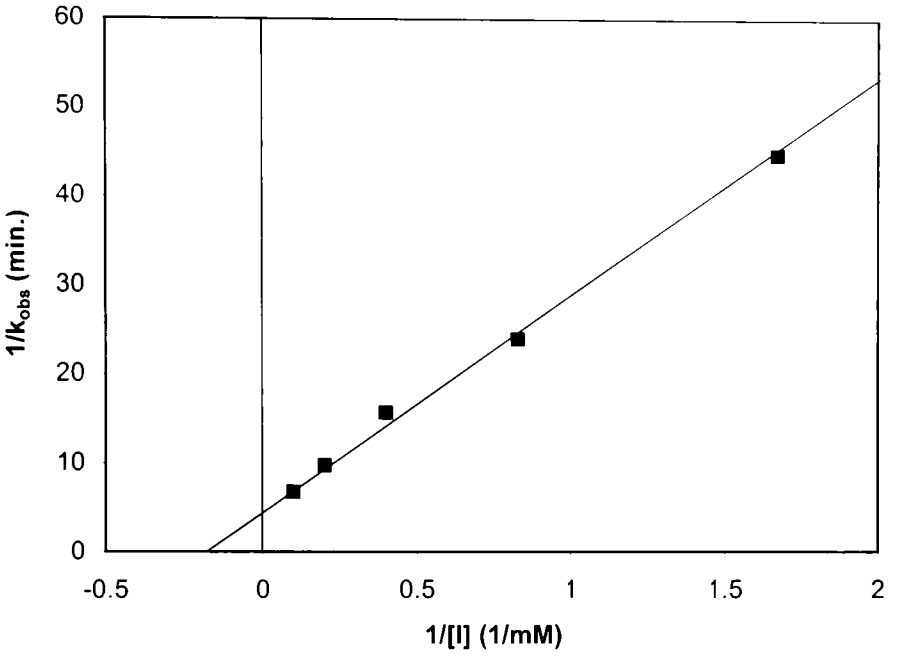

Figure 31. Double-reciprocal plot for the inactivation of *B. cereus* 5/B/6 metallo-β-lactamase activity by compound **1.**

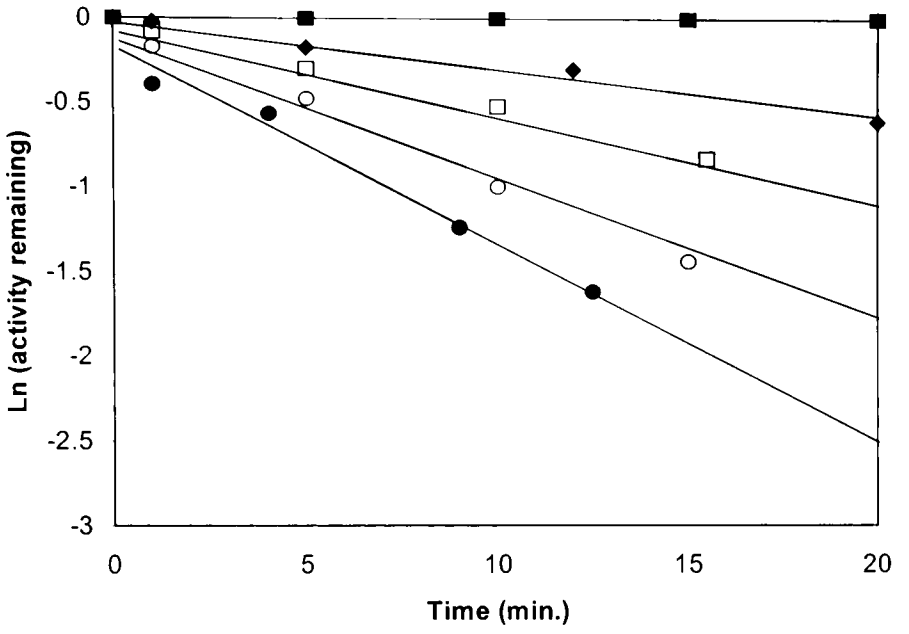

Figure 32. Time- and concentration-dependence of inactivation of *B. cereus* 5/B/6 metallo-β-lactamase activity by compound **2**. Filled square: [I] = 0 mM; filled diamond: [I] = 1.2 mM; open square: [I] = 2.5 mM; open circle; [I] = 5.0 mM; filled circle; [I] = 10.0 mM. I = compound **2**.

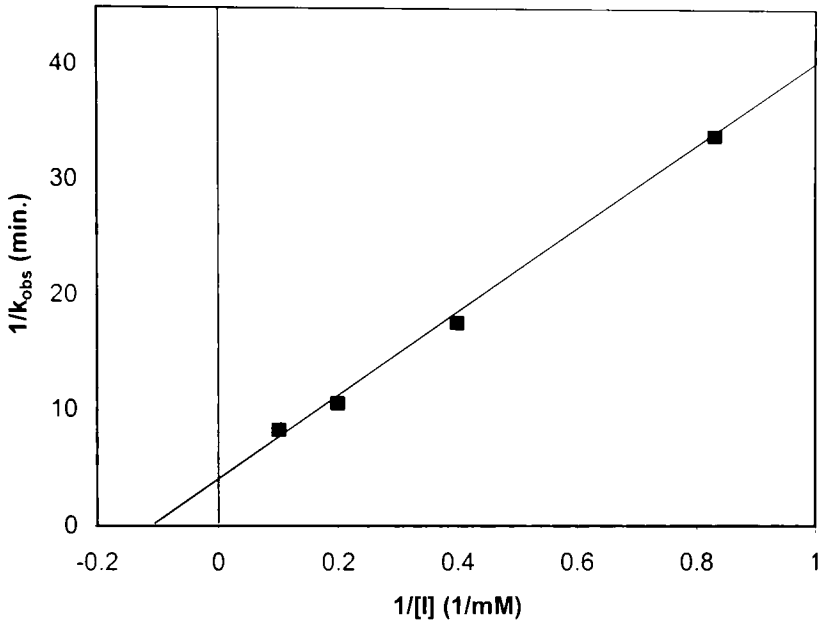

Figure 33. Double-reciprocal plot for the inactivation of *B. cereus* 5/B/6 metallo-β-lactamase activity by compound **2**.

Table 8. Effects of mechanism-based inhibitors on metallo-β-lactamases by compound **1** and compound **2**.

Inhibitors	K_{inact} (mM)	k_{inact} (min^{-1})
Compound **1**	4.7	0.20
Compound **2**	9.0	0.25

Inhibition studies of penicillin derivatives

The compounds **6** and **7** (Figure 5), which are penicillin derivatives, were tested as reversible inhibitors at different inhibitor concentrations. As a preliminary control study, EDTA (Figures 34, 35, 36 and 37) and 2-mercaptoethanol (Figures 38, 39, 40 and 41) were tested. The data is presented in Table 9. From the kinetic study, EDTA and 2-mercaptoethanol showed noncompetitive inhibition (Figures 34 and 35). The compounds **6** and **7** showed noncompetitive inhibition as well (Figures 37 and 41). The value of K_i (dissociation constant for the inhibitor from the enzyme-inhibitor complex) for compound **6** was 4.2 μM and the value of K_i' (dissociation constant for the inhibitor from the enzyme-substrate-inhibitor complex) for compound **6** was 8.6 μM as determined by slope and intercept replots (Table 9, Figures 38 and 39). On the other hand, the compound **7** showed that the value of K_i was 11 μM and the value of K_i' was 23 μM (Table 9, Figures 42 and 43).

The IC_{50} value, which represents the concentration of inhibitor required to affect a 50 % loss of activity of free enzyme, was determined by measuring the rate of enzymatic

hydrolysis of cephalosporin C after the enzyme has been preincubated for 15 minutes and assayed in presence of different amounts of inhibitor. The IC_{50} values of EDTA, 2-mercaptoethanlol, compounds **6** and **7** were 3.1 μM, 4.0 μM, 8.3 μM and 18 μM, respectively. The data is presented in Table 9, and Figures 42 and 46.

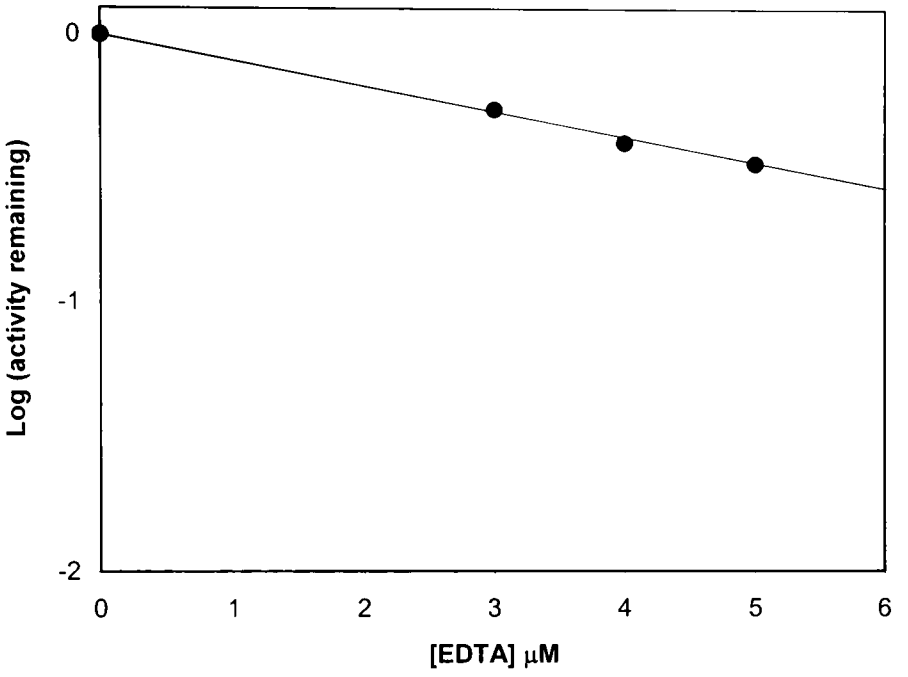

Figure 34. Determination of IC_{50} for *B. cereus* 5/B/6 metallo-β-lactamase by EDTA. The enzyme was preincubated with/without EDTA in the buffer (50 mM MOPS, pH = 7.0) for 15 min. at 30 °C. The concentration of the substrate (cephalosporin C) was 4 mM.

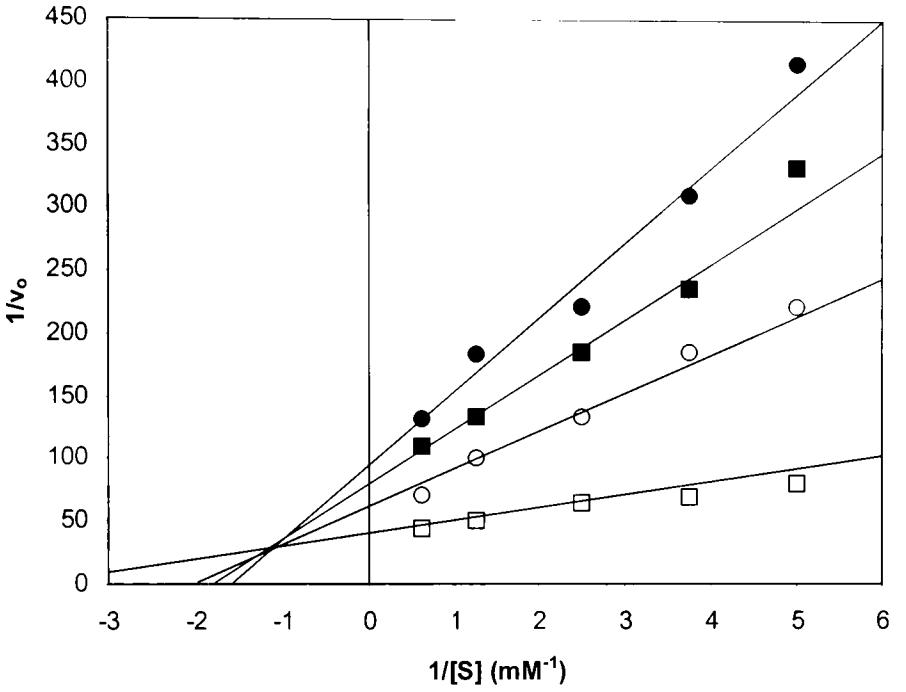

Figure 35. Lineweaver-Burk plot of inhibition of *B. cereus* 5/B/6 metallo-β-lactamase by EDTA. Open square: [I] = 0 μM; open circle: [I] = 3 μM; filled square: [I] = 4 μM; filled diamond: [I] = 5 μM. I = EDTA.

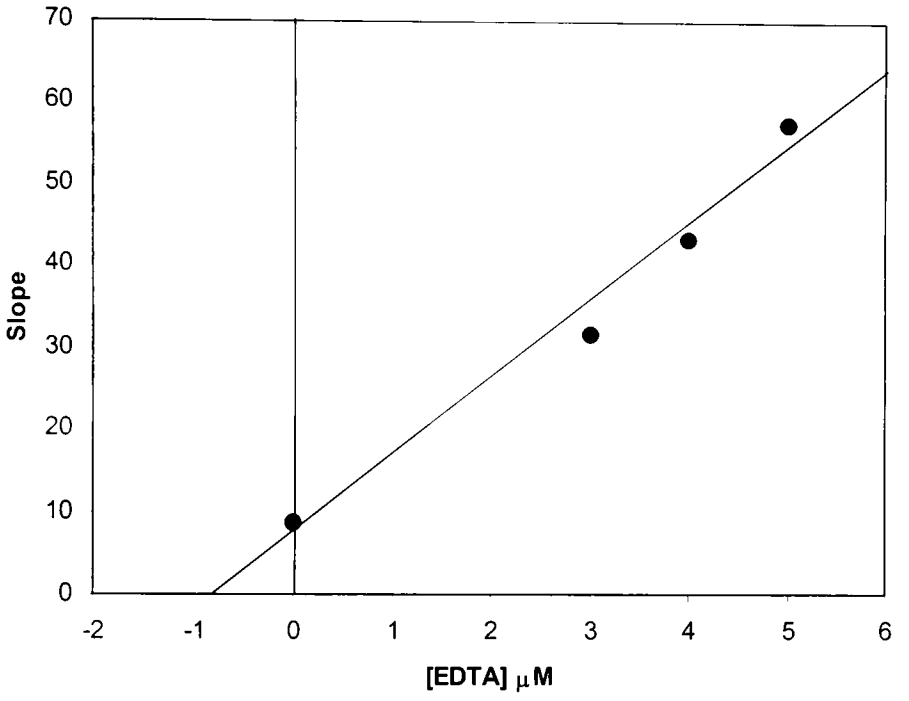

Figure 36. Slope replot to estimate K_i for EDTA. Slope values (K_m/V_{max}) for each inhibitor concentration from experimental data of Figure 35 were determined using a non-linear regression computer program (EnzymeKinetics, v. 1.2, Trinity Software). Slope values were then plotted versus corresponding inhibitor concentrations. The x-intercept in this plot is $-K_i$.

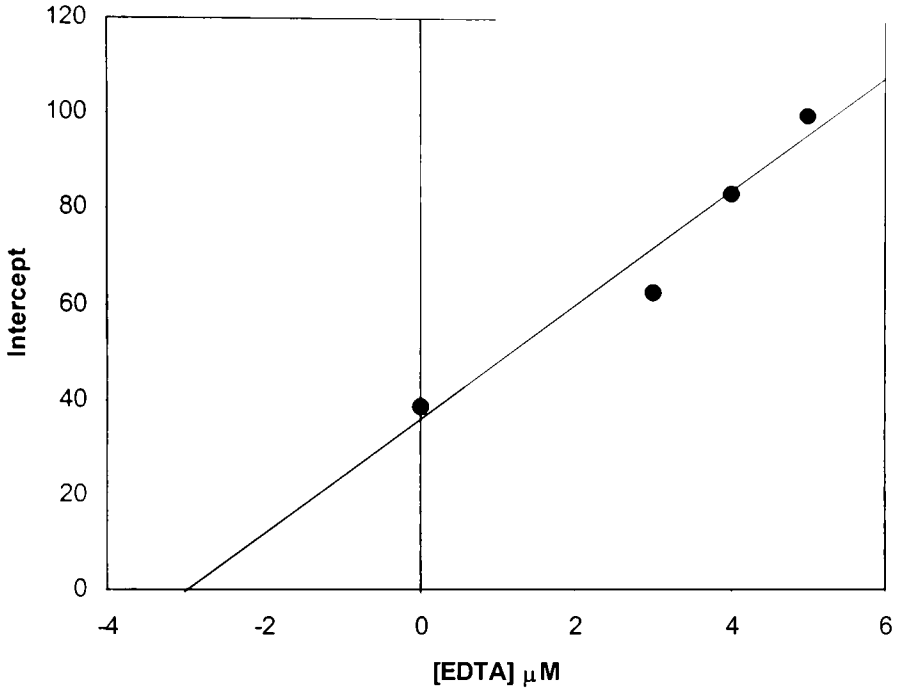

Figure 37. Intercept replot to estimate K_i' for EDTA. Intercept values ($1/V_{max}$) for each inhibitor concentration from experimental data of Figure 35 were determined using a non-linear regression computer program (EnzymeKinetics, v. 1.2, Trinity Software). Intercept values were then plotted versus corresponding inhibitor concentrations. The x-intercept in this plot is $-K_i$'.

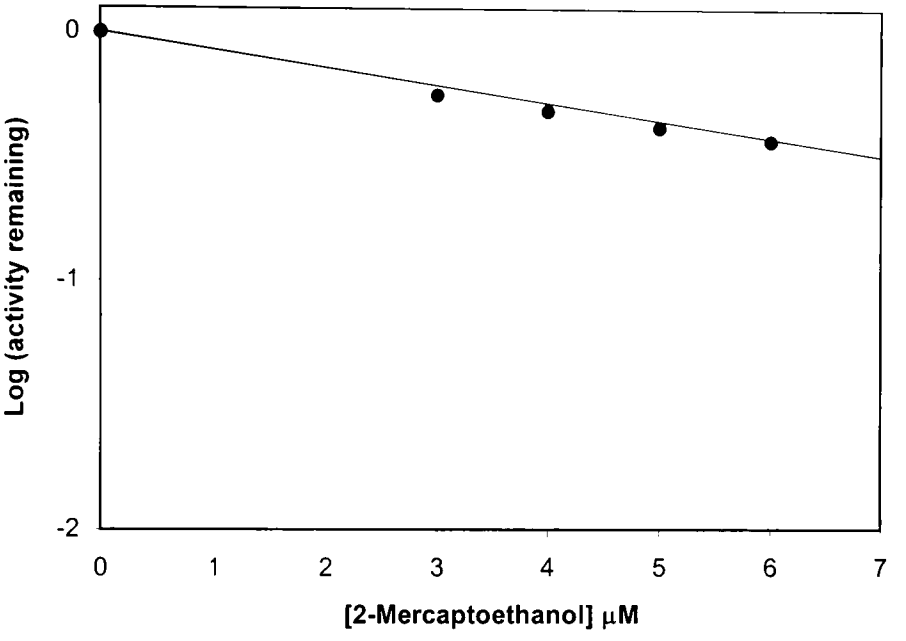

Figure 38. Determination of IC_{50} for *B. cereus* 5/B/6 metallo-β-lactamase by 2-mercaptoethanol. The enzyme was preincubated with/without 2-mercaptoethanol in the buffer (50 mM MOPS, pH = 7.0) for the 15 min. at 30 °C. The concentration of the substrate (cephalosporin C) was 4 mM.

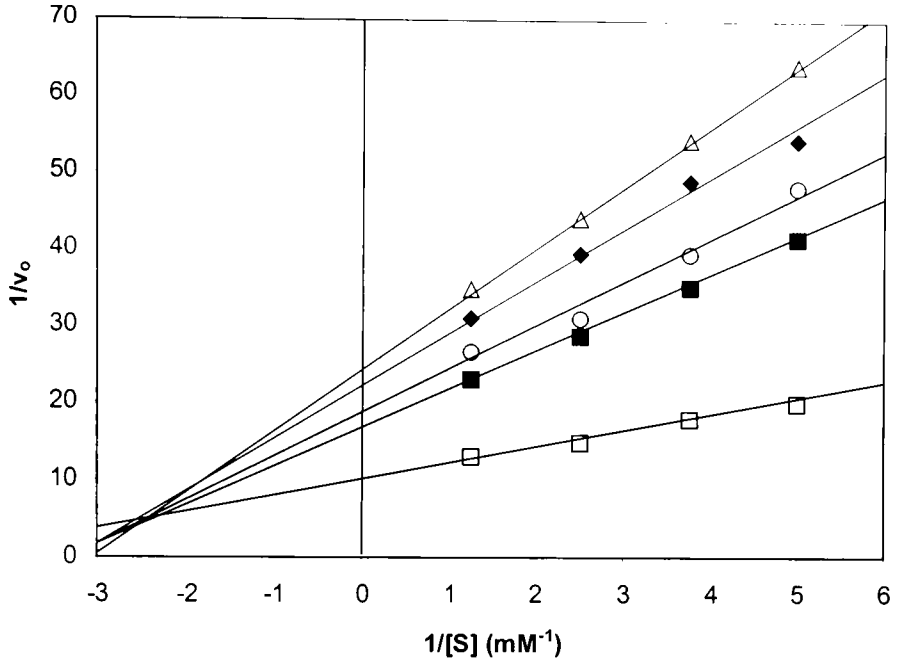

Figure 39. Lineweaver-Burk plot of inhibition of *B. cereus* 5/B/6 metallo-β-lactamase by 2-mercaptoethanol. Open square: [I] = 0 μM; filled square: [I] = 3 μM; open circle: [I] = 4 μM; filled diamond: [I] = 5 μM; open triangle: I = 6 μM. I = 2-mercaptoethanol.

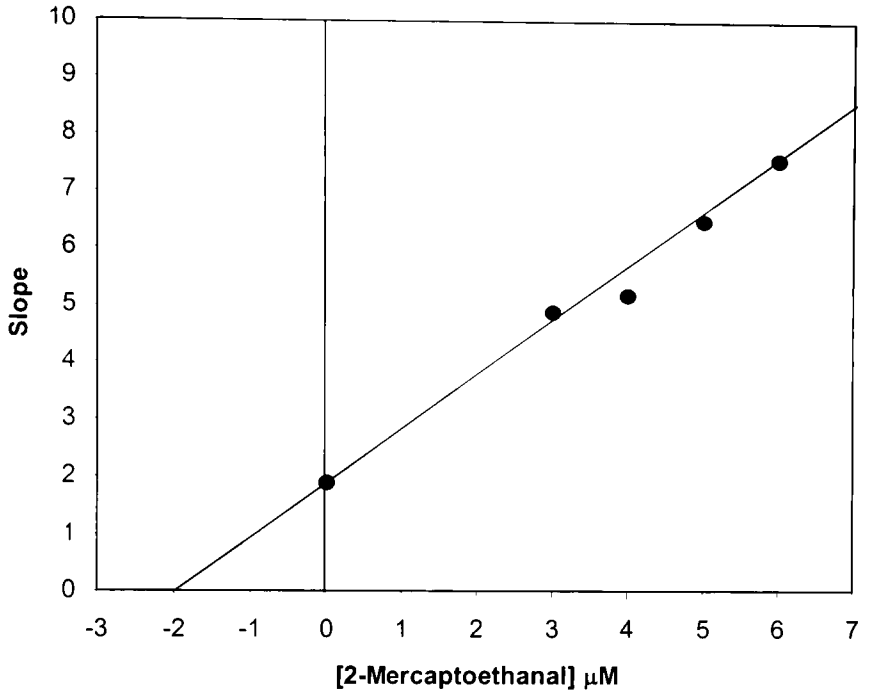

Figure 40. Slope replot to estimate K_i for 2-mercaptoethanol. Slope values (K_m/V_{max}) for each inhibitor concentration from experimental data of Figure 39 were determined using a non-linear regression computer program (EnzymeKinetics, v. 1.2, Trinity Software). Slope values were then plotted versus corresponding inhibitor concentrations. The x-intercept in this plot is $-K_i$.

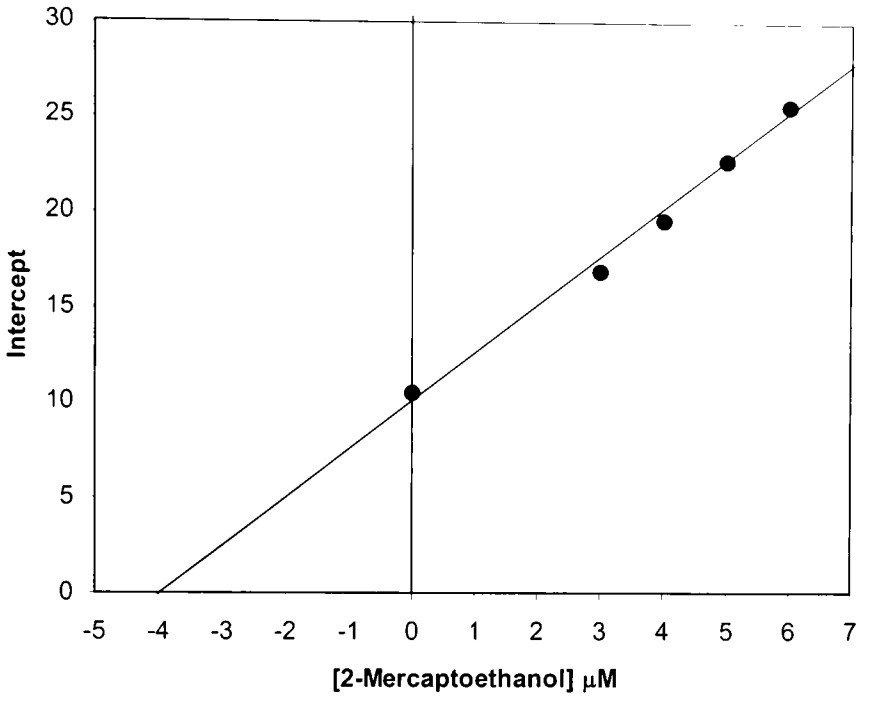

Figure 41. Intercept replot to estimate K_i' for 2-mercaptoethanol. Intercept values ($1/V_{max}$) for each inhibitor concentration from experimental data of Figure 39 were determined using a non-linear regression computer program (EnzymeKinetics, v. 1.2, Trinity Software). Intercept values were then plotted versus corresponding inhibitor concentrations. The x-intercept in this plot is $-K_i$'.

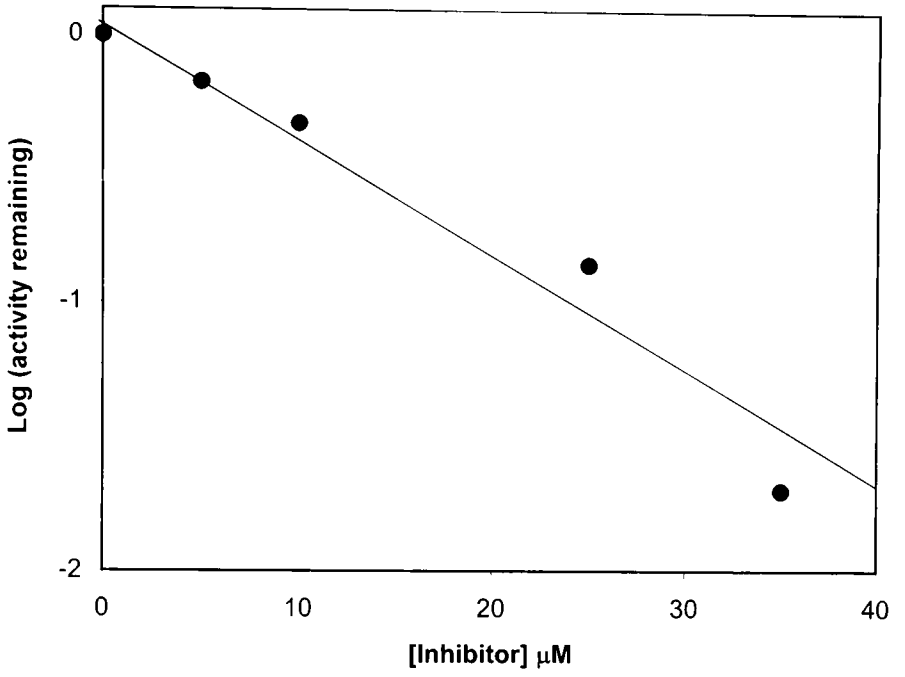

Figure 42. Determination of IC_{50} for *B. cereus* 5/B/6 metallo-β-lactamase by compound **6**. The enzyme was preincubated with/without in the buffer (50 mM MOPS, pH = 7.0) for the 15 min. at 30 °C. The concentration of the substrate (cephalosporin C) was 4 mM.

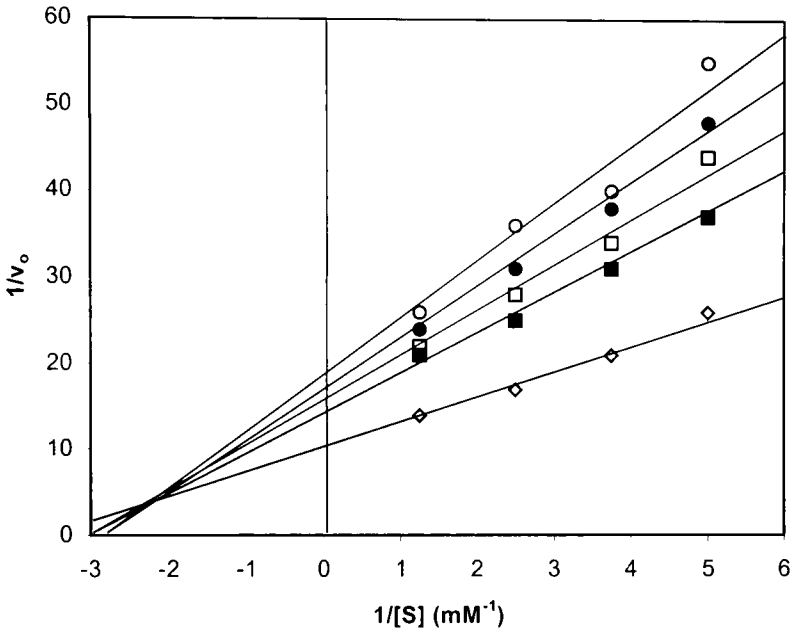

Figure 43. Lineweaver-Burk plot of inhibition of *B. cereus* 5/B/6 metallo-β-lactamase by compound **6**. Open diamond: [I] = 0 μM; filled square: [I] = 3 μM; open square: [I] = 4 μM; filled diamond: [I] = 5 μM; open circle: I = 6 μM. I = compound **6**.

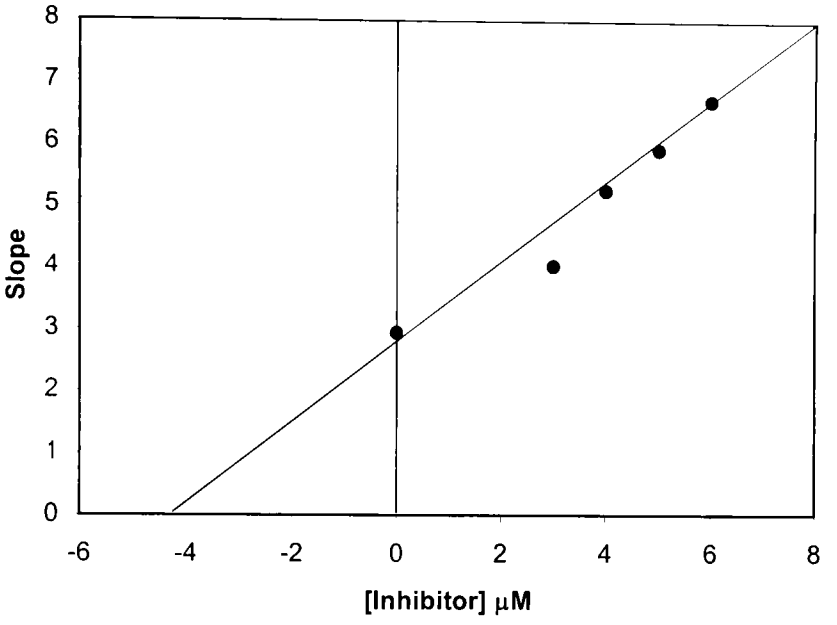

Figure 44. Slope replot to estimate K_i for compound **6**. Slope values (K_m/V_{max}) for each inhibitor concentration from experimental data of Figure 43 were determined using a non-linear regression computer program (EnzymeKinetics, v. 1.2, Trinity Software). Slope values were then plotted versus corresponding inhibitor concentrations. The x-intercept in this plot is $-K_i$.

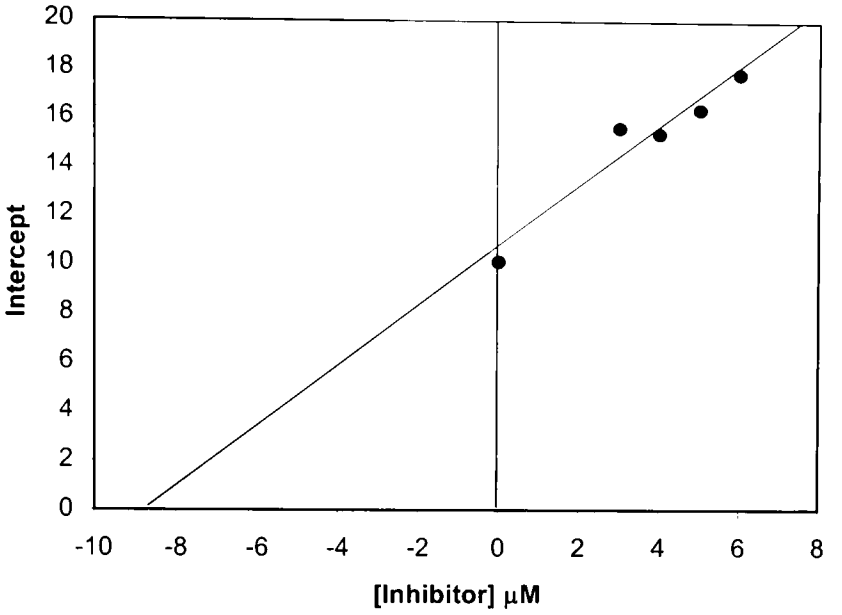

Figure 45. Intercept replot to estimate K_i' for compound **6**. Intercept values ($1/V_{max}$) for each inhibitor concentration from experimental data of Figure 43 were determined using a non-linear regression computer program (EnzymeKinetics, v. 1.2, Trinity Software). Intercept values were then plotted versus corresponding inhibitor concentrations. The x-intercept in this plot is $-K_i$'.

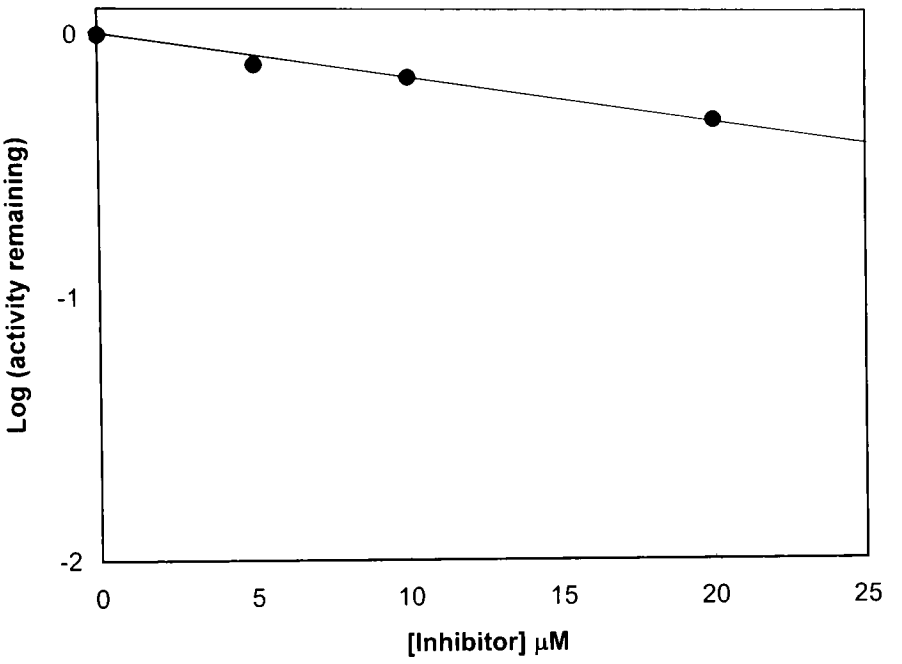

Figure 46. Determination of IC_{50} for *B. cereus* 5/B/6 metallo-β-lactamase by compound **7**. The enzyme was preincubated with/without compound **7** in the buffer (50 mM MOPS, pH = 7.0) for the 15 min. at 30 °C. The concentration of the substrate (cephalosporin C) was 4 mM.

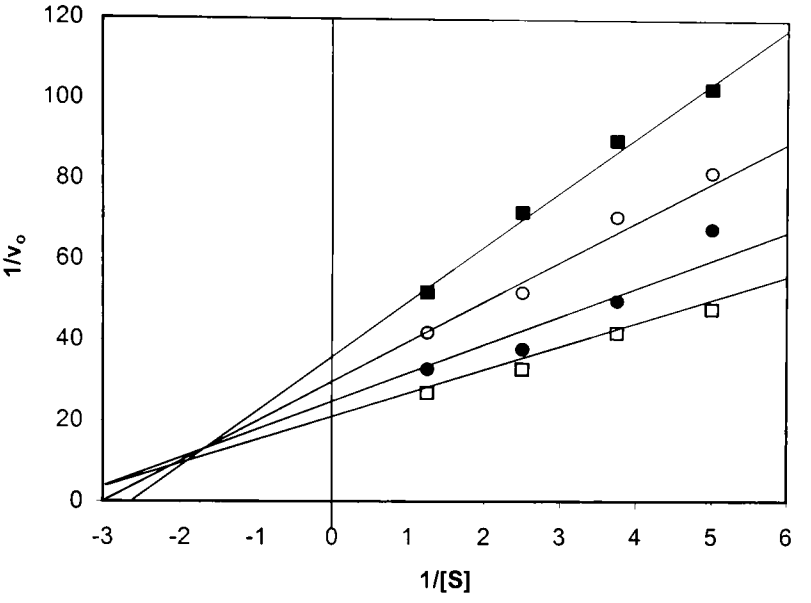

Figure 17. Lineweaver-Burk plot of inhibition of *B. cereus* 5/B/6 metallo-β-lactamase by compound **7**. Open square: [I] = 0 μM; filled diamond: [I] = 3 μM; open circle: [I] = 10 μM; filled square: [I] = 17 μM. I = compound **7**.

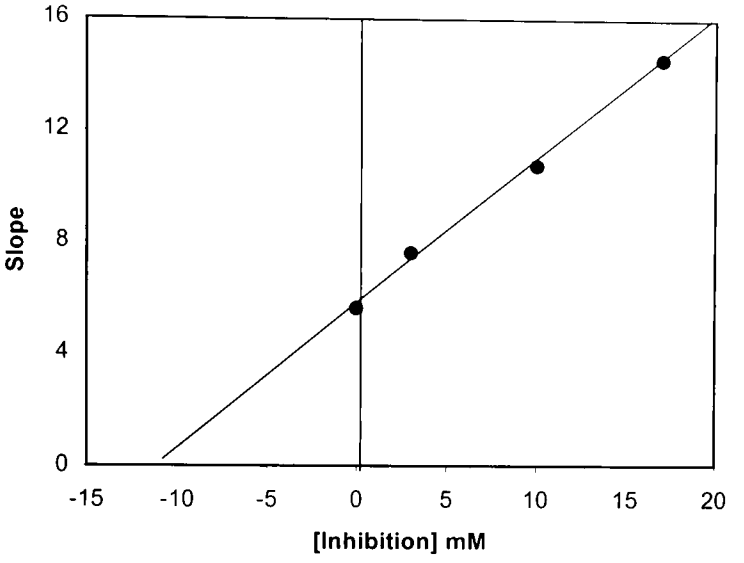

Figure 48. Slope replot to estimate K_i for compound **7**. Slope values (K_m/V_{max}) for each inhibitor concentration from experimental data of Figure 47 were determined using a non-linear regression computer program (EnzymeKinetics, v. 1.2, Trinity Software). Slope values were then plotted versus corresponding inhibitor concentrations. The x-intercept in this plot is $-K_i$.

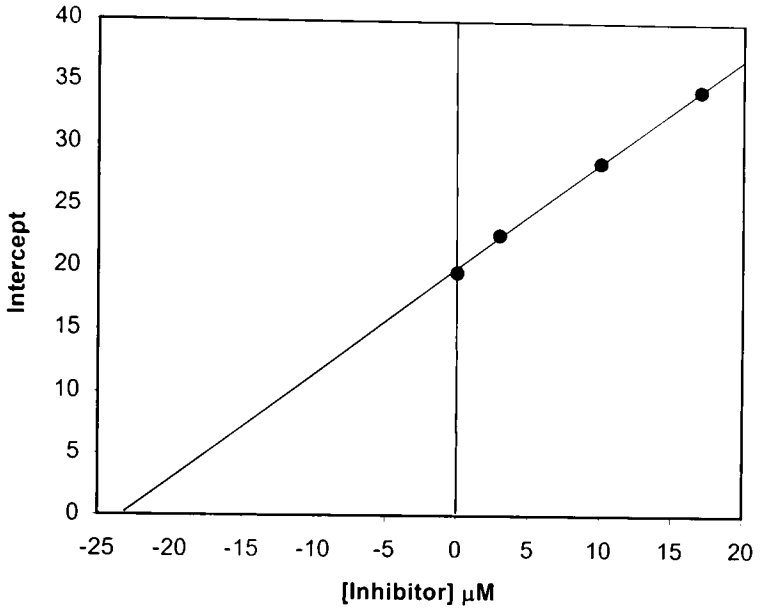

Figure 49. Intercept replot to estimate K_i' for compound **7**. Intercept values ($1/V_{max}$) for each inhibitor concentration from experimental data of Figure 47 were determined using a non-linear regression computer program (EnzymeKinetics, v. 1.2, Trinity Software). Intercept values were then plotted versus corresponding inhibitor concentrations. The x-intercept in this plot is $-K_i$'.

Table 9. Reversible inhibition of *B. cereus* 5/B/6 metallo-β-lactamase.

	IC_{50}	K_i	K_i'
EDTA	3.1 μM	0.75 μM	2.9 μM
2-mercaptoethanol	4.0 μM	2.0 μM	4.0 μM
Compound **6**	8.3 μM	4.2 μM	8.6 μM
Compound **7**	18 μM	11 μM	23 μM

Combinatorial approach to inhibition of metallo-β-lactamases: SELEX

A pool of 4^{30} (1.2×10^{18}) 61-mer oligonucleotides, that share 15 and 16 nucleotide sites for polymerase chain reaction (PCR) primers at their 5' and 3' termini respectively and also contain an internal random sequence 30-nucleotide was synthesized.

After incubating the enzyme with the pool of 61-mer oligonucleotides, the enzyme:ssDNA complex was separated from free ssDNA by electrophoresis. Figure 50 shows the existence of a nucleic acid:protein complex and was obtained by staining in ethidium bromide and Coomassie Brilliant Blue R250. The *B. cereus* 5/B/6 metallo-β-lactamase is a cationic enzyme. If there were no ssDNA binding to the enzyme, the enzyme would not migrate into the gel but would rather travel up the gel toward the cathode and out of the sample well area. The bound ssDNA provides negative charges for migration down the gel toward the anode. The bound ssDNA can be recognized by ethidium bromide fluorescence and the protein can be identified by Coomassie Brilliant Blue R250.

In Figure 51, the PCR products from SELEX migrated differently compared from the initial random ssDNA. This difference of migration and the broad nature of band of the PCR products can be due to the variety of possible secondary and tertiary structures of the PCR products.

To confirm that the excised band from the PCR products contained the sought-for ssDNA, the initial random ssDNA was compared with the ssDNA generated by PCR after SELEX on an 8 M urea gel (Figure 52). The results of the comparison showed that the electrophoretic migration of the ssDNA after SELEX was essentially identical to that of the initial random ssDNA.

A significant advantage of the electrophoretic separation is that it allows visualization of each selection step, making apparent the relative amounts of bound and free DNA. It thus indicates the stringency of selection and reveals whether ligand binding has occurred during the course of an experiment. In the early rounds (Figure 53), the enzyme was in excess, so location of the enzyme:ssDNA complex was easily accomplished. The ratio of enzyme:ssDNA in early rounds was 6.7. The ratio was then gradually decreased to give more stringency of selection in the middle rounds (Figure 54). The ratio of enzyme:ssDNA was 3.3, 3.3 and 1.3 at rounds 6, 7 and 8, respectively. The gel showed an enzyme:ssDNA complex (Figure 55). That was more intense than the band corresponding to free DNA. From the ninth round, the ratio of enzyme:ssDNA was maintained at 1:1. The concentration of the NaCl added was increased to 15 mM from 10 mM at the thirteenth round. In the late rounds, free ssDNA was the predominately visible species in the gel (Figure 57). In the sixteenth round, although the concentration of NaCl

was increased up to 20 mM NaCl, free ssDNA was significantly diminished due to selection of high affinity of the ssDNA for the enzyme (Figure 57).

The PCR products of ssDNA were located between 20 bps and 40 bps (Figures 54, 56 and 58). To test whether the ssDNA could bind and inhibit the enzyme, a preliminary inhibition test was performed at the eighth, eleventh, fourteenth and sixteenth rounds. The results of preliminary inhibition study are summarized in Table 10.

At round 8, 40 % inactivation occurred. After round 11, the inactivation increased to 75 %. The inactivation of round 11 was very close to round 14. The inactivation of round 16, however, decreased to 53 %. In this preliminary inhibition test, the results were not accurate because the concentration of ssDNA was estimated optically based on the intensity of florescence compared to the sample of ssDNA of known concentration.

After the sixteenth round, cloning of the fragment into the vector pRE2 was carried out. This made it possible to sequence the insert. The sequence was 5'-d(ANCNANNNTTNNNTNGNNGNNCATNNNNAA)-3', which contained 17 N's. To give more stringency of selection, beginning with the seventeenth round, the concentration of NaCl was increased to 50 mM. Also, the incubation time was increased to 2.5 hours. This resulted in a smearing effect on the gel due to increasing the salt concentration to 50 mM NaCl. After the twenty-first round, the cloning and sequencing were carried out again. The sequence of the 30-mer aptamer was determined to be:

5'-d(AACCAAACTTGGATCGGTGCACATGTCGAA)-3'

This final single-stranded DNA (aptamer 30-mer) was synthesized using a Beckman Oligo 1000M oligonucleotide synthesizer.

The IC_{50} value for the 30-mer was determined by measuring the rate of enzymatic hydrolysis of cephalosporin C after the enzyme has been preincubated and assayed in presence of different of amounts of the 30-mer. The IC_{50} of the 30-mer was 1.2 nM. The data is presented in Table 11 and Figure 59. From a steady-state kinetic study, the 30-mer showed a noncompetitive inhibition (Figure 60). The value of K_i (dissociation constant for the inhibitor from the enzyme-inhibitor complex) for the 30-mer was 0.92 nM and the value of K_i' (dissociation constant for the inhibitor from the enzyme-substrate-inhibitor complex) for the 30-mer was 11 nM as determined by slope and intercept replots (Table 11, Figures 61 and 62).

In order to check to see if the reversible inhibition was time-dependent, the time dependence of the inhibition of the enzyme by 0.5 nM the 30-mer was measured. As can be seen from Figure 63, the inhibition was time-independent.

The experiment of Figure 64 was performed to test the specificity of inhibition by this 30-mer. As can be seen in Figure 64, 100 nM of the 30-mer has no effect on the activity of the *B. cereus* 569/H/9 β-lactamase I (a class A β-lactamase).

In addition, the bovine carboxypeptidase A was used to test the specificity of inhibition by this 30-mer. As can be seen in Figure 65, 25 nM of the 30-mer has no effect on the activity of the carboxypeptidase A.

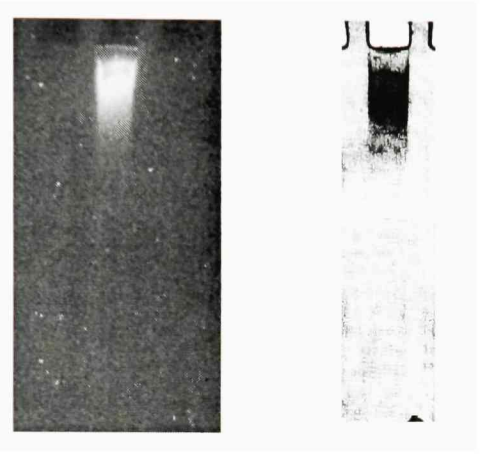

Figure 50. The evidence for a complex of the *B. cereus* 5/B/6 metallo-β-lactamase and the ssDNA. On the left, the gel was stained by ethidium bromide. On the right, the gel was stained by Coomassie Brilliant Blue R250. 20 μM enzyme and 1.5 μM ssDNA were used to make the complex. The buffer used for incubation was 20 mM TA (pH = 7.0) and 1 mM $ZnSO_4$.

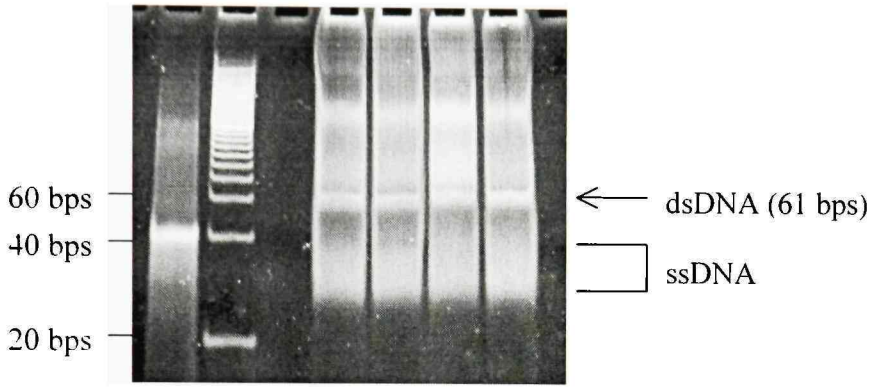

Figure 51. Comparison of the initial random ssDNA with the ssDNA after SELEX on a native gel. The first lane contained initial random ssDNA. The second lane contained the molecular size markers. The first marker from the bottom represents 20 bps. The fourth, fifth, sixth and seventh lanes contained PCR products after the eight round of SELEX. A 12 % (w/v) polyacrylamide gel (29:1 mono:bis) was used in TA buffer.

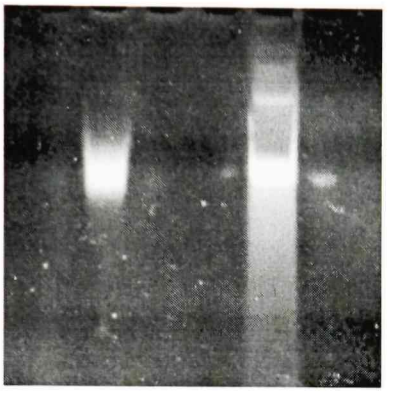

Figure 52. Comparison of the initial random ssDNA with the ssDNA after SELEX on a denaturing gel. The left lane contained ssDNA after SELEX and the right lane contained initial random ssDNA. The 12 % polyacrylamide gel (29:1 mono:bis) was run with 8M urea in TBE buffer (45 mM Tris, 45 mM boric acid and 1 mM EDTA, pH = 8.0).

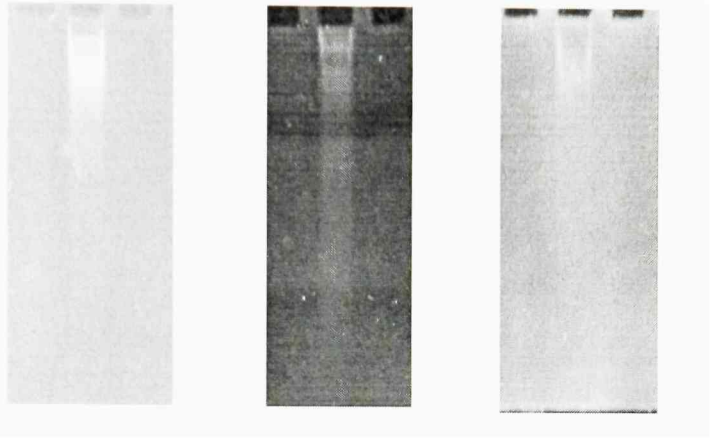

Figure 53. The early rounds of SELEX. The first, second, third lanes are for the first, third, fifth rounds of SELEX, respectively. The gel shift assays were carried out as described in Methods. The first round contained 20 μM enzyme, 3 μM ssDNA and 10 mM NaCl. The third round contained 20 μM enzyme, 1.5 μM ssDNA and 10 mM NaCl. The fifth round contained 10 μM enzyme, 1.5 μM ssDNA and 10 mM NaCl.

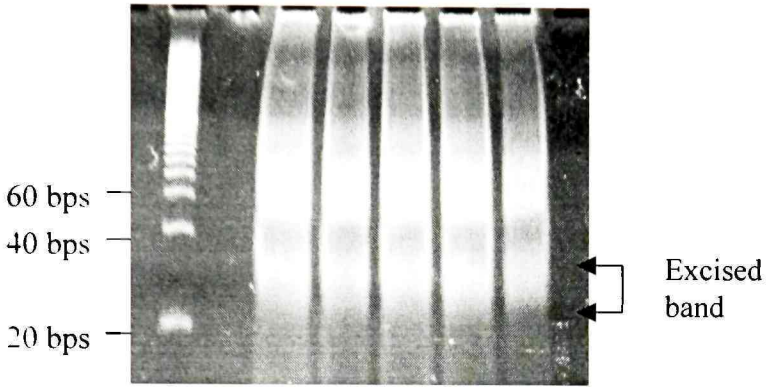

Figure 54. PCR of ssDNA from the first round of SELEX. The condition of the PCR was described in Methods. The first lane contained the molecular size markers. The first marker from the bottom represents 20 bps. The band excised was chosen because its migration on the 8 M urea gel matched the migration of the initial random ssDNA.

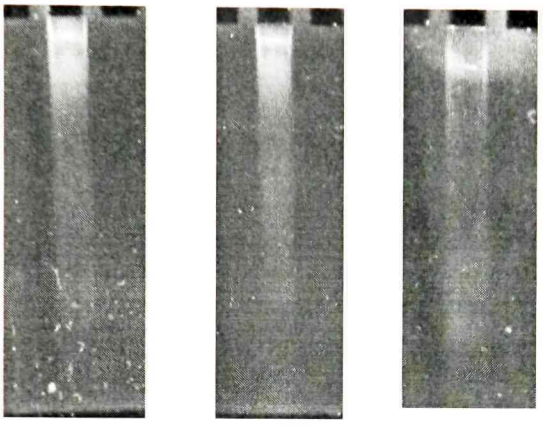

Figure 55. The middle rounds of SELEX. The first, second, third lanes are for the sixth, seventh, eighth round SELEX, respectively. The gel shift assays were carried out as described in Methods. The sixth round contained 5 μM enzyme, 1.5 μM ssDNA and 10 mM NaCl. The seventh round contained 5 μM enzyme, 1.5 μM ssDNA and 10 mM NaCl. The eighth round contained 2 μM enzyme, 1.5 μM ssDNA and 10 mM NaCl.

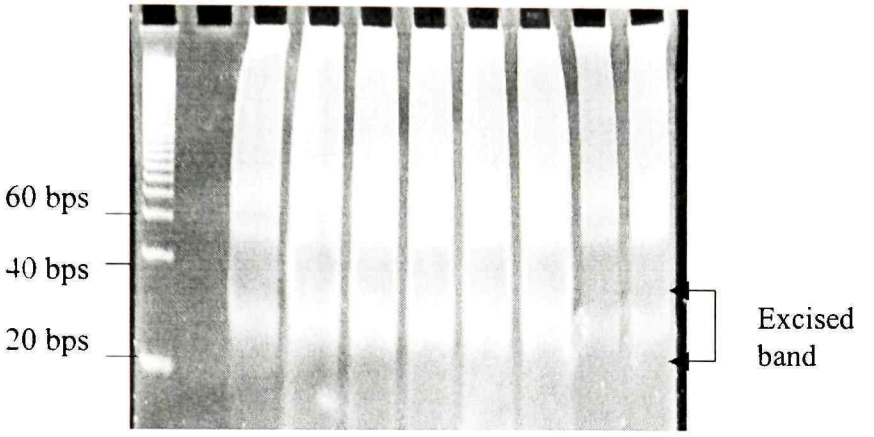

Figure 56. PCR of ssDNA from the ninth round of SELEX. The condition of the PCR was described in Methods. The first lane contained the molecular size markers. The first marker from the bottom represents 20 bps. The band excised was chosen because its migration on the 8 M urea gel matched the migration of the initial random ssDNA.

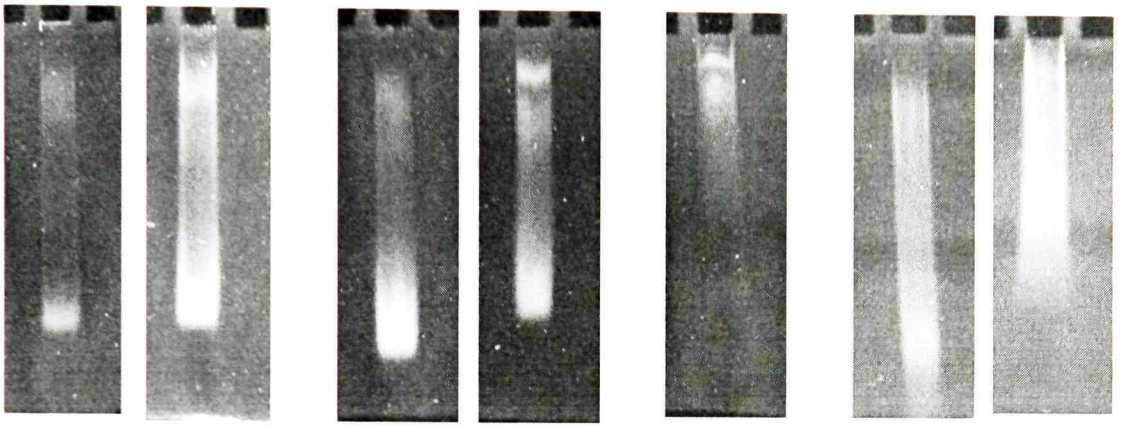

Figure 5 7. The late rounds of SELEX. The first, second, third, fourth, fifth, sixth and seventh lanes are for the ninth, twelfth, thirteenth, fifteenth, sixteenth, seventeenth, and twenty-first round SELEX, respectively. The gel shift assays were carried out as described in Methods. The ninth and twelfth round contained 1.5 μM enzyme, 1,5 μM ssDNA and 10 mM NaCl. The thirteenth and fifteenth round contained 1.5 μM Enzyme, 1.5 μM ssDNA and 15 mM NaCl. The sixteenth round contained 1.5 μM enzyme, 1.5 μM ssDNA and 20 mM NaCl. The seventeenth and twenty-first round contained 1.5 μM enzyme, 1.5 μM ssDNA and 50 mM NaCl.

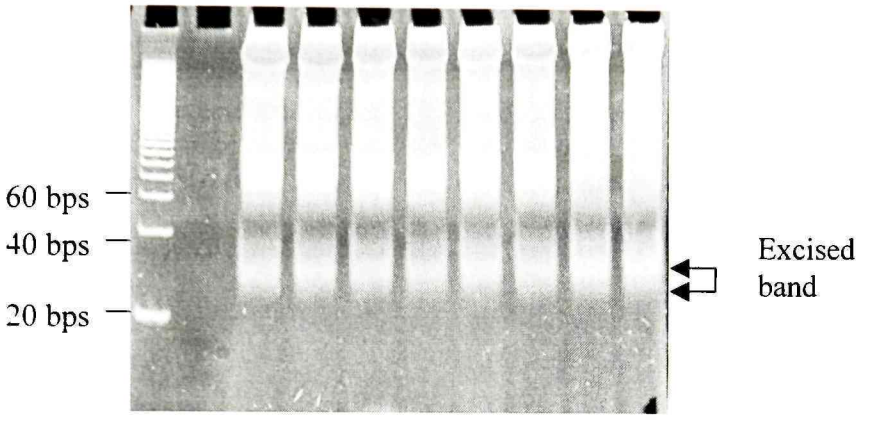

Figure 58. PCR of ssDNA from the twenty-first round of SELEX. The condition of the PCR was described in Methods. The first lane contained the molecular size markers. The first marker from the bottom represents 20 bps. The band excised was chosen because its migration on the 8 M urea gel matched the migration of the initial random ssDNA.

Table 10. Estimates of the metallo-β-lactamase activity assay in presence of selected ssDNA pools.

Inhibitor DNA	Percent control enzyme activity
oligonucleotide before SELEX	100 %
ssDNA* after the eighth round	60 %
ssDNA* after the eleventh round	25 %
ssDNA* after the fourteenth round	27 %
ssDNA* after the sixteenth round	47 %

* The approximate concentration of the ssDNA was estimated as described in the text to be 42 nM.

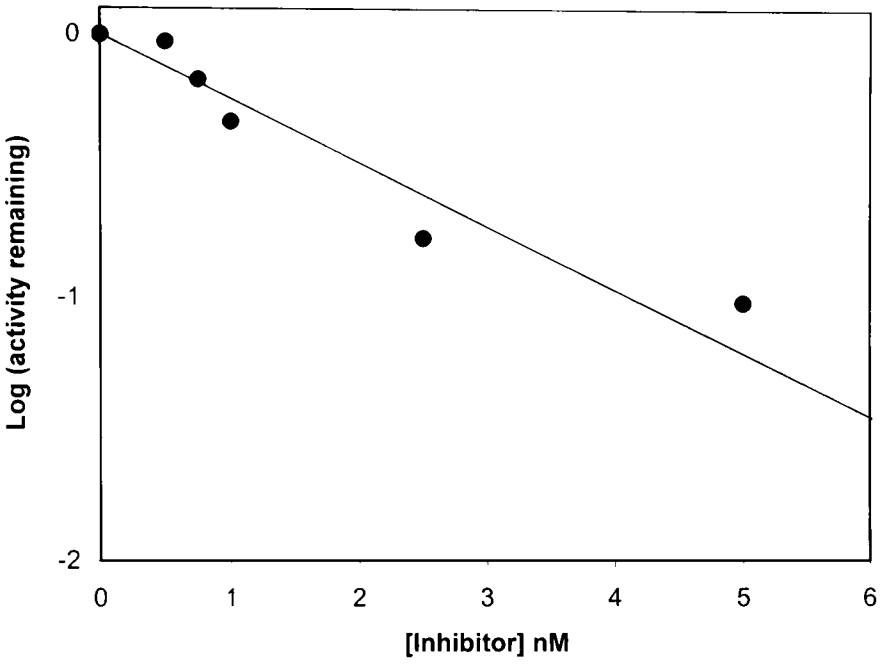

Figure 59. Determination of IC_{50} for *B. cereus* 5/B/6 metallo-β-lactamase by the 30-mer. The enzyme was incubated in the buffer (50 mM MOPS, pH = 7.0) for the 15 min. at 30 °C. The concentration of the substrate (cephalosporin C) was 4 mM.

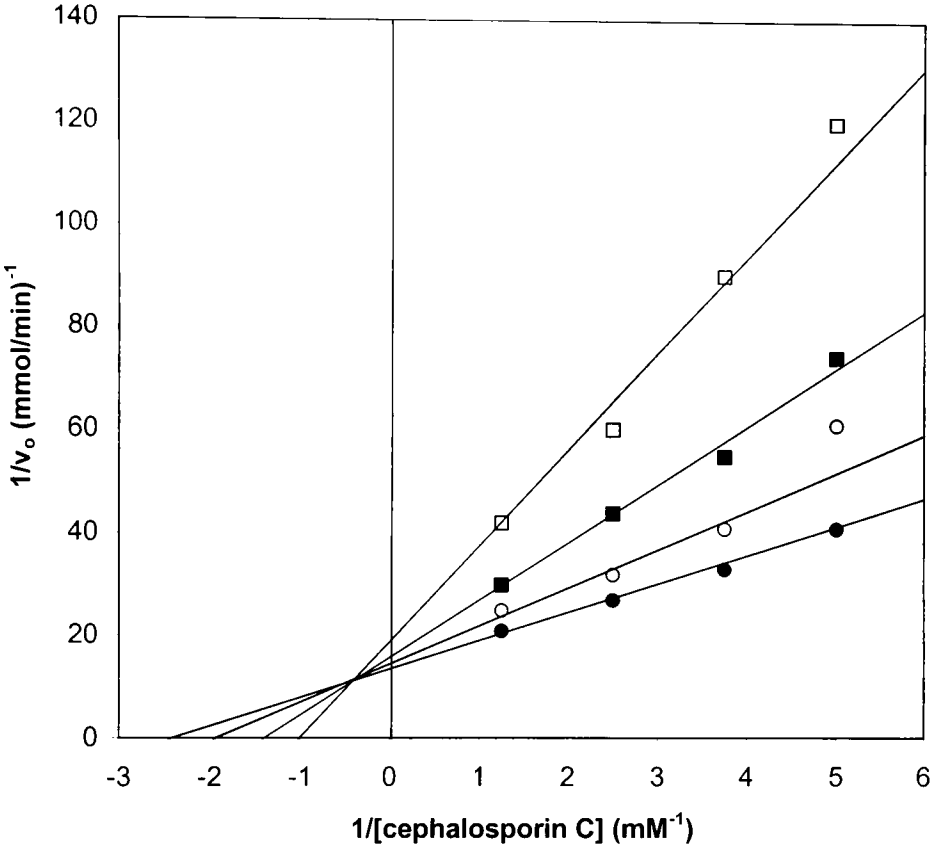

Figure 60. Lineweaver-Burk plot of inhibition of *B. cereus* 5/B/6 metallo-β-lactamase by the 30-mer. Filled circle: [I] = 0 nM; open circle: [I] = 1 nM; filled square: [I] = 2 nM; open square: [I] = 3 nM. I = the 30-mer.

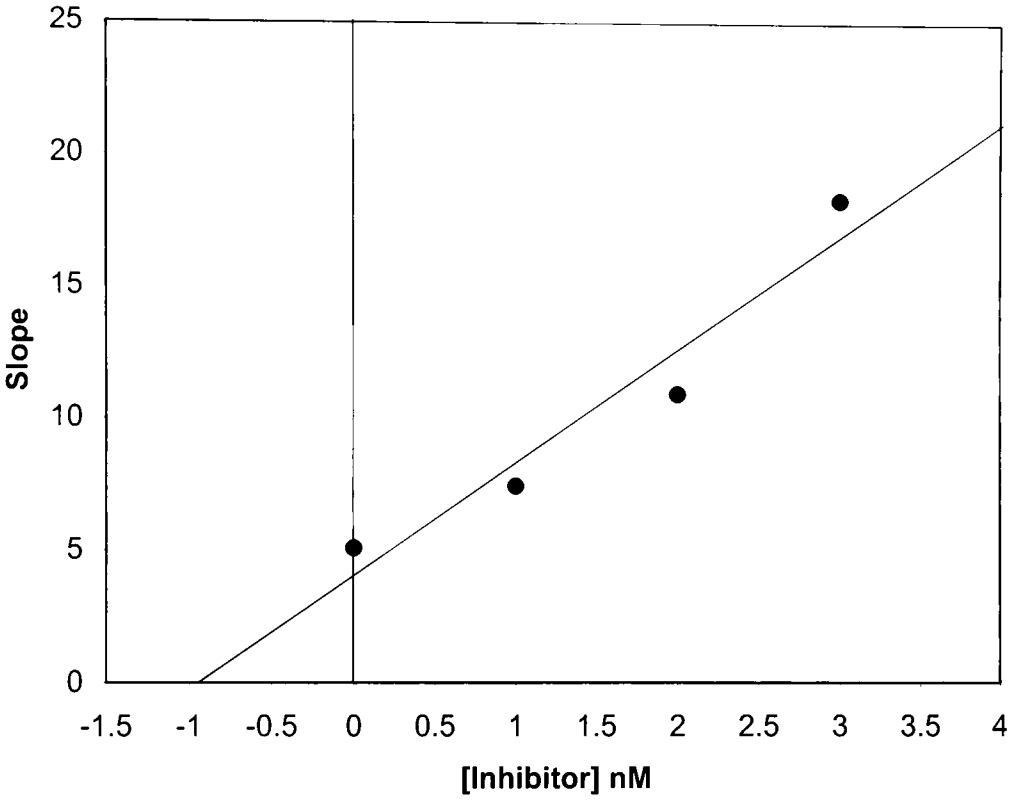

Figure 61. Slope replot to estimate K_i for the 30-mer. Slope values (K_m/V_{max}) for each inhibitor concentration from experimental data of Figure 54 were determined using a non-linear regression computer program (EnzymeKinetics, v. 1.2, Trinity Software). Slope values were then plotted versus corresponding inhibitor concentrations. The x-intercept in this plot is $-K_i$.

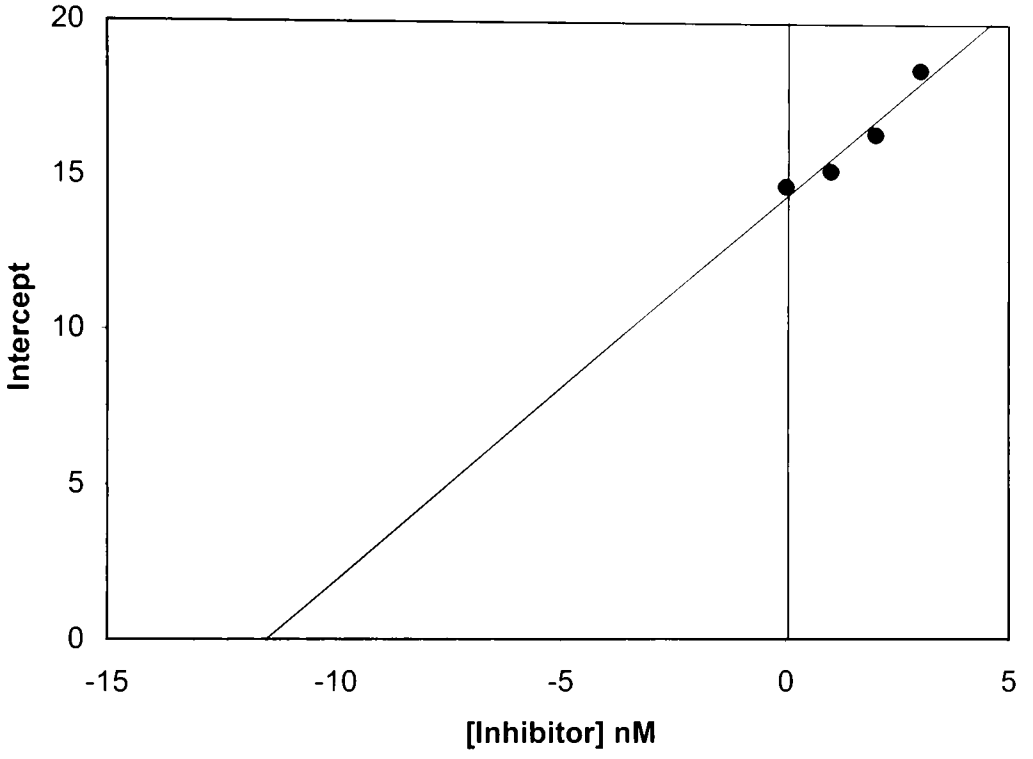

Figure 62. Intercept replot to estimate K_i' for the 30-mer. Intercept values ($1/V_{max}$) for each inhibitor concentration from experimental data of Figure 54 were determined using a non-linear regression computer program (EnzymeKinetics, v. 1.2, Trinity Software). Intercept values were then plotted versus corresponding inhibitor concentrations. The x-intercept in this plot is $-K_i$'.

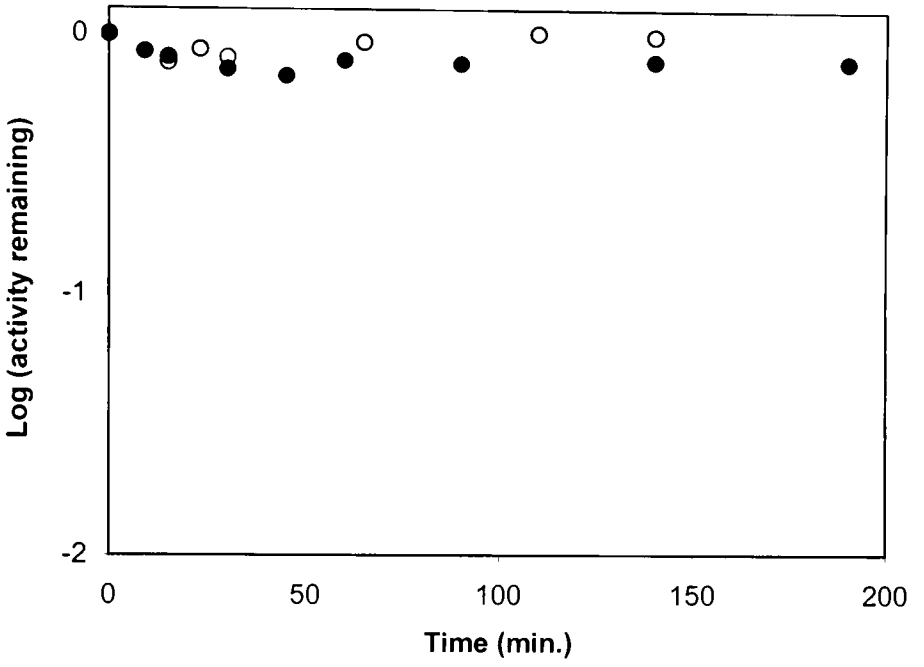

Figure 63. Time-dependence of inactivation of *B. cereus* 5/B/6 metallo-β-lactamase activity by the 30-mer. The concentration of the 30-mer was 0.5 nM. Incubation and assay buffer was 50 mM MOPS, pH = 7.0. cephalosporin C was used as substrate. Open circle: [I] = 0 nM; filled circle: [I] = 0.5 mM. I = the 30-mer.

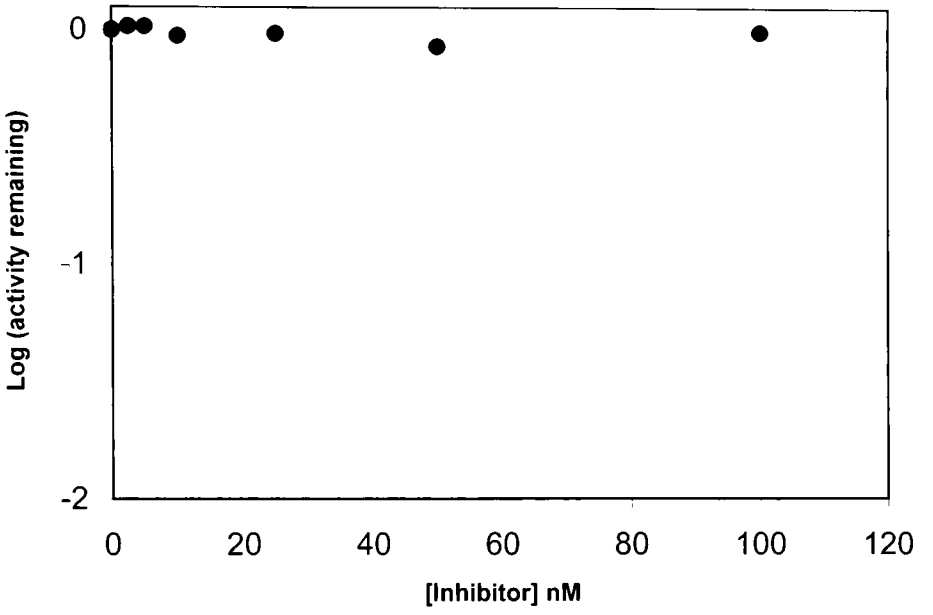

Figure 64. Inhibition of *B. cereus* 569/H/9 β-lactamase I by various concentrations of the 30-mer. The enzyme was preincubated with/without the inhibitor in the buffer (50 mM MOPS, pH = 7.0) for the 15 min. at 30 °C. The concentration of the substrate (cephalosporin C) was 4 mM.

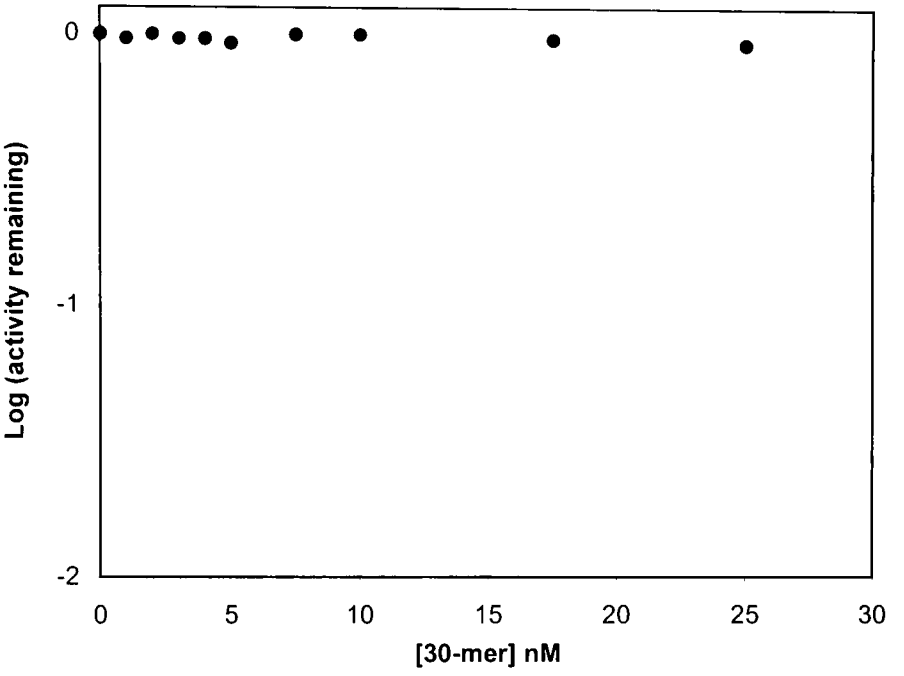

Figure 65. Inhibition of bovine carboxypeptidase A by various concentrations of the 30-mer. The enzyme was preincubated with/without the inhibitor in the buffer (0.05 M TrisHCl, pH = 7.5 with 0.5 M sodium chloride) for the 15 min. at 25 ^{o}C. The concentration of the substrate (hippuryl-L-phenylalanine) was 1 mM.

Table 11. Inhibition of *B. cereus* 5/B/6 metallo-β-lactamase by the ssDNA 30-mer.

	IC_{50}	K_i	K_i'
Synthetic 30-mer	1.2 nM	0.92 nM	11 nM

Prediction of secondary structure of aptamers and metallo-β-lactamase inhibition

The secondary structure of aptamers was predicted by the MFold program (Zuker, 1989). Two different secondary structures of the aptamer (30-mer) were predicted.

Structure 1 (Figure 66) included a one stem-loop structure, and structure 2 (Figure 67) included a two stem-loop structure. Structure 1 was predicted to be lower in energy than structure 2. The sequence of the stem-loop structure from structure 1 is 5'-d(CCAAACTTGG)-3'. This sequence is one of the two stem-loop structures from structure 2 as well. The thermodynamic parameters of folding of the aptamers were calculated by MFold program (Table 12).

The predicted secondary structure for the aptamer (61-mer) containing the primer sequence regions revealed several stem-loop structures (Figure 68). The sequence, 5'-d(CCAAACTTGG)-3', was present as a stem-loop structure in the aptamer (61-mer). This result suggests that the 5'-d(CCAAACTTGG)-3' sequence may be important for interaction with metallo-β-lactamase.

This conserved single-stranded DNA (10-mer) sequence was synthesized using a Beckman Oligo 1000M oligonucleotide synthesizer. To confirm the stem-loop structure from the conserved sequence, the secondary structure of the 10-mer was predicted by the

MFold program (Zuker, 1989). From the prediction, the same stem-loop secondary structure of the 10-mer was preserved (Figure 69).

The IC_{50} value for the 10-mer was determined by measuring the rate of enzymatic hydrolysis of cephalosporin C after the enzyme has been preincubated and assayed in presence of different of amounts of the 10-mer. The data is presented in Table 13 and Figure 70.

From a steady-state kinetic study, the 10-mer showed a noncompetitive inhibition (Figure 71). The value of K_i (dissociation constant for the inhibitor from the enzyme-inhibitor complex) for the 10-mer was 0.31 nM and the value of K_i' (dissociation constant for the inhibitor from the enzyme-substrate-inhibitor complex) for the 10-mer was 1.5 nM as determined by slope and intercept replots (Table 13, Figures 72 and 73).

In order to check to see if the reversible inhibition was time-dependent, the time dependence of the inhibition of the enzyme by 1.0 nM of the 10-mer was measured. As can be seen from Figure 74, the inhibition was time-independent.

The experiment of Figure 75 was performed to test the specificity of inhibition by this 10-mer. As can be seen in Figure 75, the 10-mer has no effect on the activity of the *B. cereus* 569/H/9 β-lactamase I (a class A β-lactamase).

In addition, the bovine carboxypeptidase A was used to test the specificity of inhibition by this 10-mer. As can be seen in Figure 76, 25 nM of the 10-mer has no effect on the activity of the carboxypeptidase A.

An 18-mer corresponding to the remainder of the 30-mer sequence was tested to check how much the conserved 10-mer from the prediction is responsible for the

inhibition of the metallo-β-lactamase. As can be seen in Figure 77, the 18-mer did not show significant inhibition up to 50 nM.

As a control experiment, in order to check to see if the 10-mer binds to metal ion(s) in the active site of the metallo-β-lactamase, the assay for the metallo-β-lactamase was carried out in the presence of 1 mM $ZnSO_4$. The IC_{50} value for the 10-mer was greatly elevated up to 32 nM because of the excess Zn^{2+} ions (Figure 78).

Figure 66. Secondary structure 1 of the 30-mer predicted by the MFold program (Zuber, 1989).

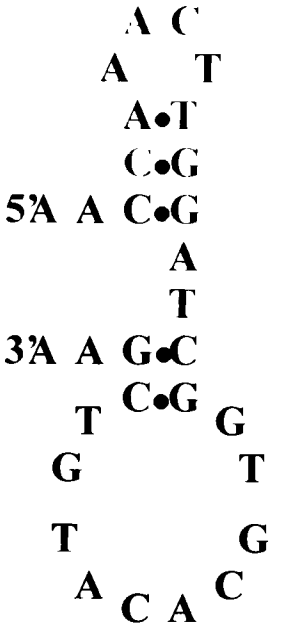

Figure 67. Secondary structure 2 of the 30-mer predicted by the MFold program (Zuber, 1989).

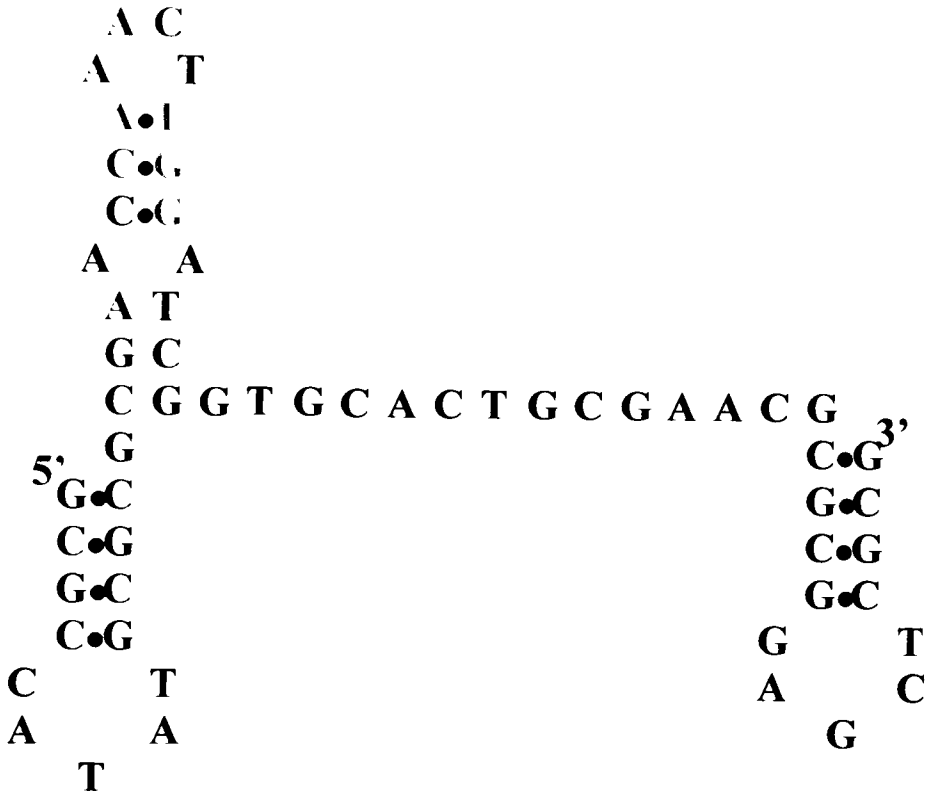

Figure 68. Secondary structure of the 61-mer predicted by the MFold program (Zuber, 1989).

Table 12. Calculation of thermodynamic parameters for folding of ssDNA aptamers in 50 mM NaCl* at 30°C* by MFold program.

	ΔG (kcal mole)	-ΔH (kcal/mole)	-ΔS (cal/(K mol))	T_m (°C)
Structure 1 of the 30-mer	2.2	29.9	91.4	54.1
Structure 2 of the 30-mer	2.2	50.3	158.7	43.9
Structure of the 61-mer	11.4	123.4	369.5	60.9
Structure of the 10-mer	0.5	21.5	69.3	37.2

* Temperature and the concentration of NaCl are the same conditions as the SELEX experiments.

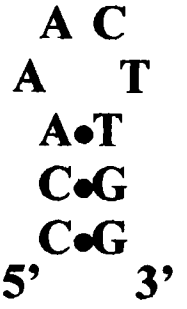

Figure 69. Secondary structure of the 10-mer produced by the MFold program (Zuber, 1989).

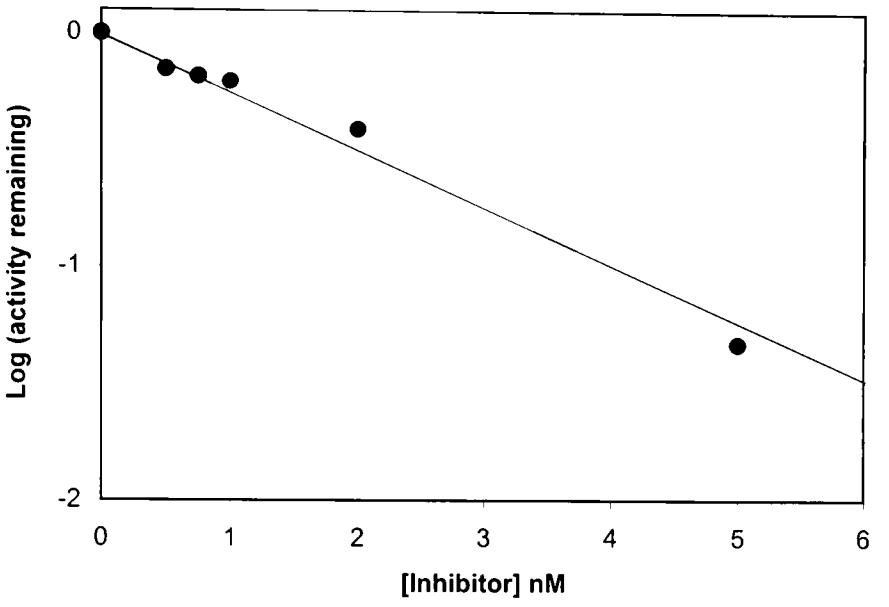

Figure 70. Determination of IC_{50} for *B. cereus* 5/B/6 metallo-β-lactamase by the 10-mer. The enzyme was preincubated with/without the inhibitor in the buffer (50 mM MOPS, pH = 7.0) for the 15 min. at 30 °C. The concentration of the substrate (cephalosporin C) was 4 mM.

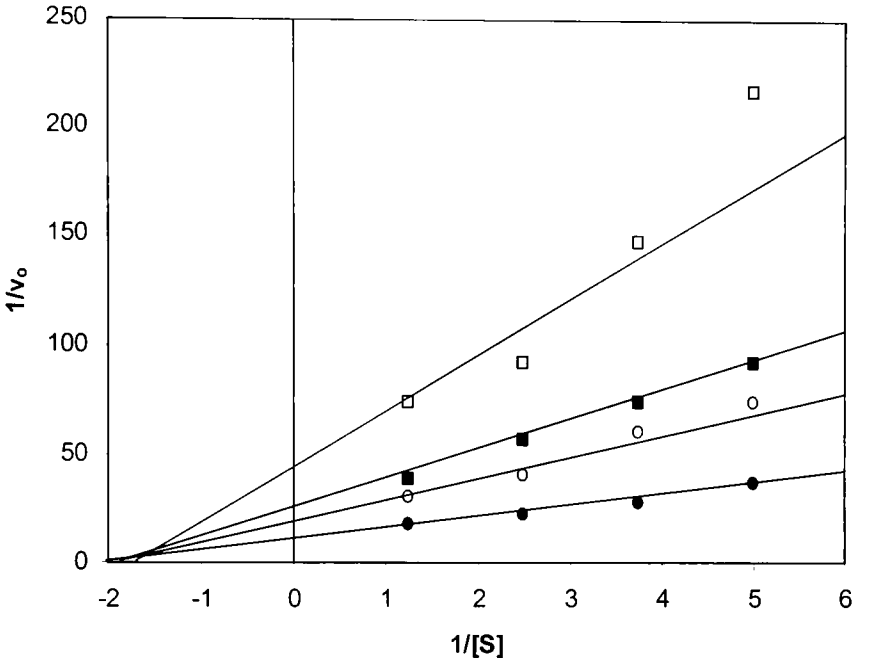

Figure 71. Lineweaver-Burk plot of inhibition of *B. cereus* 5/B/6 metallo-β-lactamase by the 10-mer. Filled circle: [I] = 0 nM; open circle: [I] = 1 nM; filled square: [I] = 2 nM; open square: [I] = 3 nM. I = the 10-mer.

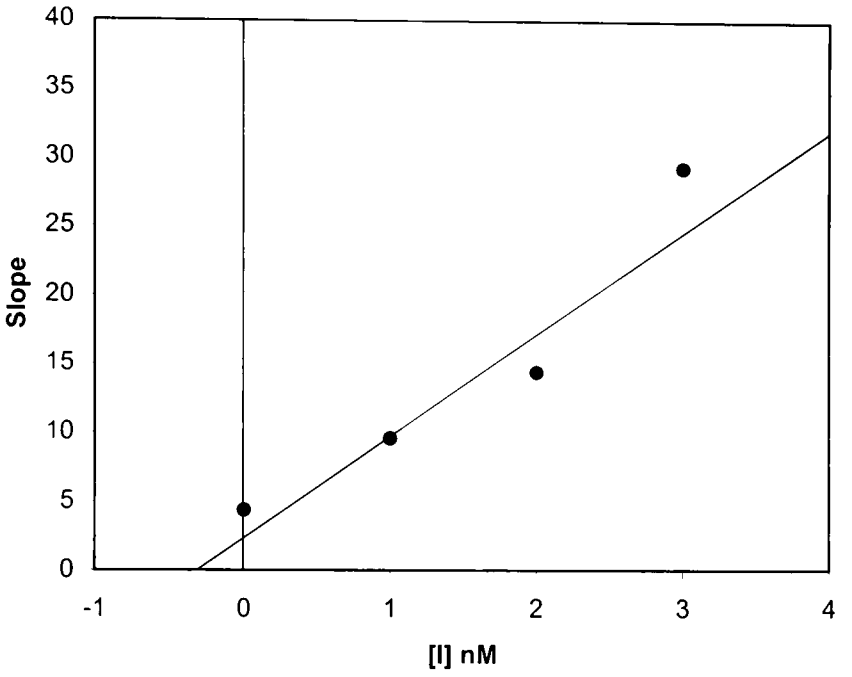

Figure 72. Slope replot to estimate K_i for the 10-mer. Slope values (K_m/V_{max}) for each inhibitor concentration from experimental data of Figure 64 were determined using a non-linear regression computer program (EnzymeKinetics, v. 1.2, Trinity Software). Slope values were then plotted versus corresponding inhibitor concentrations. The x-intercept in this plot is $-K_i$.

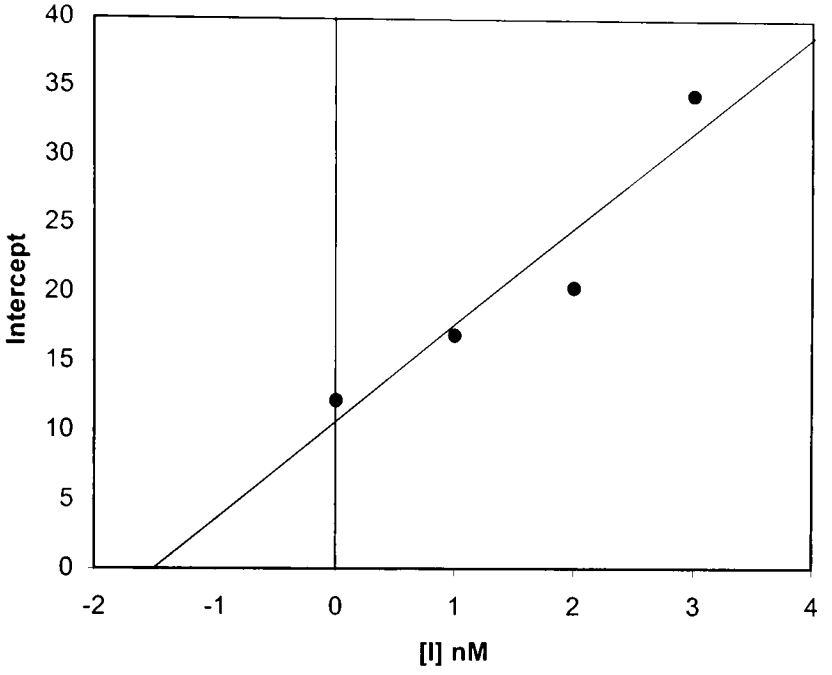

Figure 73. Intercept replot to estimate K_i' for the 10-mer. Intercept values ($1/V_{max}$) for each inhibitor concentration from experimental data of Figure 64 were determined using a non-linear regression computer program (EnzymeKinetics, v. 1.2, Trinity Software). Intercept values were then plotted versus corresponding inhibitor concentrations. The x-intercept in this plot is $-K_i$'.

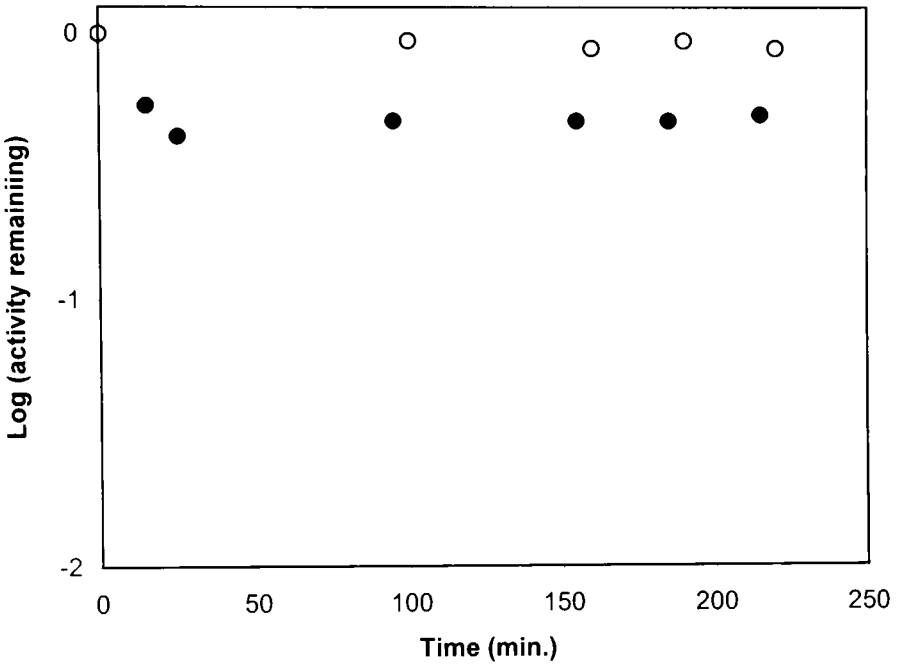

Figure 74. Time-dependence of inactivation of *B. cereus* 5/B/6 metallo-β-lactamase activity by the 10-mer. The concentration of the 30-mer was 0.5 nM. Incubation and assay buffer was 50 mM MOPS, pH = 7.0. cephalosporin C was used as substrate. Open circle: [I] = 0 nM; filled circle: [I] = 0.5 nM. I = the 10-mer.

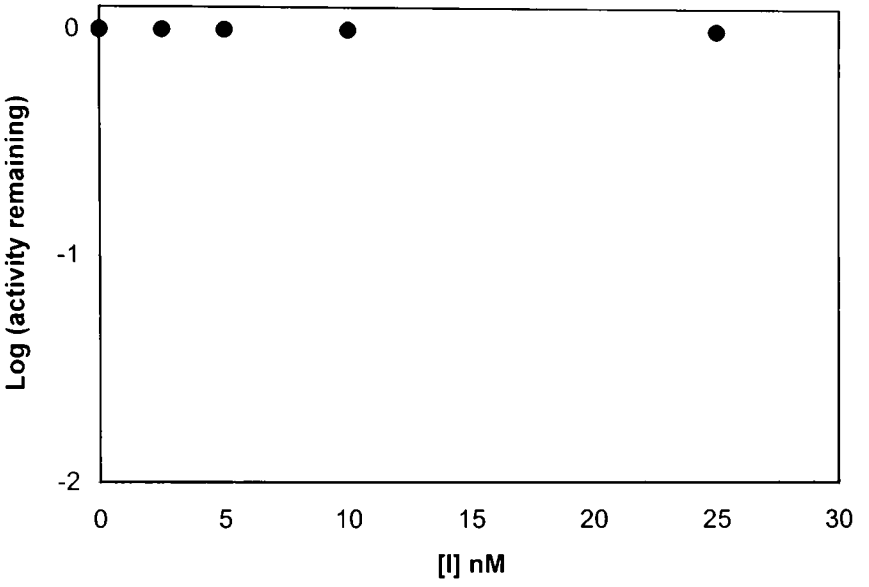

Figure 75. Inhibition of *B. cereus* 569/H/9 β-lactamase I by various concentrations of the 10-mer. The enzyme was preincubated with/without the inhibitor in the buffer (50 mM MOPS, pH = 7.0) for the 15 min. at 30 °C. The concentration of the substrate (cephalosporin C) was 4 mM.

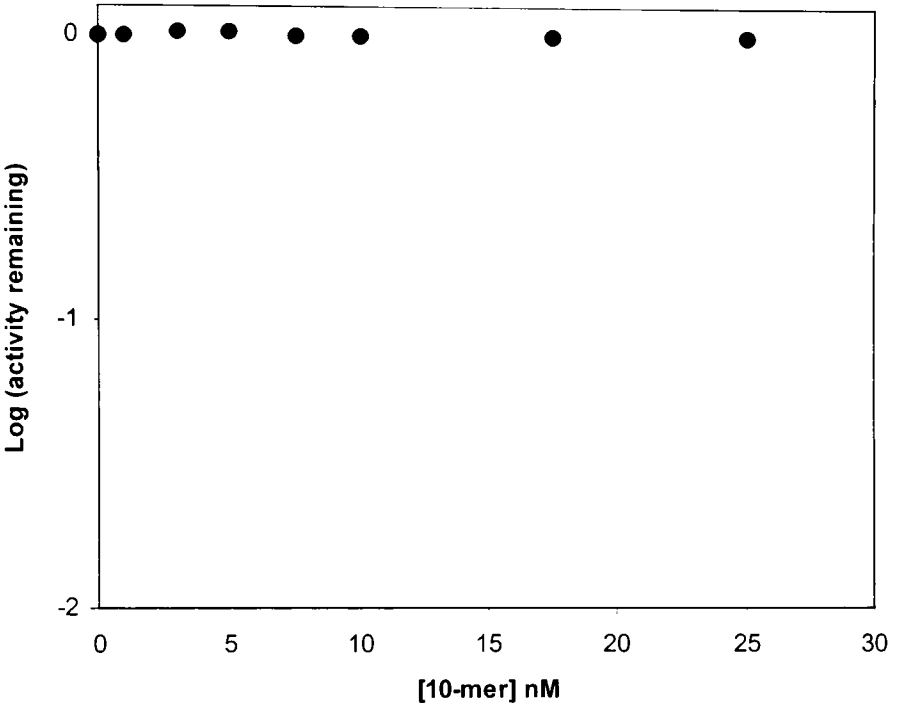

Figure 76. Inhibition of bovine carboxypeptidase A by various concentrations of the 10-mer. The enzyme was preincubated with/without the inhibitor in the buffer (0.05 M TrisHCl, pH = 7.5 with 0.5 M sodium chloride) for the 15 min. at 25 °C. The concentration of the substrate (hippuryl-L-phenylalanine) was 1 mM.

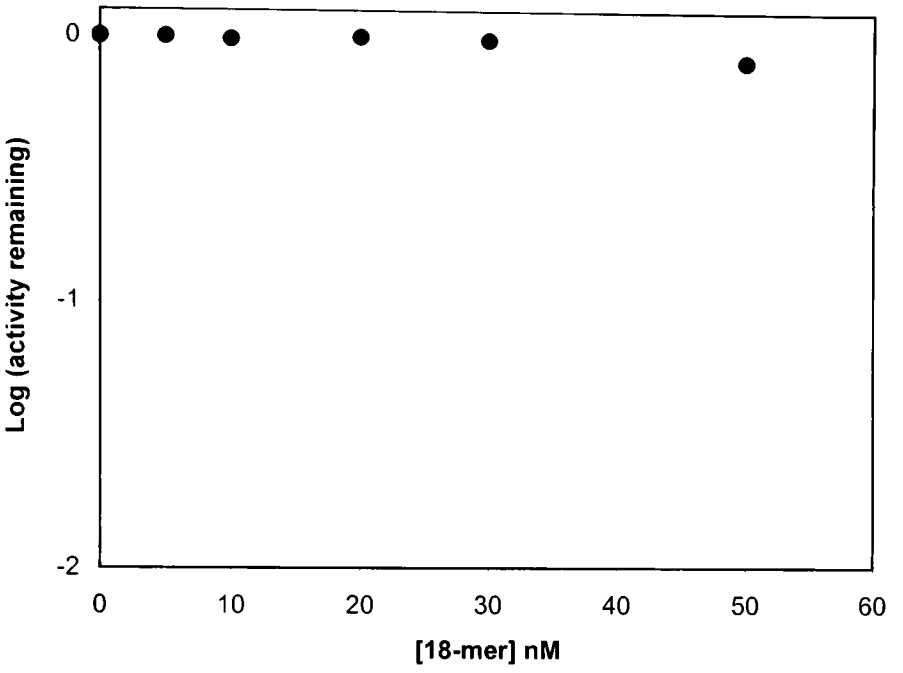

Figure 77. Inhibition of for *B. cereus* 5/B/6 metallo-β-lactamase by various concentrations of the 18-mer. The enzyme was preincubated with/without the inhibitor in the buffer (50 mM MOPS, pH = 7.0) for the 15 min. at 30 °C. The concentration of the substrate (cephalosporin C) was 4 mM.

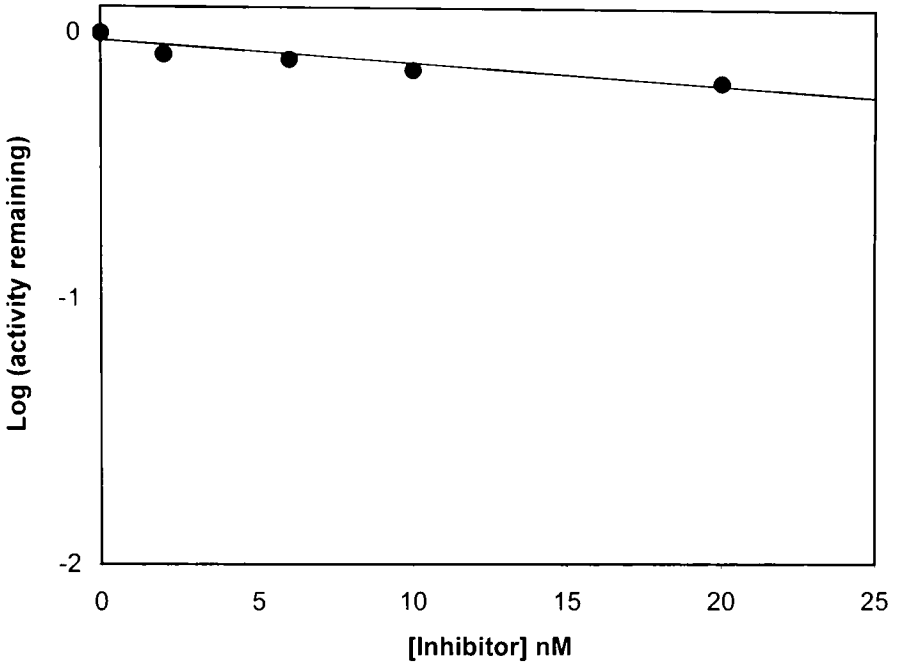

Figure 78. Determination of IC_{50} for *B. cereus* 5/B/6 metallo-β-lactamase in the presence of Zn^{2+} ions by the 10-mer. The enzyme was preincubated with/without the inhibitor in the buffer (50 mM MOPS and 1mM $ZnSO_4$, pH = 7.0) for the 15 min. at 30 °C. The concentration of the substrate (cephalosporin C) was 4 mM.

Table 13. Inhibition of *B. cereus* 5/B/6 metallo-β-lactamase by the ssDNA 10-mer.

	IC_{50}	K_i	K_i'
Synthetic 10-mer	1.2 nM	0.31 nM	1.5 nM

CHAPTER IV

DISCUSSION

ICP-AES studies

The three-dimensional structure of metallo-β-lactamase from *Bacteroides fragilis* (Concha et al., 1996) and *Bacillus cereus* (Fabiane et al., 1998) showed there were one or two Zn^{2+} ions present in the active site. From the ICP-AES results, holoenzyme has at least two Zn^{2+} ions and possibly one extra Zn^{2+} may be loosely bound in some place other than the active site that is not readily localized in the crystal structure.

Site-directed mutagenesis studies

The three-dimensional structure of metallo-β-lactamase from *B. cereus* has revealed that the residue Lys 171 may be involved in stabilization of the Mechaelis complex and/or the tetrahedral intermediate of the reaction (Fabiane et al., 1998). The mutant Lys171Ala showed 8 % of the activity of wild-type enzyme, a dramatic loss of activity. The mutant Lys171Arg, which showed 32 % of the activity of the wild-type enzyme, also displayed significantly diminished activity. These results indicate that this region of the peptide may be important to the structure and/or function of the enzyme. In fact, in the x-ray crystal structure, the residue, Lys171, is thought to hydrogen bond with a penicillin substrate (Fabiane et al., 1998). For future experiments, these mutant forms of the enzyme should be purified to obtain their accurate specific activities. A CD experiment is needed to check to see if the loss in enzyme activity is the result of a major conformational change in the protein's structure.

Metallo-β-lactamase inhibition studies by the rational drug design approach

Buynak et al. (1995) studied the inhibition the compounds **1** and **2** for two type C β-lactamases, derived from *Enterobacter cloacae* P99 and *Enterobacter cloacae* SC12368, and one type A β-lactamase, derived from *E. coli* WC3310. The compounds **1** and **2** inhibited all three β-lactamases with a micromolar range for IC_{50}.

The inhibition of compound **1** was studied for *B. cereus* 5/B/6 metallo-β-lactamase (Yi, 1998). From the time-dependent inhibition study for compound **1** at pH = 7.0, Yi (1998) suggested the inhibition mechanism involved the so-called "iso-mechanism" (Rebholz and Northrop, 1995). To confirm the behavior, the time-dependent inhibition study was repeated (Figure 7). The time-dependent inhibition for the compound **1** showed that early in incubation, there was a steep decline followed by a dramatic increase in activity as a function of time at pH = 7.0 as Yi (1998) suggested. On the other hand, at pH = 6.0 (Figure 8) that is the optimal pH for the metallo-β-lactamase, there was a monotonic sharp decrease followed by an approach to equilibrium. The change of pH allowed us to have simpler behavior of metallo-β-lactamase with compound **1**.

Compounds **1** and **2** showed inhibition as a function of time. But compounds 3, 4 and 5 did not show significant inhibition for *B. cereus* 5/B/6 metallo-β-lactamase. Compounds 1 and 2 have an acetoxymethyl group at position 3 and bromomethylidene group at position 7. However, compounds **3**, **4** and **5** do not have an acetoxymethyl group at position 3 and bromomethylidene group at position 7 at the same time. As a result, the

acetoxymethyl group at position 3 and the bromomethylidene group at position 7 appear to be required for inhibition to occur.

From the time- and concentration-dependent studies, the K_{inact} and k_{inact} values were determined. The values of k_{inact} (the rate constant for the conversion of the reversible complex to the irreversibly inhibited enzyme) for compounds **1** and **2** were the almost same. However the K_{inact} (dissociation constant for the initial reversible enzyme-inhibitor complex) of compound **2** was almost twice as high as that of compound **1**. As a result, two bromines in the compound **1** may provide a higher enzyme affinity than the one bromine in compound **2**.

The specific activity of the purified B. cereus 5/B/6 metallo-β-lactamase is 1200 units/mg of purified enzyme. One unit is defined as a 1 μmol cephalosporin C hydrolyzed per minute at 30 °C; this translates to a turnover number for the enzyme of 500 s^{-1}. Since k_{inact} for compound 1 is 0.2 min^{-1}, the turnover to kill ration for compound 1 is 500 s^{-1}/0.2 min^{-1} = 150000.

Figures 16, 17 and 18 showed that the adducts formed by the mechanism-based inhibitors were acid labile; therefore, it was difficult to determine protein peaks. Figures 16 and 19 show the mass shift of the enzyme bound to compounds **1** and **2**, respectively. The mass difference between Figure 16 and Figure 19 is about 78 Da. The difference is consistent with the molecular weight difference between compound **1** and **2** (80 Da).

In all proteins, sinapinic acid adducts were observed in addition to the MH^+ ions. These adducts are apparent at $[M + 206]^+$ and correspond to the addition of sinapinic acid accompanied with dehydration (Beavis and Chait, 1989). In the inactivation reactions, 100 % inactivation did not occur. After a steep decrease in activity, the equilibrium

between uninhibited and inhibited enzyme exists. Therefore, the broad peak in the mass spectrum for the inhibited enzyme may contain uninhibited enzyme, inhibited enzyme and the sinapinic acid adduct peaks.

Although compounds **3**, **4** and **5** did not show significant time-dependent inhibition, the compounds showed mass shifts in DE-MALDI MS. One reasonable explanation may be that the inhibition process involves the generation of a highly reactive species that is not tightly bound at the active site in the cases of compounds **3**, **4** and **5**. This reactive species may subsequently randomly react with functional groups on the surface of the enzyme in a nonspecific way. Such species may still have enzymatic activity.

Compound **6** and **7** were evaluated as reversible inhibitors of metallo-β-lactamase. Before testing these two compounds, as a preliminary experiment, inhibition patterns for EDTA and 2-mercaptoethanol were generated. From inhibition kinetic studies, noncompetitive inhibition was shown for EDTA and 2-mercaptoethanol. EDTA is well known as a good chelating reagent for Zn^{2+} ions.

The IC_{50} of compound **6** (IC_{50} = 8.3 μM) was two times lower than that of compound **7** (IC_{50} = 18.7 μM), suggesting that the stereochemistry of compound **6** may allow it to inhibit the enzyme more effectively. The inhibition patterns for compounds **6** and **7** were noncompetitive. The noncompetitive inhibition patterns for compounds **6** and **7** were similar to the inhibition patterns of EDTA and 2-mercaptoethaol as were their values of IC_{50}, K_i and K_i'. In the structure of compounds **6** and **7**, these compounds have thiolmethyl groups at position 6. Thus, their thiol groups may interact with the Zn^{2+} ion(s) in the active site of metallo-β-lactamase like 2-mercaptoethanol. For the compound

6, the K_i (dissociation constant for inhibitor from enzyme-inhibitor complex) and K_i' (dissociation constant for inhibitor from enzyme-substrate-inhibitor complex) values were 4.2 μM and 8.6 μM, respectively. This indicates that this compound binds to free enzyme more strongly than enzyme-substrate complex. For the compound **7**, the K_i (dissociation constant for inhibitor from free enzyme) and K_i' (dissociation constant for inhibitor from enzyme-substrate complex) values were 11 μM and 23 μM, respectively. This compound binds to free enzyme more strongly than substrate complex like compound **6**.

As inhibitors of metallo-β-lactamases, these compounds (compound **1**, **2**, **6** and **7**) should provide a platform for the design and synthesis of more potent metallo-β-lactamase inhibitors.

Metallo-β-lactamase inhibition studies by a combinatorial approach (SELEX)

To find an inhibitor for metallo-β-lactamase, a combinatorial approach was utilized. In this study, we have taken advantage of the SELEX methodology to generate high affinity single-stranded DNA aptamers that inhibit metallo-β-lactamase activity.

To increase the stringency of selection during the course of the SELEX experiments, the concentrations of enzyme and NaCl were varied. When the enzyme concentration was greater than the ssDNA concentration, the inhibition was approximately 40 %; higher inhibition was detected after the enzyme concentration (Table 10). This infers that the stringency of selection helped to eliminate non-specific binding ssDNA. Increasing the concentration of NaCl also favored specific binding by ssDNA resulting in selection for a specific oligonucleotide sequence. As another factor in

detecting aptamers, increasing the incubation time may be allowed to provide time for any conformational changes of the metallo-β-lactamase that might occur to "lock" onto the specific ssDNA strongly. In the early rounds, the bands of ssDNA PCR products on the gel were broad. The bands were getting sharper and more distinct throughout the SELEX rounds.

Following 21 rounds of SELEX, a single nucleic acid sequence was found. The 30-mer had IC_{50} of 1.2 nM. By comparison, this represents approximately a 7,000-fold improvement over compound **6**. From the kinetic study, noncompetitive inhibition was indicated for the 30-mer. The K_i (dissociation constant for inhibitor from enzyme-inhibitor complex) and K_i' (dissociation constant for inhibitor from enzyme-substrate-inhibitor complex) values were 0.92 nM and 11 nM, respectively. The noncompetitive inhibition pattern was similar to the noncompetitive inhibition pattern of EDTA, 2-meracptoethanol, compound **6** or compound **7**. Therefore, the 30-mer is likely to bind to one or more Zn^{2+} ions in the active site of the enzyme. The other possibility is that the 30-mer may interact with the enzyme in such a way as to block substrate access to the metal ions. This possibility could be tested by X-ray crystallographic analysis of the inhibited enzyme to determine the specific binding region of ssDNA.

This inhibition was not time-dependent, and the 30-mer did not show any inhibition for β-lactamase I and carboxypeptidase A. Hence, the inhibition is very specific for metallo-β-lactamases. Clearly, the oligonucleotide does not recognize features in the metallo-β-lactamase that bind to the substrate. The carboxypeptidase A results show the exquisite specificity for the metal ion of metallo-β-lactamase. Carboxypeptidase A has been compared to the metallo-β-lactamase as a model for the

latter enzyme, both in terms of structural and mechanistic features (Alberts et al., 1998: Bouagu et al., 1998). Hence, the demonstration that a concentration of the 30-mer that is 25 x IC_{50} for the metallo-β-lactamase has no effect on either 569/H/9 β-lactamase I activity or on the activity of bovine carboxypeptidase A is a profound observation regarding the specificity of inhibition.

A major point is that while this is considerable evidence that suggests that the mode of inhibition involves metal binding by the inhibitor, it is clear that the inhibitor does not indiscriminately chelate all zinc from all sources as does EDTA or other metal chelators.

Payne et al. (1997) have identified inhibitors for metallo-β-lactamase. One of a mercaptoacetic acid thiol esters series (SB216968) inhibited *Aeromonas hydrophila* CphA metallo-β-lactamase and was found to be an uncompetitive inhibitor (K_i = 3.9 μM). Yang and Crowder (1999) have also identified inhibitors for metallo-β-lactamase from *Stenotrophomonas maltophilia*. They showed that N-(2'-mercaptoethyl)-2-phenylacetamide and N-benzylacetyl-D-alanylthioacetic acid were competitive inhibitors with K_i values of 50 ± 3 μM and 1.6 ± 0.3 μM, respectively. Scrofani et al. (1999) suggested that the inhibitor 3-[2'-(S)-benzyl-3'-mercaptopropanoyl]-4-(S)-carboxy-5,5-dimethylthiazolidine, that exhibits many structural similarities to the β-lactam antibiotic ampicillin, "tightly" binds in a position similar to that thought to be occupied by β-lactam antibiotics for metallo-β-lactamase from *B. fragilis* using NMR characterization. A free sulfhydryl group of the inhibitor did not show a disulfide formation with one of the free cysteine side chains in the vicinity of the zinc-binding site. Mollard et al. (2001) showed

that thiomandelic acid was a competitive inhibitor of metallo-β-lactamases with K_i values (*Bacillus cereus* enzyme) of 0.09 μM for R-thiomandelic acid and 1.28 μM for the S-isomer. To date, R-thiomandelic acid appears to be the most effective published inhibitor for metallo-β-lactamase. However, the K_i value (0.92 nM) of the 30-mer that we found was more effective than any of the others. Therefore, the 30-mer is a very promising inhibitor for metallo-β-lactamase.

Prediction of secondary structure of aptamers and metallo-β-lactamase inhibition

It is desirable that the aptamer should be as small as possible, on costs grounds, reasons of target accessibility and so on. The predicted secondary structures of the 30-mer produced by the MFold program revealed a conserved stem-loop structure. The sequence was 5'-d(CCAAACTTGG)-3'. Hence, we synthesized the 10-mer.

The IC_{50} of the 10-mer was the same as the 30-mer. From the steady-state kinetic studies, the noncompetitive inhibition pattern was shown like the 30-mer. The IC_{50} value for the 10-mer was greatly elevated when the assay was carried out in the presence of inhibitor with exogenous Zn^{2+} ions. This supports idea that the 10-mer likely binds to the metal ion(s).

The K_i (dissociation constant for inhibitor from enzyme-inhibitor complex) and K_i' (dissociation constant for inhibitor from enzyme-substrate-inhibitor complex) values were 0.31 nM (290-fold lower than the K_i reported for R-thiomandelic acid (Mollard et al. (2001)) and 1.5 nM, respectively. The K_i and K_i' values for the 10-mer were lower than the 30-mer. This infers that the 10-mer binds the free enzyme and enzyme-substrate

complex more strongly than the 30-mer. Therefore, this 10-mer may be a more promising drug candidate than the 30-mer.

Like the 30-mer, this inhibition was not time-dependent and the 10-mer did not show any inhibition for β-lactamase I and carboxypeptidase A. Hence, the inhibition is very specific for metallo-β-lactamases as well.

The secondary structure of 10-mer, as proposed by the MFold program, corellated well with the experimental results. The conserved structure from the sequence 5'-d(CCAAACTTGG)-3' is responsible for the inhibition of *B. cereus* 5/B/6 metallo-β-lactamase.

For further research, major challenges to clinical applications of these ssDNA aptamers include the pharmacokinetics of oligonucleotides *in vivo*, and the rate at which they are degraded by nucleases. To overcome the latter problem, the modification of the ssDNA aptamers may be necessary to provide stability of these aptamers *in vivo* (Hicke and Stephens, 2000).

Obviously, the other important practical consideration for clinical use is related to the molecular size of the decamer. A compound this large may not have direct applicably as a drug. Further experimentation is required to determine whether or not a smaller oligonucleotide can be an efficient inhibitor. Perhaps the inhibitory activity can be identified with either the loop or stem regions of the oligonucleotide.

As an example of a commercial product using SELEX technology, Eyetech Pharmaceuticals, Inc. has a product in clinical trials that is an aptamer that inhibits vascular endothelial growth factor (VEGF). The aptamer was discovered using SELEX (Jellinek et al., 1994; Ruckman et al., 1998; Willis et al., 1998). Known as EYE001, the

aptamer is an oligonucleotide that acts like a high affinity antibody to VEGF. This anti-VEFG aptamer blocks vessel growth and inhibits neovascularization in pre-clinical models.

Single-stranded DNA (Bock et al., 1992; Macaya et al., 1995; Tsiang et al., 1995) was found using the SELEX process for thrombin that is a multifunctional serine protease. The DNA ligands that have quadruplex/duplex were shown to bind the fibrinogen-recognition exosite at the base of the active site cleft. The ligand inhibits thrombin-catalyzed clot formation *in vitro* (Tasset et al., 1997). Tasset et al. (1997) showed that a 15-mer containing quadruplex motif from the previous ssDNA inhibitor binds to the active cleft. Such structural features may be important in metallo-β-lactamase inhibition as well.

Even if it should prove to be impractical to directly utilize the decamer or its derivatives in drug form as a metallo-β-lactamase inhibitors, such compounds show great promise as lead compounds for a new generation of highly effective metallo-β-lactamase inhibitors.

LIST OF REFERENCES

Abraham, E. P. and Waley, S. G. (1979) in *Beta-lactamases* (Hamilton-Miller, J. M. T. and Smith, J. T., eds.) pp. 311-338, Academic Press, New York.

Alberts, I. L., Katalin, N. and Wodak, S. J. (1998) *Protein Science* **7**, 1700-1716.

Ambler, R. P. (1980) *Phil. Trans. R. Soc. Lond.* **B289**, 321-331.

Ambler, R. P., Coulson, A. F. W., Frere, J.-M., Ghysen, J.-M., Joris, B., Forsman, M., Levesque, R. C., Tiraby, G. and Waley, S. G. (1991) *Biochem. J.* **276**, 269-270.

Ambler, R. P., Daniel, M., Fleming, J., Hermoso, J.-M., Pang, C. and Waley, S. G. (1985) *FEBS Lett.* **189**, 207-211.

Ausubel, F. M., Brent, R., Kingston, R. E., Moore, D. D., Seidman, J. G., Smith, J. A. and Struhl, K. (1992) *Short Protocols in Molecular Biology* pp. 26-27, Greene Publishing Associates and Wiley-Interscience, John Wiley & Sons, New York.

Bartel, D. P. and Szostak, J. W., (1993) *Science* **261**, 1411-1418.

Beavis, R. C. and Chait, B. T. *Rapid Commun. Mass Spectrom.* (1989) **3**, 432-435.

Bicknell, R., Schaeffer, A., Waley, S. G. and Auld, D. S. (1986) *Biochemistry* **25**, 7208-7215.

Bock, L. C., Griffin, L. C., Latham, J. A., Vermass, E. H. and Toole, J. J. (1992) *Nature* **355**, 564-566.

Bouagu, S., Laws, A., Galleni, M. and Page, M. (1998) *Biochem. J.* **331**, 703-711.

Brenner, D. G. and Knowles, J. D., (1984) *Biochemistry* **23**, 5834-5846.

Buynak, J. D., Khasnis, D., Bachmann, B., Wu, K. and Lamb, G. (1994) *J. Am. Chem. Soc.* **116**, 10955-10965.

Buynak, J. D., Wu, K., Bachmann, B., Khasnis, D., Hua, L., Ngyen, H. K. and Carver, C. L. (1995) *J. Med. Chem.* **38**, 1022-1034.

Carfi, A., Pares, S., Duee, E., Galleni, M., Duez, C., Frere, J. M. and Dideberg, O. (1995) *The EMBO Journal*, **14**, No. 20, 4914-4921.

Chen, H. and Gold, L., (1994) *Biochemistry* **33**, 8746-8756.

Concha, N. O., Janson, C. A., Rowling, P., Pearson, S., Cheever, C. A., Clarke, B. P., Lewis, C., Galleni, M., Frere, J. M., Payne, D. J., Bateson, J. H. and Abdel-Meguid, S. S. (2000) *Biochemistry* **15**, 4288-4298.

Concha, N. O., Rasmussen, B. A., Bush, K. and Herzberg, O. (1996) *Structure* **4**, 823-836.

Crompton, B., Jago, M., Crawford, K., Newton, G. G. F and Abraham, E. P. (1962) *Biochem. J.* **83**, 52-63.

Danziger, L. H. and Pendland, S. L. (1995) *Am. J. health Syst. Pharm.* **52** (Suppl 2), S3-8.

Davies, R. B. and Abraham, E. P (1974) *Biochem. J.* **143**, 129-135.

Davies, R. B. Abraham, E. P. and Melling, J. (1974) *Biochem. J.* **143**, 115-127.

Davies, R. B. Abraham, E. P. Melling, J. and Pollock, M. R. (1975) *Biochem. J.* **143**, 409-411.

Ellington A.D. and Szostak J. W. (1990) Nature 346, 818-822.

Fabiane, S. M., Sohi, M. K., Wan, T., Payne, D. J., Bateson, J. H., Mitchell, T. and Sutton, B. J. (1998) *Biochemistry* **37**, 12404-12411.

Farmulok, M. and Szostak, J. W. (1992) *Angew. Chem. Int. Ed. Engl.* **31**, 979-988.

Felici, A. and Amicosante, G. (1995) *Antimicrob. Agents Chemother.* **39**, 192-199.

Felici, A., Amicosante, G., Oratore, A., Strom, R., Ledent, P., Joris, B., Fanuel, L. and Frere, J.-M. (1993) *Biochem. J.* **291**, 151-155.

Felici, A., Perilli, M., Franceschini, N., Rossolini, G. M., Galleni, M., Frere, J.-M., Oratore, A. and Amicosante, G. (1997) *Antimicrob. Agents Chemother.* **41**, 866-868.

Fisher, J., Charnas, R. L, Bradley, S. M. and Knowles, J. R. (1981) *Biochemistry* **20**, 2726-2731.

Folk, J. E. and Schirmer, E. W. (1963) *J. Biol. Chem.* **238**, 3884-3894.

Frere, J. M. (1995) *Mol. Microbiol.* **16** (3), 385-395.

Ghuysen, J.-M. (1988) in *Antibiotic Inhibition of Bactrial Cell surface Assembly and Function* (Actor, P., Daneo-Moore, L., Higgins, M. L., Salton, M. R. J. and

Shockman, G. D., Ed.) pp. 268-284, American Society for Micro biology, Washington, D. C

Gold, L., Polisky, B., Uhlenbeck, O. and Yarus, M., (1995) *Annu. Rev. Biochem.* **64**, 763-797

Hanahan, D. (1983) *J. Mol. Biol.* **166**, 557-580.

Hicke, B. J. and Stephens, A. W. (2000) *J. Clin. Invest.* **106**, 923-928.

Hilliard, N. P., (1995) Ph.D thesis , Texas Tech University

Hilliard, N. P. and Shaw, R. W. (1992) The *FASEB J.* **6**, p. A1008.

Hussain, M., Pastor, F. I. J. and Lampen, J. O. (1987) *J. Bacteril.* **169**, 579-586.

Jaeger, J. A., Turner, D. H. and Zuker, M. (1989) *Proc. Natl. Acad. Sci. USA* **86**, 7706-7710.

Jaeger, J. A., Turner, D. H. and Zuker, M. (1990) *In Methods in Enzymology* **183**, 281-306.

Jellinek, D., Green, L. S., Bell, C. and Janjic, N. (1994) *Biochemistry* **33**, 10450-10456.

Joris, B., Ledent, P., Dideberg, O., Fonze, E., Lamotte-Brasseur, J., Kelly, J. A., Ghuysen, J.-M. and Frere, J.-M. (1991) *Antimicrob. Agents Chemother.* **35**, 2294-2301.

Joyce, G. F. (1989) *Gene* **82**, 83-87.

Kelly, J. A., Knox, J. R., Moews, P. C., Moring, J. and Zhao, H. C. (1988) in *Antibiotic Inhibition of Bactrial Cell surface Assembly and Function* (Actor, P., Daneo-Moore, L., Higgins, M. L., Salton, M. R. J. and Shockman, G. D., Ed.) pp. 261-267, American Society for Micro biology, Washington, D. C.

Kitz, R. and Wilson, I. B. (1962) *J. Biol. Chem.* **237**, 3245-3249.

Kogut, M., Pollock, M. R. and Tridgell, E. J. (1956) *Biochem. J.* **62**, 391-401.

Kuwabara, S., Adams, E. P. and Abraham, E. P. (1970) *Biochem. J.* **118**, 467-474.

Kuwabara, S. and Lloyd, P. H. (1971) *Biochem. J.* **124**, 215-220.

Ledent, P., Raquet, X., Joris, B., Van Beeumen, J. and Frere, J.-M. (1993) *Biochem. J.* **292**, 555-562.

Lim, H. M., Pene, J. J. and Shaw, R. W. (1988) *J. Bacteriol.* **170**, 2873-2878.

Livermore, D. M. (1991) Scand. J. Infect. Dis., Suppl. **78**, 7-16

Lowry, O. H., Rosebrough, N. J., Farr, A. L. and Randall, R. J. (1951) *J. Biol. Chem.* **193**, 265-275.

Macaya, R. F., Waldron, J. A., Beutel, B. A., Gao, H., Joeston, M. E., Yang, M., Patel, R., Bertelsen, A. H. and Cook, A. G. (1995) *Biochemistry* **34**, 4478-4492.

Matagne, A., Ledent, P., Monnaie, D., Felici, A., Jamin, M., Raquet, X., Galleni, M., Klein, D., Francois, I. and Frere, J. M. (1995) *Antimicrob. Agents Chemother* **39**, 227-231.

Maugh, T. M. (1981) *Science* **214**, 1225-1228.

Maxam, A. M. and Gilbert, W. (1977) *Proc. Natl. Acad. Sci. USA* **74**, 560-564.

Meyers, J. L. and Shaw, R. W. (1989) *Biochem. Biophys. Acta* **995**, 264-272.

Mollard, C., Moali, C., Papamicael, C., Damblon, C., Vessilier, S., Amicosante, G., Schofield, C. J., Galleni, M., Frere, J. M. and Roberts, G. C. (2001) *J. Biol. Chem.* **276**,45015-45023.

Nagai, K. and Thogersen, H. C. (1984) *Nature* **309**, 810-812.

Neu, H. C. (1992) *Science* **257**, 1064-1073.

Papworth, C., Braman, J. and Wright, D. A. (1996) *Strategies* **9**, 3-4.

Payne, D. J. (1993) *J. Med. Microbiol.* **39**, 993-999.

Payne, D. J., Bateson, J. H., Gasson, B. C., Proctor, D., Khushi, T, Farmer, T. H., Tolson, D. A., Bell, D., Skett, P. W., Marshall, A. C., Reid, R., Ghosez, L., Combret, Y. and Marchand-Brynaert, J. (1997) *Antimicrob. Agents Chemother.* **41**, 135-140.

Pitout, J. D. D., Sanders, C. C. and Sanders, W. E. (1997) *Am. J. Med.* **103**, 51-59.

Rahil, J. and Pratt, R. F. (1991) *Biochem. J.* **275**, 793-795.

Rasmussen, B. A., Yang, Y., Jacobs, N. and Bush, K. (1994) *Antimicrob. Agents Chemother.* **38**, 2116-2120.

Reddy, P., Peterkofsky, A. and McKenney, K. (1989) *Nucleic Acids Res.* **17**, 10473-10488.

Robertson, D. L. and Joyce, G. F (1990) *Nature* **344**, 467-468.

Ruckman, J., Green, L. S., Beeson, J., Waugh, S., Gillette, W. L., Henninger, D. D., Claesson-Welsh, L. and Janjic, N. (1998) *Journal of Biological Chemistry* **273**, 20556-20567.

Sabath, L. D. and Abarham, E. P (1966) *Biochem. J.* **98**, 11c-13c.

Sambrook, J., Fritsch, E. F. and Maniatis, T. (1989) *Molecular Cloning: a laboratory manual*, 2ed, pp. 7.70-7.76, Cold Spring Harbor Laboratory Press, New York.

SantaLucia, J. Jr. and Allawi, H. T. (1977) *Biochemistry* **36**, 10581-10594.

Scrofani, S. D., Chung, J., Huntley, J. J., Benkovic, S. J., Wright, P. E. and Dyson, H. J. *Biochemistry* (1999) **44**, 14507-14514.

Shaw, R. W., Clark, S. D., Hilliard, N. P and Harman, J. G. (1991) *Prot. Exp. Purif.* **2**, 151-157.

Suskoviae, B., Vajtner, Z. and Naumski, R. (1991) *Tetrahedron* **47**, 8407-8416.

Sutton, B. J., Artymiuk, P. J., Cordero-Borboa, A. E., Little, C., Philips, D. C. and Waley, S. G. (1987) *Biochem. J.* **248**, 181-188.

Tasset, D. M., Kubik, M. F. and Steiner, W. (1997) *J. Mol. Biol.* **272**, 688-698.

Thatcher, D. R. (1975) *Biochem. J.* **147**, 313-326.

Tsiang, M., Gibbs, C. S., Griffin, L. C., Dunn, K. E. and Leung, L. K. (1995) *J. Biol. Chem.* **270**, 19370-19376.

Tuerk, C. and Gold, L. (1990) *Science* **249**, 505-510.

Turner, D. H., Sugimoto, N. and Freier, S. M. (1988) *Annu. Rev. Biophys. Biophys. Chem.* **17**, 167-192.

Willis, M. C., Collins, B. D., Zhang, T., Green, L. S., Sebesta, D. P., Bell, C., Kellogg, E., Gill, S. C., Magallanez, A., Knauer, S., Bendele, R. A., Gill, P. S., Janjic, N. and Collins, B. (1998) *Bioconjug Chem* **9**, 573-582.

Wolf, B. P., Sumner, L. W., Shields, S. J., Nielsen, K., Gray, K. A. and Russell, D. H. (1998) *Analytical Biochemistry* **260**, 117-127.

Yang, K. W. and Crowder, M. W. (1999) *Arch. Biochem. Biophys.* **368**, 1-6.

Yu, X. (1998) Ph.D. thesis, Texas Tech University.

Zuber, M., Patterson, T. A. and Court, D. L. (1987) *Proc. Natl. Acad. Sci. USA* **84**, 4514-4518.

Zuker, M. (1989) *Science* **244**, 48-52.